Dissertation zur Erlangung des Doktorgrades
der Fakultät für Chemie und Pharmazie
der Ludwig-Maximilian-Universität München

Arabidopsis flavonoid glycosylation impacts on phenylpropanoid biosynthesis and plant growth

Ruohe Yin

aus

Anhui, P.R. China

2010

Erklärung

Diese Dissertation wurde im Sinne von § 13 Abs. 3 bzw. 4 der Promotionsordnung vom 29. Januar 1998 von PD Dr. Anton R. Schäffner betreut.

Ehrenwörtliche Versicherung

Diese Dissertation wurde selbstständig, ohne unerlaubte Hilfe erarbeitet.
München, am 08.10.2010

Ruohe Yin

Dissertation eingereicht am: 08.10.2010

1. Gutachter: PD Dr. Anton R. Schäffner

2. Gutachter: Prof. Dr. Roland Beckmann

Mündliche Prüfung am: 10.12.2010

SUMMARY

Flavonols, a class of phenylpropanoids, have protective and regulatory functions in plants and are important nutritional ingredients. The hydrophobic compounds are glycosylated consecutively at their 3-OH and 7-OH positions in *Arabidopsis thaliana*. UGT78D1 and UGT78D2 are the major glycosyltransferases involved in flavonol 3-*O*-glycosylation in leaves of this plant. Accordingly, the *ugt78d1 ugt78d2* double mutant was strongly compromised in the primary conjugation of flavonol aglycones. Instead of alternative modifications or aglycone accumulation, flavonol biosynthesis was repressed in *ugt78d1 ugt78d2* retaining only one third of the wild-type flavonol level. The reduced flavonol amounts were associated with a repressed transcription of many flavonol-biosynthetic key genes including the committed step of flavonoid biosynthesis catalyzed by CHALCONE SYNTHASE (TT4). In addition, the expression of PHENYLALANINE AMMONIA LYASE (PAL), which constitutes the committed step of the general phenylpropanoid pathway, was repressed at the level of gene transcription and enzyme activity. However, a strong repression of total flavonol biosynthesis in the *flavonol synthase 1* mutant did not negatively affect PAL expression nor was it repressed by a compromised downstream 7-*O*-glycosylation. PAL activity was also reverted back to wild-type level in *tt4 ugt78d1 ugt78d2* lines eliminating flavonoid biosynthesis in addition to the repressed 3-*O*-glycosylation capacity. Chemical complementation of *tt4 ugt78d1 ugt78d2* plants using naringenin, a flavonoid intermediate, could restore the reduction in PAL expression. Thus, these studies revealed a novel feedback inhibition of the flavonol-biosynthetic pathway, which was specifically linked to a compromised flavonol 3-*O*-glycosylation, but at the same time dependent on flavonol formation itself. Although the molecular mechanism of flavonol-dependent feedback inhibition remains obscure, this regulation may serve as a mean to avoid the accumulation of hydrophobic and potentially toxic flavonol aglycones.

The *ugt78d2* mutant possesses an altered flavonol glycoside pattern and showed severe shoot growth defects including dwarfism and loss of apical dominance. The *ugt78d2* growth defects were eliminated by blocking flavonoid biosynthesis, suggesting that they were flavonoid-dependent. The modular combination of mutants in flavonoid biosynthesis or glycosylation and their flavonol glycoside profiles identified kaempferol 3-*O*-rhamnoside-7-*O*-rhamnoside (k1) as the *ugt78d2* phenotype-inducing metabolite. Flavonoids and in particular flavonols have been postulated to modulate auxin transport. However, the active flavonoids involved in this process have not yet been identified in plants. Basipetal auxin transport was reduced in the k1-overaccumulating *ugt78d2* mutant. Preliminary data showed that auxin transport was reverted close to wild-type level in an *ugt78d2* mutant complemented line. The

expression of *UGT78D1*, which is required for the synthesis of k1, was detected in all the tissues examined, but particularly high in the tissues where the modulation of auxin transport by flavonoids occurs. These results suggest that k1 is an endogenous auxin transport inhibitor.

Curriculum Vitae

Name: Ruohe Yin
Date of birth: Sep. 01, 1977
Place of birth: Anhui, P.R. China
Nationality: P.R. China
Gender: Male
Marital status: Married

Education

1996.9 - 2004.7 Study of Biology (Bachelor and Master) at the Huazhong Agricultural University, China. Advisor: Prof. Dr. Zhibiao Ye

2006.3 - 2007.5 Study of Plant Biochemistry at the Technische Universität München, Germany. Advisor: PD Dr. Erich Glawischnig

2007.6 – 2010.12 PhD study of Biochemistry at the Ludwig-Maximilians-Universität München, Germany. Advisor: PD Dr. Anton R. Schäffner

Publications

1. **Ruohe Yin, Monika Frey, Alfons Gierl and Erich Glawischnig** (2010) Plants contain two distinct classes of functional tryptophan synthase beta proteins. *Phytochemistry*, **71**, 1667-1672.

2. **Ruohe Yin, Burkhard Meßner, Thomas Hoffmann, Wilfried Schwab, Theresa Faus-Kessler, Veronica von Saint Paul, Werner Heller and Anton R. Schäffner**: Feedback inhibition of phenylpropanoid and flavonol-biosynthetic pathways upon a compromised flavonol-3-*O*-glycosylation. (*J. Biol. Chem.* in revision)

3. **Ruohe Yin, Kerstin Schuster, Petr I. Dobrev, Eva Zažímalová, Werner Heller and Anton R. Schäffner**: The over-accumulation of kaempferol 3-*O*-rhamnoside-7-*O*-rhamnoside in the *ugt78d2* mutant results in decreased basipetal auxin transport and plant growth defects. (Manuscript in preparation).

4. **Burkhard Meßner, Ruohe Yin and Anton R. Schäffner**: *Arabidopsis* UGT74F1 and UGT74F2 do conjugate salicylic acid *in planta*, but are not responsible for stress-related salicylic acid glucosylation. (Manuscript in preparation).

1 Chapter 1: General Introduction

1.1 Glycosyltransferase

Glycosyltransferases exist in all living organisms; they transfer a glycosyl moiety from an activated donor to an acceptor molecule. The glycosylation reaction is illustrated in Figure 1. 1. Glycosylation is an important mechanism for regulating the bioactivity, metabolism and localization of small molecules in living cells. In plants, a large multigene family of glycosyltransferases is involved in these processes, i.e. glycosylating secondary metabolites, phytohormones, and environmental toxins. The transfer of a sugar to an aglycone changes its chemical properties and bioactivities. A consensus amino acid sequence has been identified in the carboxyl terminus of many of these glycosyltransferases, leading to the classification of a single UDP-glycosyltransferase (UGT) superfamily (Li *et al.,* 2001). The nomenclature system of the UGT superfamily is based primarily on amino acid sequence identity and is summarized in Figure 1. 2.

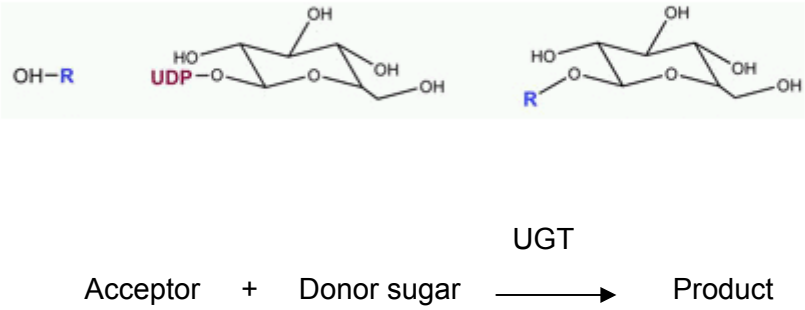

Figure 1. 1 Illustration of the glycosylation reaction.

About 120 putative *UGT* genes were identified based on the presence of the consensus amino acid sequence and therefore were classified as family 1 glycosyltransferase in *Arabidopsis* (Li *et al.,* 2001; Ross *et al*., 2001; von Saint-Paul *et al.*, unpublished data). A comprehensive phylogenetic analysis to all the discovered *Arabidopsis UGT* genes revealed that the superfamily is likely to contain 14 distinct phylogenetic clusters (Li *et al.,* 2001). The level of amino acid sequence similarity between these *UGT* genes varies from above 95% to lower than 30% identity. After the discovery of the large number of *UGT* genes the analysis of their functions in plants is becoming a challenging task.

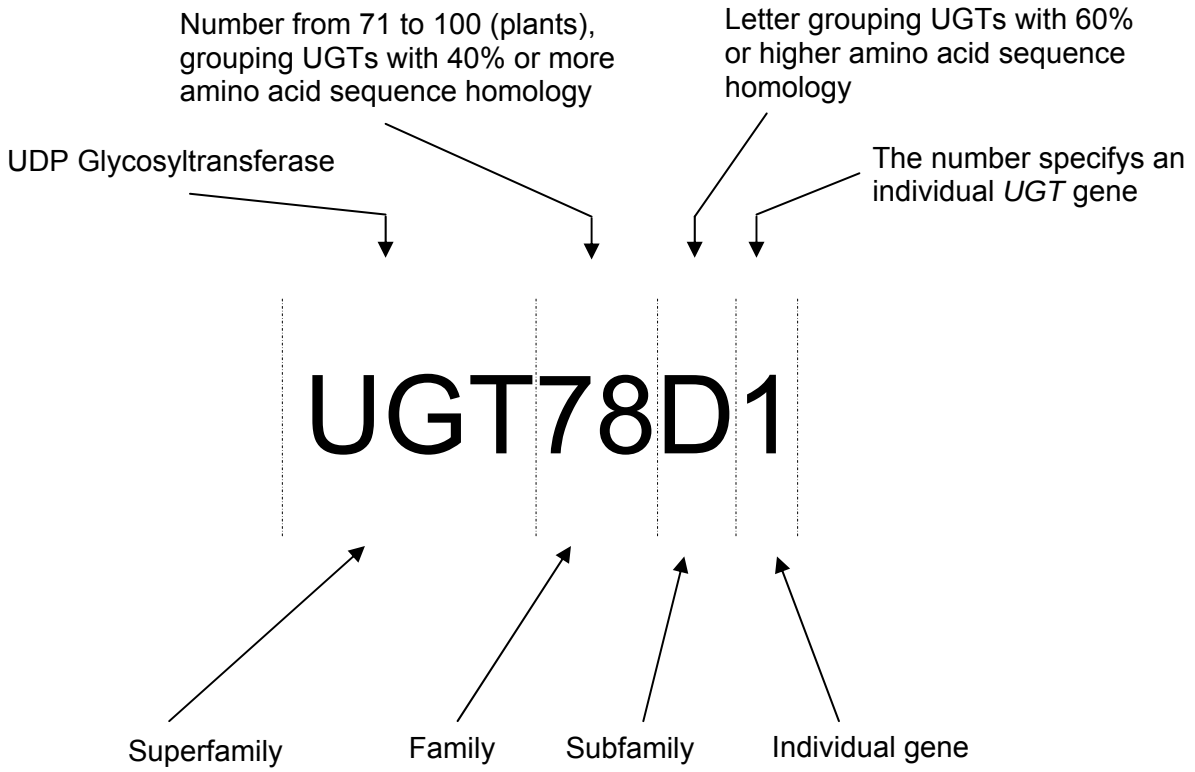

Figure 1. 2 Nomenclature system of the UGT superfamily (modified from Ross *et al.,* 2001).

1.2 Flavonoid biosynthesis in *Arabidopsis*

Three subclasses of flavonoids are present in *Arabidopsis*, including flavonols, anthocyanins and proanthocyanidins. In this thesis, I particularly studied flavonols. The structures of major flavonol glycosides in *Arabidopsis* are illustrated in Figure 1. 3.

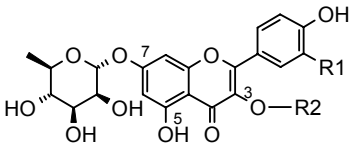

Figure 1. 3 Major flavonol glycosides in *Arabidopsis* (accession Columbia). R1 = H (kaempferol), = OH (quercetin). R2 = glucose (flavonol-3-*O*-glucoside-7-*O*-rhamnoside), = rhamnose (flavonol-3-*O*-rhamnoside-7-*O*-rhamnoside), or = rhamnose (1->2)-glucose (flavonol-3-*O*-[rhamnosyl (1->2 glucoside]-7-*O*-rhamnoside).

The *Arabidopsis* flavonoid biosynthesis pathway, as illustrated in Figure 1. 4, is one of the most well-studied secondary metabolic pathways. In *Arabidopsis*, flavonoids are synthesized

by a branched pathway that yields both colourless compounds (flavonols) and coloured pigments (anthocyanins and proanthocyanidins). Phenylalanine ammonia-lyase (PAL) commits the flux of primary metabolism into the phenylpropanoid pathway, which mainly leads to the formation of lignin, sinapate esters and flavonoids. There are four *PAL* genes in the *Arabidopsis* genome (*PAL1-4)*. However, only *PAL1* and *PAL2* have been shown to be involved in flavonoid biosynthesis (Lillo *et al.,* 2008).

Chalcone synthase (CHS) is at the entry point of the flavonoid pathway and it produces an intermediate used in the synthesis of all flavonoids. The *Arabidopsis* plants carrying a mutation of *CHS* accumulate no flavonoids (Burbulis *et al.,* 1996). Chalcone isomerase (CHI) catalyzes the isomerisation of naringenin chalcone to the flavanone naringenin. Naringenin is then hydroxylated to form dihydrokaempferol by flavanone 3-hydroxylase (F3H). From dihydrokaempferol or dihydroquercetin, flavonols are synthesized by flavonol synthase (FLS) and anthocyanins are synthesized by dihydroflavonol 4-reductase (DFR). Except for FLS, the enzymes of the central flavonoid pathway, including CHS, CHI, F3H, F3'H, DFR, ANS and anthocyanidin reductase, are encoded by single genes. Six homologues have been identified to encode FLS, however, in the *Arabidopsis* genome (Owens *et al.,* 2008). It was proposed that among the six FLS homologues only AtFLS1 contributes to flavonol synthesis in *Arabidopsis*. However, FLS3 was recently shown to be a second functional flavonol synthase (Preuss *et al.,* 2009). Apart from the FLS genes, leucoanthocyanidin dioxygenase (LDOX) was also shown to have FLS function (Prescott *et al.,* 2002; Turnbull *et al.,* 2004). The FLS activity of LDOX and FLS3 may be relevant only in the *fls1* mutant background (Preuss *et al.,* 2009).

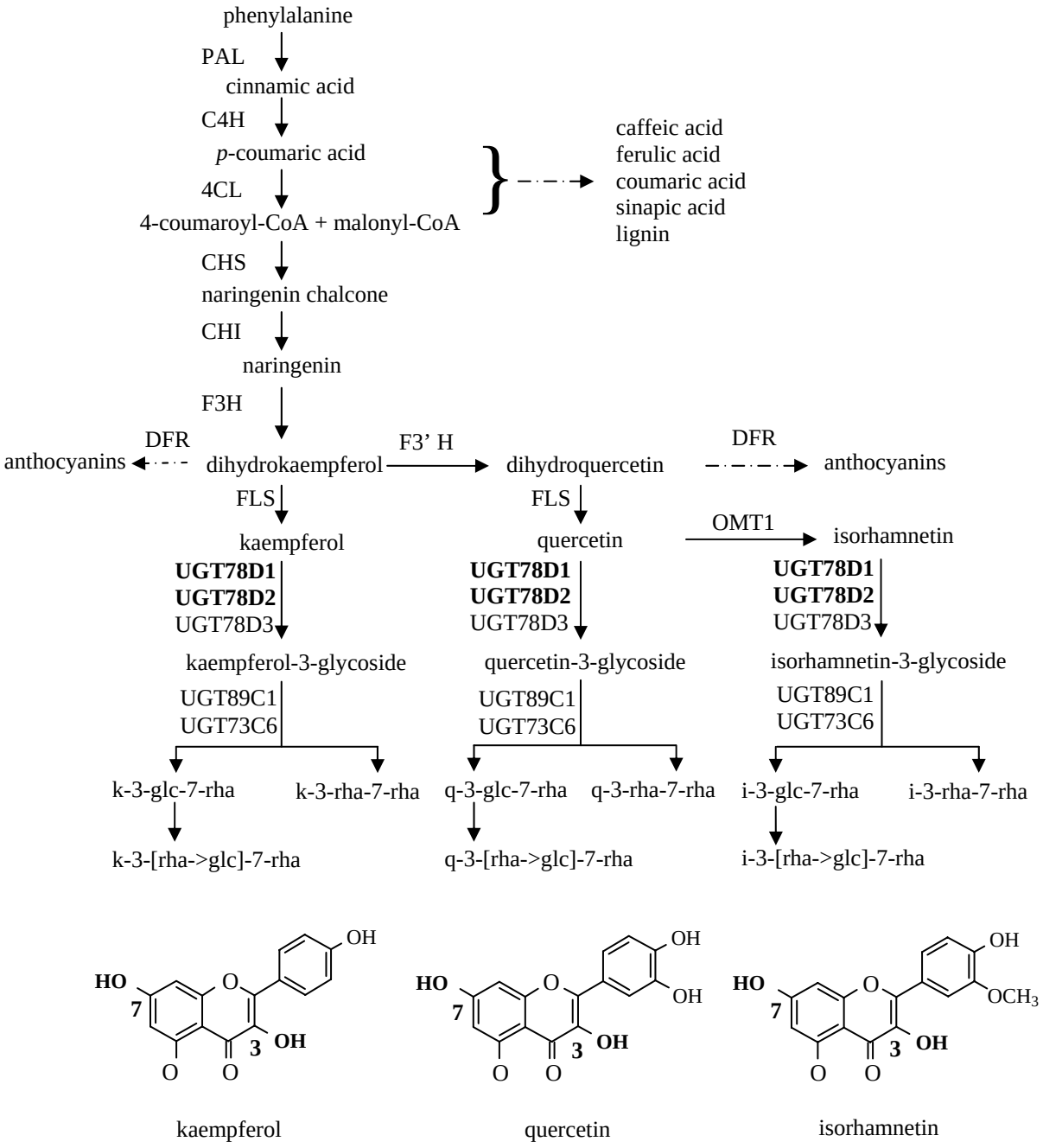

Figure 1. 4 Phenylpropanoid and flavonoid biosynthesis pathways in *Arabidopsis*.

The pathways leading from the central precursor phenylalanine to flavonols and anthocyanins as well as other phenylpropanoids like sinapic acid derivatives and lignin are displayed (Winkel-Shirley, 2006; Yonekura-Sakakibara *et al.,* 2008). Phenylalanine ammonia lyase (PAL), cinnamate 4-hydroxylase (C4H), 4-coumarate-CoA ligase (4CL), chalcone synthase (CHS), chalcone isomerase (CHI), flavanone 3-hydroxylase (F3H), flavonoid 3'-hydroxylase (F3'H), flavonol synthase (FLS), *O*-methyltransferase (OMT1), dihydroflavonol 4-reductase (DFR), flavonol 3-*O*-rhamnosyltransferase (UGT78D1), flavonoid 3-*O*-glucosyltransferase (UGT78D2), flavonol 3-*O*-arabinosyltransferase (UGT78D3), flavonol 7-

O-rhamnosyltransferase (UGT89C1), flavonol 7-*O*-glucosyltransferase (UGT73C6). Abbreviations: k-3-glc-7-rha, kaempferol 3-*O*-glucoside-7-*O*-rhamnoside; k-3-rha-7-rha, kaempferol 3-*O*-rhamnoside-7-*O*-rhamnoside; k-3-[rha->glc]-7-rha, kaempferol-3-*O*-[rhamnosyl (1->2 glucoside)]-7-*O*-rhamnoside. The structurally equivalent quercetin (q) and isorhamnetin (i) glycosides are abbreviated in a similar way as for kaempferol glycosides. The chemical structures of the three flavonol aglycones are given below the pathway. The bold printing highlights the 3-OH and 7-OH positions, which are targets for the indicated glycosylations.

1.3 Flavonoid glycosyltransferases in *Arabidopsis*

Most flavonoid end products exhibit complex glycosylation patterns in *Arabidopsis*. Recently, much progress has been made toward the elucidation of flavonoid glycosylation in *Arabidopsis*. First, UGT78D1 and UGT73C6 were characterized as the flavonol 3-*O*-rhamnosyltransferase and flavonol 7-*O*-glucosyltransferase, respectively (Jones *et al.,* 2003). UGT78D2 and UGT75C1 were identified as the flavonoid 3-*O*-glucosyltransferase and anthocyanin 5-*O*-glucosyltransferase, respectively (Tohge *et al.,* 2005). UGT89C1 was characterized as the flavonol 7-*O*-rhanosyltransferase. Recently, UGT78D3 was identified as the flavonol 3-*O*-arabinosyltransferase. Integration of transcriptome co-expression analysis with a reverse genetic approach has been shown to be a powerful tool to identify UGT genes involved in flavonoid glycosylation (Tohge *et al.,* 2005; Yonekura-Sakakibara *et al.,* 2007). Obviously, there have to be yet-to-identify genes involved in flavonoid glycosylation because (1) genes involved in 3-*O*-secondary glycosylation are still not identified; (2) the *ugt78d2* mutant still accumulates significant amount of flavonol 3-*O*-glucoside derivatives, suggesting the presence of an unknown flavonol 3-*O*-glucosyltransferase.

Recently, Saito and colleagues (2008) carried out a comprehensive study on the distribution of flavonol glycosides in different organs of *Arabidopsis* plants, revealing that flavonol glycosides are distributed in an organ-dependent manner. For example, kaempferol 3-*O*-rhamnoside-7-*O*-rhamnoside, one of the three abundant flavonol glycosides in leaves and flowers, is present only at a very low level in roots. I reasoned that the flavonol UGT might also have an organ specific expression to generate the organ dependent accumulation of flavonol glycosides. Flavonols are mainly glycosylated at 3-OH and 7-OH positions. Based on the combination of flavonol glycoside profiling of the above mentioned five UGT mutants and the *in vitro* substrate preference of recombinant UGT proteins, the 3-*O*-glycosylation is considered to be the first step of flavonol glycosylation, followed by 7-*O*-glycosylation, then further followed by secondary glycosylation at 3-*O* position in *Arabidopsis* (Jones *et al*., 2003; Yonekura-Sakakibara *et al.,* 2008). UGT78D1, UGT78D2 and UGT78D3, are highly

homologous. Interestingly, these three UGT78D isoforms share the same aglycone substrates, but their specificity for donor sugars was different, with UGT78D1 using UDP-Rha and UGT78D2 using UDP-Glc and UGT78D3 using UDP-Arabinose. It is very intriguing that such a specificity and complexity in glycosylation patterns exist. Presumably nature won't produce complex patterns if simple ones sufficed. Therefore there should be some distinct biological functions associated with these *UGT* genes.

1.4 Transcriptional regulation of flavonol biosynthesis

Flavonol biosynthesis is tissue specific and developmentally regulated. Among several proposed mechanisms, transcriptional regulation is the best studied one. AtMYB11, AtMYB12 and AtMYB111 have been identified as the regulators of flavonol biosynthesis in *Arabidopsis* (Mehrtens *et al.,* 2005; Stracke *et al.,* 2007). These three regulators show a high degree of functional similarity and display very similar target gene specificity for several genes of the flavonoid pathway, including *CHS*, *CHI*, *F3H* and *FLS1* (Stracke *et al*., 2007). AtMYB11, AtMYB12 and AtMYB111 have different spatial activity. AtMYB12, for instance, regulates flavonol formation mainly in roots, whereas AtMYB111 functions primarily in cotyledons. No flavonols are formed in the *myb11 myb12 myb111* triple mutant seedling, while the accumulation of anthocyanins is not affected (Stracke *et al*., 2007). Two *UGT* genes, *UGT84A1* and *UGT91A1*, were identified as the target genes of the MYB transcription factors, and the expression domains of the different MYB transcription factors correlated with the accumulation of distinct flavonol glycosides in seedlings. Thus, these MYB genes were referred to as *PFG1-3* for '*PRODUCTION OF FLAVONOL GLYCOSIDES*' by Stracke and colleagues (Stracke *et al*., 2007).

1.5 Enzyme complexes in the phenylpropanoid and flavonoid pathway

Transcriptional regulation plays an important role in regulating the overall activity of flavonoid metabolism. This level of regulation might be not sufficient to control the flux subcellularly. To regulate the flavonols at the subcellular level, the flavonoid biosynthetic enzymes are thought to be organized as multi-enzyme complexes and the substrates are channelled among the complexes (Winkel-Shirley 1999). Several studies (see below) have suggested the existence of a flavonoid enzyme complex.

The existence of a flavonoid enzyme complex was first proposed early in 1974 (Stafford 1974). Fritsch and Grisebach (1975) suggested that flavonoid biosynthesis takes place partly or completely on membranes. Substrate channelling, size-exclusion chromatography, and cell fractionation were employed to suggest that PAL, cinnamate-4-hydroxylase (C4H), CHS,

and a UGT function as part of one or more membrane-associated enzyme complexes in amaryllis, buckwheat, and red cabbage (Hrazdina and Wagner 1985). Immunocytochemical studies indicated that CHS was located at the cytoplasmic face of the rough endoplasmic reticulum (Hrazdina *et al.,* 1987). Integration of these results led to a model in which flavonoid pathways are organized as a linear array of enzymes loosely associated with the endoplasmic reticulum and anchored via C4H and F3'H (Hrazdina and Wagner 1985). Burbulis and Winkel-Shirley (1999) provided evidence for specific protein-protein interactions among four enzymes of flavonoid biosynthesis in *Arabidopsis*, including CHS, CHI, F3H and DFR. Recently, FLS1, -3 and -5 were shown to interact with CHS, F3H and DFR using the yeast two-hybrid assay (Owens *et al*., 2008). Despite the convincing evidence listed here, the exact organization of the protein complex is still not known largely due to the inability to isolate the protein complex from plants.

1.6 The influence of flavonoids on plant growth and development

Flavonoids are usually not essential for *Arabidopsis* plant growth and development as suggested by the normal development of flavonoid-less mutant, such as *chs.* However, there are some examples that flavonoids have diverse roles in the regulation of many aspects of plant development (see below). It was shown that one flavonol glycoside, kaempferol 3-*O*-2^{G}-glycosyl-gentiobioside (K9), has an important role on leaf development in soybean (Buttery and Buzzell 1987). The K9 was correlated with reduction in leaf mass, chlorophyll content, rate of photosynthesis and stomata density (Buttery and Buzzell 1987). The leaf traits were restored to normal by blocking the formation of K9 (Buttery and Buzzell 1987). Flavonoids were shown to be required for pollen fertility in petunia. Chemical complementation of the infertile, flavonoid-less, petunia pollen using kaempferol aglycone could restore fertility (Mo *et al.,* 1992). Flavonoids also appear to be required for proper pollen development in *Arabidopsis* (Preston *et al.,* 2004). Flavonoids are involved in seed dormancy or viability (Debeaujon *et al.,* 2003). Most *transparent testa* mutants showed reduced seed dormancy, as evidenced by a high germination rate and a lower requirement for after-ripening (Debeaujon *et al.,* 2000). Expression of transcription factors regulating flavonoid biosynthetic genes during early embryogenesis suggested the functions of flavonoid in development (Hennig *et al.,* 2004). Interestingly, during the converting from flowering stage I to stage II and stage III, the flavonol branch is predominantly down-regulated, the anthocyanin branch is transiently induced, and the proanthocyanin branch is continuously activated, suggesting that different subclasses of flavonoids have different functions (Henning *et al*., 2004). Recently, it was shown that the changes in the flavonol glycosylation pattern i.e., strong increases of kaempferol 3-*O*-monoglucoside, in *rol1-2* (*ROL1* encodes RHM1, one of the three rhamnose synthase proteins, that convert UDP-D-glucose to UDP-L-rhamnose in *Arabidopsis*),

correlate with, and therefore may be responsible for the observed aberrant growth phenotypes of the mutant (Ringli *et al.,* 2008). It appears that the function of flavonoids in regulating plant growth and development is plant species-specific.

1.7 Flavonoids and auxin transport

Flavonoids have been shown to modulate transport of the phytohormone, indole-3-acetic acid (IAA) (Murphy *et al.,* 2000; Brown *et al.,* 2001; Buer and Muday, 2004; Peer *et al.,* 2004). Flavonol aglycones including quercetin and kaempferol were shown to be able to displace the auxin efflux inhibitor 1-naphthylphthalamic acid (NPA) from zucchini (*Cucurbita pepo*) hypocotyl microsomes (Jacobs and Rubery, 1988). Evidence for the regulation of auxin transport by flavonoids is accumulating by analyzing the auxin transport in *Arabidopsis* flavonoid biosynthetic mutants: *tt4* (lacking flavonoids); *tt7* (accumulating excess kaempferol); and *tt3* (accumulating kampferol and quercetin) (Winkel-Shirley *et al.,* 1995; Peer *et al*., 2004). The auxin transport was found to be elevated in *tt4* compared with the wild-type, while the flavonol-overproducing mutant *tt3* exhibited reduced auxin transport, consistent with an inhibitory role of flavonols for auxin transport (Murphy *et al*., 2000; Peer *et al*., 2004). These experiments have laid a solid foundation for the concept that flavonoids are the endogenous auxin transport modulators. However, the effective flavonoids in modulating auxin transport *in planta* are still unknown.

In situ flavonoid localization study using diphenylboric acid 2-aminoethyl ester (DPBA), which conjugates flavonoids, revealed that flavonoids accumulate at the regions where auxin is abundant, including shoot apex, cotyledon apex, shoot-root junction site and root tip. This co-localization offers another line of evidence for the modulation of auxin transport by flavonoids *in vivo*. A few studies claimed that flavonoid aglycones, not flavonoid glycosides, modulate auxin transport *in vivo* (Peer *et al.,* 2001). This conclusion is questionable, because flavonol aglycones have never been detected with various sensitive approaches, including LC-MS, CID-MS/MS and CapLC-ESI-QqTOF-MS from *Arabidopsis* wild-type or several *tt* mutant plants (von Roepenack-Lahaye *et al.,* 2004; Böttcher *et al.,* 2008; Yonekura-Sakakibara *et al.,* 2008). DPBA staining cannot differentiate flavonol aglycones from glycosides. Flavonol glycosides are the predominant forms of flavonols in plants. Therefore, the co-localization of flavonoids with auxin as concluded from DPBA staining probably reflected the co-localization of auxin with flavonoid glycosides, rather than the aglycones. The *in vitro* studies have shown that some flavonol glycosides are inactive in regulating auxin transport (Jacobs and Rubery, 1988). However, the authors used only ‘rare’ flavonoid glycosides, which are present at low levels, or even not detectable in *Arabidopsis* (Jacobs and Rubery, 1988). The most abundant flavonol glycosides *in planta*, including kaempferol 3-*O*-rhamnoside-7-*O*-rhamnoside and

quercetin 3-*O*-rhamnoside-7-*O*-rhamnoside, were not tested. In conclusion, the previous studies cannot rule out the possibility that flavonoid glycosides act as the endogenous auxin transport regulators.

Flavonoids are normally glycosylated in cells. But the complex glycosylation patterns make it difficult to study the role of a specific flavonoid glycoside in regulating auxin transport. However, the high specificity of the well characterized flavonoid UGT provides a possibility of using genetic approaches to study the consequences of a specific flavonol glycoside compostion. For example, the kaempferol 3-*O*-rhamnoside-7-*O*-rhamnoside is absent in *ugt78d1* knockout mutant, thus *ugt78d1* could be a suitable material to study the function of this metabolite. Moreover, combination of different glycosylation mutants or combination of a glycosylation mutant with a central biosynthetic mutant, such as *tt7*, can manipulate the flavonoid glycoside profiles and allow studying the function of specific flavonoid glycosides in plants.

1.8 Aims of the thesis

Previous work has characterized UGT78D1 and UGT78D2 as the major flavonol 3-*O*-rhamnosyltransferase and flavonoid 3-*O*-glucosyltransferase, respectively. Flavonol aglycones are potentially phytotoxic and the elimination of possible accumulation of flavonol aglycones is carried out by efficient 3-*O*-glycosylation.

1) The first part of this thesis addressed the question how the plants can cope with the severe loss of flavonol 3-*O*-glycosylation activity (i.e. most flavonol aglycones cannot be glycosylated).

Flavonoids particular flavonols were postulated to be endogenous polar auxin transport inhibitors. However, the specific effective flavonols have not been identified in this process.

2) The second part of the thesis aimed at identifying a specific flavonol glycoside functioning as an *Arabidopsis* plant growth regulator through the inhibition of auxin transport.

Previously, recombinant UGT74F1 and UGT74F2 were shown to glucosylate salicylic acid (SA) *in vitro* (Lim *et al.,* 2002). In our laboratory, Meßner *et al*. (unpublished data) showed that single mutants of either gene maintained wild-type levels of both free SA and SA glucosides.

3) The third part of the thesis attempted to generate *ugt74f1 ugt74f2* double mutants using the artificial microRNA-mediated gene silencing approach. SA and its glycosides were determined in the resultant double mutant plants.

2 Chapter 2: Materials and Methods

2.1 Materials

2.1.1 Plant material

Arabidopsis wild-type plants used in this thesis were of Columbia (Col-0) and Nossen (Nö-0) ecotypes. T-DNA inserted mutant lines are of Columbia background except for *fls1*, which is of Nossen background. The single mutants, including *ugt78d1*, *ugt78d2*, *ugt73c6*, *ugt89c1*, *tt4, tt7* and *tt18* mutants are described elsewhere and listed in Table 2. 1 (Jones *et al.,* 2003; Buer and Muday 2004; Tohge *et al.,* 2005; Yonekura-Sakakibara *et al.,* 2007; Stracke *et al.,* 2009).The double mutants, including *ugt78d1 ugt78d2*, *ugt89c1 ugt73c6, tt4 ugt78d2*, *ugt78d2 ugt73c6*, *tt7 ugt78d2*, *ugt89c1 ugt78d2*, and the *tt4 ugt78d1 ugt78d2* triple mutant were generated by genetic crossing and confirmed by PCR-based genotyping. The mutants mentioned above were all generated in this study except for *ugt78d1 ugt78d2*, which had been generated previously by Burkhard Meßner. Transgenic plants harboring promoter:*GUS-GFP* constructs with the promoter of *UGT78D1* and *UGT78D2* had been generated previously by Burkhard Meßner. I selected individual lines for this thesis.

AGI code	Mutant name	Line	Ecotype	Reference
At1g30530	*ugt78d1*	SAIL_568_F08	Col-0	Jones *et al.,* 2003
At5g17050	*ugt78d2*	SALK_049338	Col-0	Tohge *et al*., 2005
At2g36790	*ugt73c6*	SAIL_525_H07	Col-0	Jones *et al.,* 2003
At1g06000	*ugt89c1*	SALK_071113	Col-0	Yonekura *et al.,* 2007
At5g13930	*tt4*	SALK_020583	Col-0	Alonso *et al.,* 2003
At5g07990	*tt7*	GK_349F05	Col-0	Rosso *et al.,* 2003
At5g08640	*fls1*	RIKEN_PST16145	Nö-0	Stracke *et al.,* 2009
At4g22880	*tt18*	SALK_028793	Col-0	Stracke *et al.,* 2009

Table 2. 1 *Arabidopsis* single mutants used in this work.

2.1.2 Buffers and media

Typical solutions, buffers and media were prepared according to common protocols used in molecular biology. The preparation of special media and solutions is described in the corresponding methods.

2.1.3 Vectors

The vectors used in the thesis are listed below.

Name	Application	Reference or resource
pDONR221	Cloning	(Invitrogen, Germany)
pDEST15	Protein expression	(Invitrogen, Germany)
PGEM-T easy	Cloning	(Promega, Germany)
pBGW	Complementation	(Karimi *et al*., 2002)
pKGW	Complementation	(Karimi *et al*., 2002)
pRS300	Cloning (amiRNA)	(Ossowski *et al*., 2008)
pET-32a(+)	Protein expression	(Novagen, Germany)
pAlligator2	Protein expression	(Bensmihen *et al*., 2004)
pBGWFS7	Protein expression	(Karimi *et al*., 2002)

Table 2. 2 Vectors used in this work.

2.1.4 Restriction endonucleases and DNA modifying enzymes

The restriction enzymes were purchased from New England Biolabs (Frankfurt, Germany) and MBI Fermentas Life Sciences (St. Leon-Rot, Germany). DNA modifying enzymes, e.g. *Taq* DNA polymerase, iproof™ high fidelity DNA polymerase, T4-DNA-ligase, DNase, RNase A and H, Reverse transcriptase Superscript II were obtained from Amersham Gibco-BRL, MBI Fermentas, Pharmacia, Promeg, Q-Biogene, Stratagene, Roche and Sigma.

2.1.5 Oligonucleotides and sequencing

Primers were generated by using Primer 3 (http://frodo.wi.mit.edu/cgi-bin/primer3/primer3_www.cgi) and Primer Express 2.0 (for RT-qPCR). Oligonucleotides were obtained from Thermo Electron (Ulm, Germany). Nucleotide sequencing was done by Eurofins (mwg/operon, Germany).

2.2 Methods

2.2.1 Plant growth conditions

Arabidopsis plants were grown at 22-23°C under 100-200 µmol m^{-2} s^{-1} with a 16/8 hr long day photoperiod. For GUS reporter analyses, plants were cultured on ½ MS medium containing 1.5% sucrose and 0.6% phyto-agar. For *tt4 ugt78d1 ugt78d2* triple mutant naringenin feeding experiment, seeds were surface sterilized and planted on ½ MS medium (same composition as above) and seedlings were allowed to grow for 12 days under a 11.5/12.5 hr photoperiod. Then seedlings were transferred to water containing 3% Sucrose and 100 µM naringenin (100 mM naringenin stock was dissolved in ethanol). After growing

for 45 hr under continuous light on a rotary shaker at 110 rpm, the whole rosettes were washed with water and harvested for further analyses.

2.2.2 Seed surface sterilization

For *in vitro* culture, *Arabidopsis* seeds were surface-sterilized under a sterile hood with 80% (v/v) ethanol. About 100 *Arabidopsis* seeds together with two pieces of toothpicks were placed on the top of two layers of filter paper (Roth, Karlsruhe, Germany). 80% ethanol was sprayed onto the seeds until the filter papers were totally wet. Seeds were left under the sterile hood for about 5 to 10 min to dry. The dry seeds were then transferred to Agar plates for *in vitro* culture.

2.2.3 Bacterial strains

The *E. coli* DH5α was used for standard cloning. The *Agrobacterium tumefaciens* strain GV3101 (pMP90) was used for plant transformation.

2.2.4 Preparation of *E. coli* competent cells

A single colony of *E. coli* DH5α or *E. coli* DB3.1 was inoculated into 5 ml of Lysogeny broth (LB) medium and cultivated at 37°C overnight with moderate shaking. 100 ml LB medium was inoculated with the 5 ml overnight culture. The cells were grown to an OD_{600} of ~0.5, and were then collected by centrifugation at 4°C and at 5,000 rpm for 5 min. The pellet was suspended and incubated in 100 ml ice-cold TFB1 (30 mM potassium acetate, 100 mM RbCl, 10 mM $CaCl_2$, 50 mM $MnCl_2$, 15% glycerol, pH 5.8 with acetic acid) for 5 min on ice. The cells were pelleted by centrifugation at 4°C at 5,000 rpm for 5 min. The pellet was re-suspended gently in 10 ml cold TFB2 (10 mM MOPS, 10 mM MOPS, 75 mM $CaCl_2$, 10 mM RbCl, 15% glycerol, pH 5.8 with acetic acid) and incubated on ice for 15-60 min. Aliquots of 60 µl were snap-frozen in liquid nitrogen, then stored at -80°C. Both solutions, TFB1 and TFB 2, were filter-sterilized (0.45 µm filter Millipore, Germany).

2.2.5 *E. coli* transformation by heat shock

An aliquot of competent *E. coli* cells (DH5α or BL21 or DB3.1) was thawed on ice. 5-10 µL of template DNA (ligation assay, Plasmid DNA 80-200ng) was added, mixed and incubated on ice for 10 min. The mixture in an Eppendorf tube was then incubated in a 42°C water bath for 45 sec and then immediately cooled on ice for 2 min. 900 µl of LB medium was added and the sample was incubated for 30-60 min at 37°C with gentle agitation. 25-150 µl of the transformed bacterial suspensions were plated on agar plate with the addition of the appropriate antibiotic.

2.2.6 *Agrobacterium* transformation by electroporation

An aliquot of competent *E. coli* cells (DH5α or BL21) was thawed on ice. Less than 1 µl of plasmid DNA (less than 50 ng) was added and incubated for 2 min on ice. The sample was then transferred to a prechilled 0.2 cm electroporation cuvette. Electroporation was carried out with the BioRad Gene-Pulser using the following conditions: resistance 400Ω, capacitance: 25 µF and voltage: 2.5 kV. After an electroporation, 1.2 ml of SOC medium was immediately added into the cuvette and the bacterial suspension was transferred to a 1.5 ml eppendorf tube. The culture was incubated for 2 hr at 28°C with gentle agitation. A 50 µl aliquot of the culture was plated on LB agar plate containing appropriate antibiotics. Plates were incubated at 28°C for 2-3 days.

2.2.7 *Arabidopsis* Transformation by floral dip

A 5 ml of preculture, inoculated from fresh single colony of *Agrobacterium*, containing an appropriate binary vector, were incubated at 28°C with appropriate antibiotics for 1 day with vigorous agitation. 250 ml of LB medium was inoculated with 1 ml of the preculture and incubated further under conditions as above for 24 h. The cells were collected by centrifugation at RT, at 5,500 rpm for 20 min. The pellet was resuspended in 5% (w/v) sucrose solution to a final OD_{600} of approximately 0.8. Silwet L-77 was added to the suspension to a final concentration of 0.05%. Inflorescence shoots from 8-10 *Arabidopsis* plants, fertilized one week ago, were dipped into the suspension and soaked for 45 sec. Dipped plants were then covered with a transparent plastic bag to maintain the humidity and kept in a low light intensity location for 24 hr. The plastic cover was then removed and the plants were moved to normal growth conditions. After about 4 weeks the seeds were harvested when the siliques were brown and dry.

2.2.8 Selection of transformed *Arabidopsis* plants

Selection was carried out either by antibiotic resistance or visible markers using seed coat specifically expressed GFP (pAlligator2 vector).

2.2.9 Histochemical GUS assay

Genomic fragments upstream of the start codon of both *UGT78D* isoforms (1469bp for *UGT78D1* or 1481bp for *UGT78D2*) were amplified from Col-0 genomic DNA by PCR and introduced into the vector pBGWFS7 (Karimi *et al*., 2002), forming $UGT78D_{pro}$*:GUS-GFP* fusions were transformed into Col-0 *Arabidopsis* plants. Histochemical analysis of the GUS reporter gene was performed as described before (Deruere *et al.,* 1999) at different developmental stages.

2.2.10 Preparation of plant genomic DNA

To facilitate quick and efficient PCR-based genotyping, an Extract-N-Amp™ plant PCR kit was used according to the manufacturers protocol (Sigma). The normal CTAB DNA isolation approach is as following: Plant material (young leaf piece about 0.5 cm^2) was squeezed with small pistil in an Eppendorf tube with 250 µl extraction buffer (1.4 M NaCl, 100 mM Tris-HCl (pH 8.0), 2% (w/v) CTAB, 20 mM EDTA (pH 8.0), 1% (w/v) polyvinylpyrrolidone, Mr 40,000 (Sigma PVP-40 or P-0930)). The tube was vortexed briefly and incubated at 65°C for 10 min. 200 µl of chloroform-isoamyl alcohol (24:1) was added and centrifuged at 1, 4000 rpm at room temperature for 2 min. The upper aqueous phase was transferred to a new Eppendorf tube containing 1 µl of 1% linear polyacrylamide. For DNA precipitation, 3 volumes of Ethanol p.a were added, mixed and left at -20°C for 30 min. This step was followed by a centrifugation at 4°C with 14000 rpm for 15 min. The DNA pellet was then washed once with 70% Ethanol p.a., centrifuged at full speed for 10 min at 4°C. The pellet was allowed to dry on the bench and dissolved in 100 µl TE buffer. For PCR amplification 1-2 µl were used.

2.2.11 Preparation of plasmid DNA

Plasmid DNA from *E. coli* and *Agrobacterium tumefaciens* was prepared with Qiaprep® Spin Miniprep Kit (Qiagen, Hilden, Germany), according to the manufacturer's instructions.

2.2.12 Isolation of total RNA for RT-PCR

The RNA isolation protocol from Chang *et al*. (1993) was modified and used in this study. About 100 mg plant material were ground to a very fine powder with a cold mortar and pestle and transferred to a 2 ml Eppendorf tube. 500 ml of pre-warmed (65°C) extraction buffer (2% CTAB, 2% PVP K30, 100 mM Tris/HCl pH 8.0, 25 mM EDTA, 2 M NaCl, 0,5 g/l Spermidine, 2% 2-Mercaptoethanol) were then added. Samples were vortexed thoroughly and total RNA was extracted by addition of 500 µl chloroform/isoamylalcohol (24:1) followed by centrifugation at 10,000 rpm at 4°C for 5 min. This step was repeated once to increase the purity of the RNA sample. The supernatant was then transferred to an new Eppendorf tube and total RNA was precipitated overnight at 4°C by addition of 1/4 volume of 10 M Lithium chloride. Samples were then centrifuged at 14,000 rpm at 4°C for 20 min. 500 µl SSTE buffer (1 M NaCl, 0.5 % SDS, 10 mM Tris/HCl pH 8.0, 1 mM EDTA) was added to the pellet and incubated at RT for 1 h with agitation to suspend the pellet. After a new extraction with 500 µl chloroform/isoamylalcohol (24:1), the supernatant was transferred into a fresh Eppendorf tube and 1/10 Volume of 3 M Sodium-Acetate (NaOAc, pH 5.2) and 1 volume of isopropanol were added. After incubation for 20 min at -20°C samples were centrifuged at 14,000 rpm at 4°C for 20 min. The pellet was then washed with 75% ethanol p.a. and centrifuged as above. The pellet was then dried on the bench and resuspended with 500 µL of TM buffer (40 mM

Tris/HCl pH 7.5, 6 mM $MgCl_2$). Any traces of DNA were removed by addition of 1 µl DNase and incubation at 37°C for 15 min. RNA was then purified again with 500 µl chloroform/isoamylalcohol (24:1). Samples were centrifuged and RNA precipitated from the supernatant by addition of 1/10 volume 3 M Sodium Acetate (pH 5.2) and 2 volumes of absolute ethanol p.a. and incubation for 30 min at -20°C. After centrifugation and washing with 75% ethanol as mentioned above, the pellet was dried and resuspended in 20 µl DEPC-treated sterile water. Quality and concentration of RNA samples were than assessed by measuring the absorption at 260 nm in a spectrophotometer.

2.2.13 Determination of nucleic acid concentrations

The concentrations of DNA or RNA were determined by measuring the absorption at 260 nm and 280 nm, respectively. Double distilled water was used to zero the spectrophotometer (Nanodrop ND-1000, Kisker-biotech, Germany). The ratio of A260/A280 was used to estimate the purity of total DNA or RNA with respect to contaminants that absorb in the UV (e.g. proteins absorb at 280 nm). A ratio between 1.8 and 1.9 indicates high quality DNA; a ratio of 2.0 indicates high quality RNA.

2.2.14 Gel electrophoresis

Nucleic acids were subjected to electrophoresis using 0.8 to 2.5% Agorose gels containing 0.5 µg/ml ethidium bromide. Gels were cast and run in TAE buffer (40 mM Tris, 5 mM sodium acetate, 1 mM EDTA, adjusted to pH7.8 with glacial acetic acid). pUC 19 and λ /Hind III DNA ladders were routinely used as size markers. After electrophoresis DNA fragments were visualized under UV light and recorded with Bio-Rad Gel Doc 2000 (Bio-Rad, Munich, Germany).

2.2.15 Purification of PCR products

After PCR reactions DNA fragments were purified with Qiaquick® PCR Purification Kit (Qiagen, Hilden, Germany) following manufacturer's instructions.

2.2.16 DNA gel extraction

Gel pieces containing desired DNA fragments were excised from the agarose gel. DNA was then isolated using Qiaquick® Gel Extraction Kit (Qiagen, Hilden, Germany), according to the manufacturer's instructions.

2.2.17 Real-Time Quantitative RT-PCR

Rosette leaves of 21-DAG plants were collected. Total RNA was isolated with Trizol Reagent (Invitrogen) according to the manufacturer's instructions. The first-strand cDNAs were synthesized using a High-Capacity cDNA Reverse Transcription Kit (Applied Biosystems).

Data were collected with the 7500 real time PCR system (Applied Biosystems). In all experiments, three biological replicates of each sample and two technical (PCR) replicates were performed. The Ubiquitin 9 (At5g18380) and S16 (At4g20890) were used as reference genes. The stability of the reference genes was tested using geNorm (Vandesompele *et al.,* 2002). The gene expression was compared between genotypes by the paired t-test. The paired testing takes into account the dependency of the data produced by the experimental design. The paired t-test tests the mean difference of the log intensities against zero. In addition, t-test based 95%-confidence intervals were calculated for the mean difference of the log intensities which is identical to the log fold change. The results were back-transformed by taking the power to base 10 to obtain the fold change and a confidence interval for the fold change. For all calculations, the R software package was employed (R-Development-Core-Team 2009). The absolute expression levels of the *PAL* and *4CL* isoforms analyzed were different in Col-0 leaves. The C_t values of *PAL1*, *PAL2*, *PAL3*, *PAL4*, *4CL1*, *4CL2* and *4CL3* were about 25, 30, 34, 35, 32, 39 and 32 cycles, respectively, under our qRT-PCR conditions.

2.2.18 Molecular cloning using the Gateway technology

The Gateway technology was used for cloning all constructs except for the UGT74F2amiRNA-pAlligator2 construct in this work. The detailed cloning information is available in the corresponding section. Briefly, the cloning of the fragment of interest into the destination was achieved by two steps of site-specific recombination reactions, BP and LR reaction. The BP reaction is between an attB-flanked DNA fragment and an attP-containing donor vector and an entry clone is generated. Next, the LR reaction takes place between the entry clone and an attR-containing destination vector and the final vector used is generated.

2.2.19 Bioinformatics tool

Computer analyses of DNA and protein sequences were performed using Vector NTI (Invitrogen).

2.2.20 Construct for *ugt*78d1 mutant genetic complementation

A genomic fragment containing the coding region of *UGT*78D1 and its promoter region was first amplified from Col-0 plant genomic DNA with iproof™ high fidelity DNA polymerase using the primers: UGT78D1_F-1747 (5'-GGGATTGTTTCTGCTGTGGT-3') and UGT78D1_R-2143 (5'-TCTCTCTCTTTCCCCGTCAA-3'). The PCR product was Kit-purified and used as the template for the second round PCR amplification with primers (containing both GATEWAY BP recombination sequence and gene specific sequence): 78D1_CO_GW_R1900 (5'-GGGGACCACTTTGTACAAGAAAGCTGGGT

tgtcaaattccaattcttgct-3' and 78D1_Pro_GW_F-1460 (5'-ggggACAAGTTTGTACAA AAAAGCAGGCTgcagtttccgttgacaacaa-3'). The PCR product was cloned into pDONR221 (Karimi *et al*., 2002) via BP recombination (Gateway technology) and the desired sequence was confirmed by sequencing. The genomic fragment was further cloned into the vector pKGW (Karimi *et al*., 2002) via LR recombination (Gateway technology). The resulting binary vector was used to transform *ugt78d1* knock out mutant plants by *Agrobacterium tumefaciens* mediated transformation.

2.2.21 Construct for *ugt*78d2 mutant genetic complementation

A genomic fragment containing the coding region of *UGT*78D2 and its promoter region was amplified from Col-0 plant genomic DNA using the primers (containing both GATEWAY BP recombination sequence and gene specific sequence):78D2_Pro_GW_F (5'-ggggAC AAGTTTGTACAAAAAAGCAGGCTttcggtccaaaggatttcag-3') and 78D2_CO_GW_R (5'-GGGGACCACTTTGTACAAGAAAGCTGGGTagattttctgagccgtgcat-3'). The PCR product was cloned into pDONR221 vector via BP recombination (Gateway technology) and the desired sequence was confirmed by sequencing. The genomic fragment was further subcloned into the vector pBGW (Karimi *et al*., 2002) via LR recombination (Gateway technology). The resulting binary vector was used to transform *ugt78d2* knock out mutant plants by *Agrobacterium tumefaciens* mediated transformation.

2.2.22 Construct for artificial miRNA

An artificial miRNA (amiRNA) targeting *UGT*74F2 mRNA was designed with a Web MicroRNA Designer (WMD 2 http://wmd2.weigelworld.org/cgi-bin/mirnatools.pl?page=1). One of the recommended amiRNAs (5'-GAACACCAGACTAGTGATAAA-3') was chosen. The amiRNA containing precursor is generated by PCR using pRS300 as template (Ossowski *et al*., 2008). The PCR products were gel-purified and cloned into pENTR™1A vector via EcoRI and BamHI sites. The amiRNA sequence was then confirmed by sequencing and subsequently mounted into the pAlligator2 vector via Gateway LR recombination reactions. The resulting expression clone (Figure 2. 1) was introduced into *ugt74f1* knock-out mutant background to knock-down the closely linked *UGT74F2* gene.

Figure 2. 1 Illustration of the construct for amiRNA-UGT74F2
EN35S: double-enhanced 35S promoter
HA: 3X HA (hemagglutinin) tag
T-NOS: Nopaline synthase terminator

T-35S: 35S terminator

E-GFP: endoplasmic reticulum targeted GFP

At2S3: *Arabidopsis* seed storage protein promoter

2.2.23 Extraction and determination of free and glucose-conjugated SA

The method to quantify salicylic acid (SA) was adapted from B. Meßner *et al* (unpublished). Metabolites of pooled 4-week-old rosette leaves from 4-6 individual plants (snap-frozen in liquid nitrogen and stored at -80°C) were extracted with a 1 + 2 mixture of methanol and 2% (v/v) formic acid. The content of free SA as well as SA released from conjugates was determined by an optimized method. Briefly, SA was extracted under acidic conditions using reversed-phase sorbent cartridges, recovered under basic conditions, and subsequently analyzed via reverse phase HPLC. Quantification was based on SA fluorescence (excitation 305 nm/ emission 410 nm) with o-anisic acid added as an internal standard and authentic SA standards. Enzymatic digestion of parallel aliquots of the leaf extract with (1) 2-glucosidase or with (2) esterase prior to reversed-phase extraction allowed to determine (1) total SA glucose conjugates plus free SA and (2) SA ester conjugates plus free SA, respectively. Thus, the contents of free, not conjugated SA, glucose-conjugated SA, and esterified SA could be determined.

2.2.24 PAL activity assay

The assay method was modified from a recently published one (Olsen *et al*., 2008). Approximately 100 mg leaves were thoroughly homogenized with 3 ml extraction buffer (containing 100 mM Tris-HCl, pH 8.8, and 12 mM 2-mercaptoethanol). After centrifugation at 14,000 g for 10 min at 4°C the supernatant was desalted by a Sephadex G25 column. The protein fraction was used for the PAL assay. The assay mixture contained 450 µl buffer (100 mM Tris-HCl, pH 8.8), 500 µl protein extract and 50 µl 100 mM L-phenylalanine. After incubation for two hours at 37°C, 50 µl 5 M HCl were added to terminate the reaction. The UV absorbance was recorded at 290 nm. The blank made in the same way as the assay, but without Phenylalanine. Assays were performed five times (technical repeats) for each of the three independent experiments. The activity was expressed as nmol trans-cinnamic acid formed per gram plant tissue, per hour.

2.2.25 Construction of the calibration curves for different flavonols

A calibration curve was generated from HPLC data and used to calculate the amount of kaempferol (µg) per g FW of *Arabidopsis* tissues. The calibration curve was obtained by plotting the measured area (mAU) against different amounts of kaempferol (Roth). The calibration curve was obtained using Microsoft Excel (Figure 2. 2). The formula generated by Microsoft Excel was used to calculate the concentration of kaempferol in plant extracts. The

calibration curves for isorhamnetin (Figure 2. 3) and quercetin (Figure 2. 4) were generated in an analogous way.

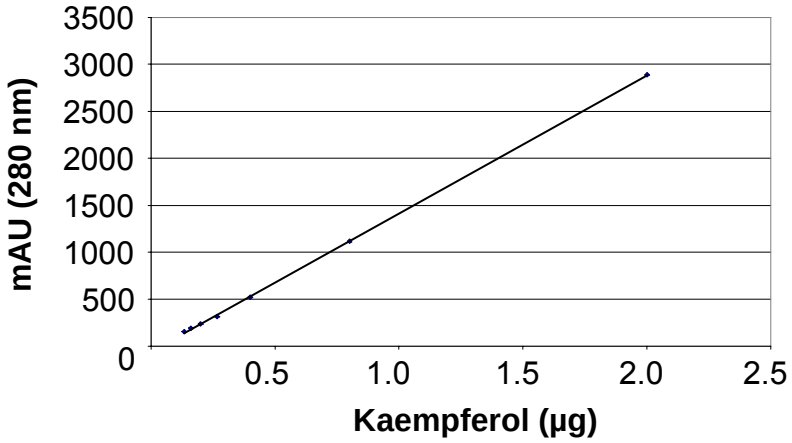

Figure 2. 2 The kaempferol calibration curve. The formula of the calibration curve obtained is y = 1469.6x-56.442 (y = mAU, x = µg). The error bars are means ± SD, n = 3. The error bars are very small.

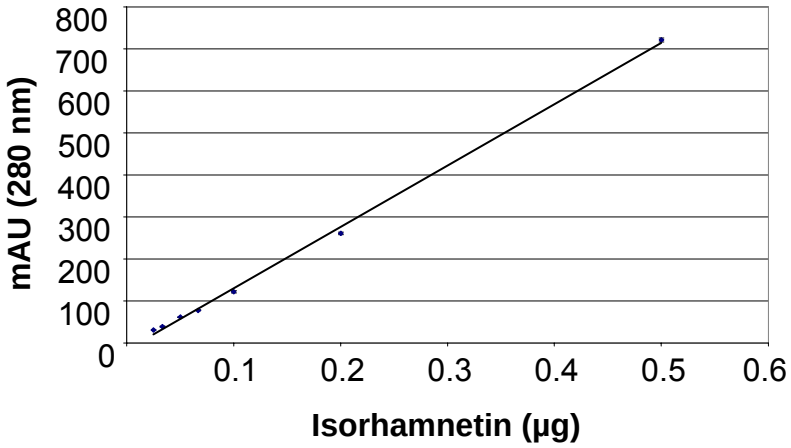

Figure 2. 3 The isorhamnetin calibration curve. The formula of the calibration curve obtained is y = 1460.3x-15.733 (y = mAU, x = µg). The error bars are means ± SD, n = 3. The error bars are very small.

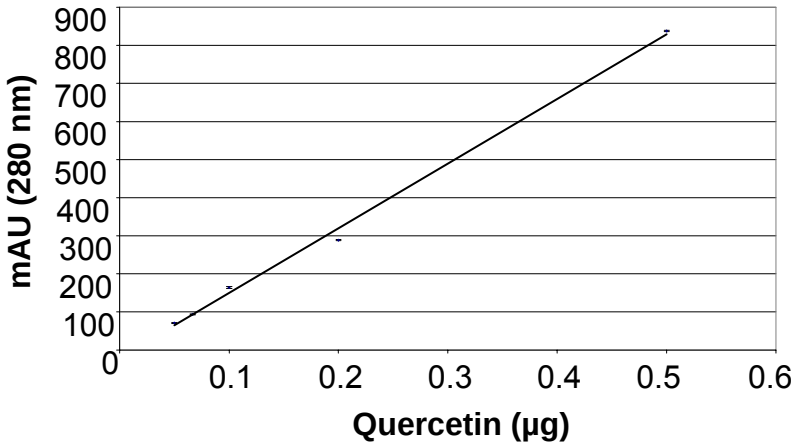

Figure 2. 4 The quercetin calibration curve. The formula of the calibration curve obtained is y = 1700x-20.607 (y = mAU, x = µg). The error bars are means ± SD, n = 3. The error bars are very small.

2.2.26 Extraction of flavonol metabolites for HPLC analysis

Rosette leaves from soil-grown plants 21 days after germination (DAG) and roots from 14 DAG agar-grown seedlings were collected for flavonol extraction. Extracts were prepared by adding 1 ml methanol (with naringenin as internal standard) to 100 mg fresh weight plant materials. Samples were ground to a fine suspension and incubated for 1 h with moderate rotation at 4°C. The extracts were then clarified by centrifugation at 14,000 g for 10 min with a table centrifuge. One third volume of distilled water was added to the extract and centrifuged as above to remove the chlorophyll. 20 µl of the clear extract were analyzed by HPLC. For flavonol aglycone analysis the clear extract was hydrolyzed by the adding of an equal volume of 2 N HCl, incubation was performed at 70°C for 40 min. An equal volume of methanol was added to prevent the precipitation of the aglycones. Samples were centrifuged at 14,000 rpm for 15 min. 20 µl of the sample was analyzed by HPLC.

2.2.27 HPLC analysis of flavonols and sinapate esters

Samples were analyzed using a reverse phase HPLC system at a flow rate of 1ml/min using a Luna 5 µ C18 column (Phenomenex, P/No: 00G-4252-E0). Solvent A was 20% formic acid with 1% ammonium formate, and solvent B was 88% methanol with 1% ammonium formate. The elution gradient program was a linear gradient from solvent A to solvent B (45 min), and maintained at 100% B for 5 min. Absorbance at 280 nm was used for detection. The flavonol aglycones, including kaempferol, quercetin and isorhamnetin, were identified by their diode array spectra and by comparison with authentic standards.

2.2.28 Photometric determination of anthocyanins

Extraction of anthocyanins of 21-DAG *Arabidopsis* plants was performed as following. 250 µl of acidic methanol (1% HCl, w/v) was added to 50 mg of fresh plant material. The plant material was homogenized on ice and then incubated at 4°C for 1h with moderate shaking. The suspension was clarified by centrifugation (14,000 rpm, room temperature, for 5 min). Absorption of the extracts at 530- and 657-nm wavelength was determined photometrically. Quantification of anthocyanins was performed using the following equation: $Q_{\text{Anthocyanins}} = (A_{530} - 0.25^* A_{657}) \text{ X } M^{-1}$, where $Q_{\text{Anthocyanins}}$ is a corrected absorption value linearly correlated with the amount of anthocyanins, A_{530} and A_{657} is the absorption at the indicated wavelengths and M is the weight of the plant material used for extraction (g). All samples were measured in triplicate in three independent biological replicates. Error bars indicate the SD of the average of the anthocyanin content.

2.2.29 LC-ESI-MS^n

A Bruker Daltonics esquire 3000^{plus} ion trap mass spectrometer (Bruker Daltonics, Bremen, Germany) connected to an Agilent 1100 HPLC system (Agilent Technologies, Waldbronn, Germany), equipped with a quaternary pump, and a variable wavelength detector, was utilized for all experiments. Components were separated with a Phenomenex (Aschaffenburg, Germany) Luna C-18 column (150 mm long x 2.0 mm inner diameter, particle size 5 µm) that was held at 25°C. The electrospray ionization voltage of the capillary was set to -4000 V and the end plate to -500 V. Nitrogen was used as dry gas at a temperature of 300°C and a flow rate of 10 l/min. The full scan mass spectra were obtained in a scan range from 50 to 800 m/z with a scan resolution of 13000 m/z/s until the ICC target reached 20000 or 200 ms, whichever was achieved first. Tandem mass spectrometry was carried out using helium as the collision gas (3.56 x 10^{-6} mbar) with the collision voltage set at 1 V. Spectra were acquired in the positive and negative ionization mode. The LC parameters went from 100% A (0.1% formic acid in water) to 50% B (0.1% formic acid in methanol) in 30 minutes, then in 5 minutes to 100% B, held for 15 min at these conditions, then returned to 100% A in 5 min at a flow rate of 0.2 ml min^{-1}. The detection wavelength was 280 nm.

2.2.30 LC-ESI-MS^n Metabolite analysis

One hundred mg of freeze-dried *Arabidopsis* leaf powder were extracted with 500 µl methanol containing 0.1 mg/ml 4-methylumbelliferyl-β-D-glucuronid as an internal standard. Methanol was removed in a rotary vacuum concentrator and the extract was re-dissolved in 35 µl water for analysis by LC-ESI-MS^n. Metabolites were identified by their retention times, mass spectra and product ion spectra in comparison with the data determined for authentic

reference materials. Relative metabolite quantification was performed using the DataAnalysis 3.1 and QuantAnalysis 1.5 software (Bruker Daltonics, Bremen, Germany) normalizing all results to the internal standard. The extraction and analyzing of metabolites were performed by T. Hoffmann (Weihenstephan, Freising, Germany).

2.2.31 Auxin transport assay

The auxin transport assay was modified according to previously published methods (Okada *et al.,* 1991; Przemeck *et al.,* 1996; Besseau *et al.,* 2007). Briefly, fragments of 2.5 cm in length cut from the basal part of the primary stem were used for the assay. The auxin solution contained 30 µl mixture of Murashige and Skoog (MS) medium (pH 5.5) with 10 µM IAA and 1 µM ^{3}H-IAA (1 µCi/µl). One end of the stem fragment (Apical end for basipetal auxin transport; basal end for acropetal auxin transport) was dipping into the assay mixture. After six hours incubation at room temperature in the dark in a closed Eppendorf tube, a 5 mm fragment was cut off from the non-submerged basal end and the radiation was measured by scintillation counting.

2.2.32 IAA quantification

Col-0 and *ugt78d2* plants were grown for 28 days before the inflorescence stems were harvested. Segments of 2.5 cm long were collected from apex, middle and base of inflorescence stems. The extraction and quantification of plant IAA were carried out by Petre I. Dobrev (Institute of Experimental Botany, Acad. Sci. Czech Rep.,Prague) as previously described (Dobrev and Kaminek, 2002).

2.2.33 Imaging methods

Plant images were taken using binocular (Olympus SZ-PT), fluorescence microscopy (Zeiss) and digital camera (Nikon D300). Some pictures were further processed with Adobe Photoshop CS2.

3 Chapter 3: FEEDBACK INHIBITION OF PHENYLPROPANOID AND FLAVONOL-BIOSYNTHETIC PATHWAYS UPON A COMPROMISED FLAVONOL-3-*O*-GLYCOSYLATION

3.1 ABSTRACT

Flavonols, a class of phenylpropanoids, have protective and regulatory functions in plants and are important nutritional ingredients. The hydrophobic compounds are glycosylated consecutively at their 3-OH and 7-OH positions in *Arabidopsis thaliana*. UGT78D1 and UGT78D2 are the major glycosyltransferases involved in flavonol 3-*O*-glycosylation in leaves of this plant. Accordingly, the *ugt78d1 ugt78d2* double mutant was strongly compromised in the primary conjugation of flavonol aglycones. Instead of alternative modifications or aglycone accumulation, flavonol biosynthesis was repressed in *ugt78d1 ugt78d2* retaining only one third of the wild-type flavonol level. The reduced flavonol amounts were associated with a repressed transcription of many flavonol-biosynthetic key genes including the committed step of flavonoid biosynthesis catalyzed by CHALCONE SYNTHASE (TT4). In addition, the expression of PHENYLALANINE AMMONIA LYASE (PAL), which constitutes the committed step of the general phenylpropanoid pathway, was repressed at the level of gene transcription and enzyme activity. However, a strong repression of total flavonol biosynthesis in the *flavonol synthase 1* mutant did not negatively affect PAL expression nor was it repressed by a compromised downstream 7-*O*-glycosylation. PAL activity was also reverted back to wild-type level in *tt4 ugt78d1 ugt78d2* lines eliminating flavonoid biosynthesis in addition to the repressed 3-*O*-glycosylation capacity. Chemical complementation of *tt4 ugt78d1 ugt78d2* plants using naringenin, a flavonoid intermediate, could restore the reduction in PAL expression. Thus, these studies revealed a novel feedback inhibition of the flavonol-biosynthetic pathway, which was specifically linked to a compromised flavonol 3-*O*-glycosylation, but at the same time dependent on flavonol formation itself.

3.2 INTRODUCTION

Phenylalanine-derived flavonoids are important plant secondary metabolites. In *Arabidopsis thaliana*, flavonoids comprise flavonols, anthocyanins and proanthocyanidins. Among them flavonols received intense research interest because they were shown to have diverse roles

such as protection from oxidative damage and UV radiation, inhibition of auxin transport, control of pollen function and signalling to symbiotic organisms (Li *et al.,* 1993; Mo *et al.,* 1992; Peer *et al.,* 2004; Peer *et al.,* 2007; Santelia *et al.,* 2008; Harrison *et al.,* 2005; Wasson *et al.,* 2006; Taylor *et al.,* 2005; Buer *et al.,* 2010). In addition, flavonols taken in as food and feed ingredients have been also implicated as either protective, regulatory or cytotoxic molecules in mammals (Lin *et al.,* 2006).

The biosynthesis of flavonols as well as the general phenylpropanoid pathway supplying the flavonoid precursor *p*-coumaroyl-CoA has been well characterized in many plant species including *A. thaliana* (Dixon *et al.,* 1999; Harborne *et al.,* 2000; Harborne *et al.,* 2001) (Fig. 1). Phenylalanine ammonia-lyase (PAL) catalyzes the committed step of the phenylpropanoid pathway and locates at the link of primary and secondary metabolism. Different PAL isoforms were proposed to have different metabolic roles in *A. thaliana*. PAL1 and PAL2 are important for both flavonoid and lignin biosyntheses, while PAL4 appears to be important for lignin biosynthesis (Raes *et al.,* 2003; Rohde *et al.,* 2004). Chalcone synthase (CHS) catalyzes the committed step of flavonoid biosynthesis and is encoded by a single gene in *A. thaliana* (Winkel-Shirley 2006). The *chs* mutant (or *transparent testa 4*, *tt4*) is completely devoid of flavonoids, which provides a good tool for analyzing the consequences of a complete loss of flavonoids in plants. Although six *Arabidopsis* flavonol synthase (FLS) isoforms were identified, only FLS1 considerably contributed to the last step of the formation of the flavonol aglycones (Owens *et al.,* 2008; Stracke *et al.,* 2009). FLS3 had a low activity, but it might be relevant only under an *fls1* background *(Preuss et al.,* 2009).

Flavonol aglycones are further glycosylated in a complex manner in plant cells. Glycosylation is frequently involved in the biosynthesis of secondary metabolites to modify their stability, solubility or localization and thereby the biological properties of the conjugated molecules (Li *et al.,* 2001; Bowles *et al.,* 2006; Meßner *et al.,* 2003). In case of the hydrophobic flavonols, glycosylation renders them more water-soluble and less toxic, and it may enable flavonol transport and compartmentation (Winkel-Shirley 2006; Bowles *et al.,* 2006; Cos *et al.,* 2001; Moreira *et al.,* 2007; Xiao *et al.,* 2009). However, the physiological significance of the complex glycosylation pattern found in plants remains unclear. Glycosylation is achieved by UDP-carbohydrate dependent glycosyltransferases (UGTs), which transfer sugars to target molecules by the formation of a glycosidic bond (Li *et al.,* 2001). Flavonols are usually glycosylated at their 3-OH and 7-OH positions in *A. thaliana* (Veit *et al.,* 1999; Bloor *et al.,* 2002; Jones *et al.,* 2003; Tohge *et al.,* 2005; Yonekura-Sakakibara *et al.,* 2007; Yonekura-Sakakibara *et al.,* 2008). Based on the *in vitro* substrate preferences of recombinant UGT proteins and the flavonol glycoside profiles of the *Arabidopsis* mutants deficient for

glycosylation at these two positions, the 3-*O*-glycosylation is considered to be the first step of conjugation followed by 7-*O*-glycosylation. Five UGTs involved in flavonol glycosylation have been identified including UGT78D1, UGT78D2, UGT78D3, UGT73C6, and UGT89C1 (Figure 1. 4) (Jones *et al.,* 2003; Tohge *et al.,* 2005; Yonekura-Sakakibara *et al.,* 2007; Yonekura-Sakakibara *et al.,* 2008). In leaves, UGT78D1 and UGT78D2 are the major 3-*O*-glycosyltransferases, whereas UGT78D3 has, if any, only a negligible contribution to the overall 3-*O*-glycosylation (Jones *et al.,* 2003; Tohge *et al.,* 2005; Yonekura-Sakakibara *et al.,* 2008). UGT73C6 has only a minor contribution to 7-*O*-glycosylation in leaves as only trace amount of flavonols are 7-*O*-glucosylated. Instead, 7-*O*-rhamnosylation by UGT89C1 is the major form of 7-*O*-conjugation (Yonekura-Sakakibara *et al.,* 2007).

The phenylpropanoid and flavonoid biosynthesis pathways are subject to multiple levels of control. They are dependent on developmental stages and tissues as well as on exogenous stimuli, in particular on irradiation and temperature (Winkel-Shirley 2006; Kubasek *et al.,* 1992; Kaffarnik *et al.,* 2006; Götz *et al.,* 2010). Both post-transcriptional modification and transcriptional controls have been implicated in these regulations (Winkel-Shirley 2006; Franken *et al.,* 1991; Pairoba *et al.,* 2003). In addition, the committed step into phenylpropanoid pathway has been shown to be metabolically regulated through negative feedback by cinnamic acid on *PAL* transcription exerted at the level of C4H activity (Blount *et al.,* 2000).

Here, an *Arabidopsis ugt78d1 ugt78d2* double mutant was characterized that was to lead to a compromised initial 3-*O*-glycosylation of flavonols. However, instead of an accumulation of flavonol aglycones or alternative conjugations in this line, the biosynthesis of flavonols was repressed. This repression was correlated with a reduced expression of both flavonol biosynthetic and *PAL* genes. A further genetic analysis suggested a novel feedback repression of PAL that was directly related to the strongly compromised initial 3-*O*-conjugations, yet dependent on flavonol aglycone formation.

3.3 RESULTS

3.3.1 *The ugt78d1 ugt78d2* double mutant has strongly reduced total flavonol content in leaves

Three major flavonol glycosides, kaempferol 3-*O*-rhamnoside-7-*O*-rhamnoside (k1), kaempferol 3-*O*-glucoside-7-*O*-rhamnoside (k2), and kaempferol 3-*O*-rhamnosyl (1->2) glucoside-7-*O*-rhamnoside (k3), accumulated in leaves of *Arabidopsis* plants grown in a growth chamber under non-stressed conditions (Bloor and Abrahams 2002) (Figure 3. 1 A).

In *ugt78d1* single mutant leaves k1 was not detectable, whereas k2 and k3 were accumulated to higher levels (Jones *et al.,* 2003) (Figure 3. 1 A). However, in *ugt78d2* single mutant leaves k2 and k3 were strongly decreased while k1 was increased (Tohge *et al.,* 2005) (Figure 3. 1 A). Although the flavonol glycoside pattern was altered in the *ugt78d1* and *ugt78d2* single mutants, they appeared to maintain wild-type levels of total flavonol glycoside. These observations suggest that UGT78D1 and UGT78D2 compete for flavonol aglycones as substrates and the loss of flavonol 3-*O*-glycosylation in either single mutant is fully compensated for by the remaining active flavonol 3-*O*-glycosylatranferases.

However, when studying the flavonol glycoside profile in leaves of the *ugt78d1 ugt78d2* double mutant, k2 and k3 were strongly reduced and k1 was not detectable. Furthermore, no other forms of flavonol derivatives or flavonol aglycones were detected (Figure 3. 1 A). LC-MS analysis could not detect any flavonol aglycone (Table 3. 1). It appeared that total flavonol content was reduced in *ugt78d1 ugt78d2* double mutant leaves. To precisely quantify total flavonol content I hydrolyzed the methanolic leaf extracts and measured the flavonol aglycones by HPLC analysys. Consistent with flavonol glycoside observation, both the *ugt78d1* and *ugt78d2* single mutants maintained wild-type total flavonol content (Figure 3. 1C). In the *ugt78d1 ugt78d2* double mutant, kaempferol and quercetin contents were reduced to 21% and 18% of the wild-type levels, respectively (Figure 3. 1 B & C). Interestingly, isorhamnetin, a low abundant flavonol in wild-type plants, accumulated to about 3.5-fold in the *ugt78d1 ugt78d2* double mutant (Figure 3. 1 B & C). Through both LC-MS and FT-ICR-MS analyses, I detected a strongly increased compound corresponding to the molecular mass of isorhamnetin-glucoside-rhamnoside, which may at least partly account for the increased isorhamnetin in the *ugt78d1 ugt78d2* double mutant (Table 3. 1). The total amount of flavonols (including the increased isorhamnetin) in leaves of *ugt78d1 ugt78d2* double mutant was reduced to about 32% of the wild-type level. Thus, the drastic loss of flavonol 3-*O*-glycosylation results in a strong reduction of total flavonol content.

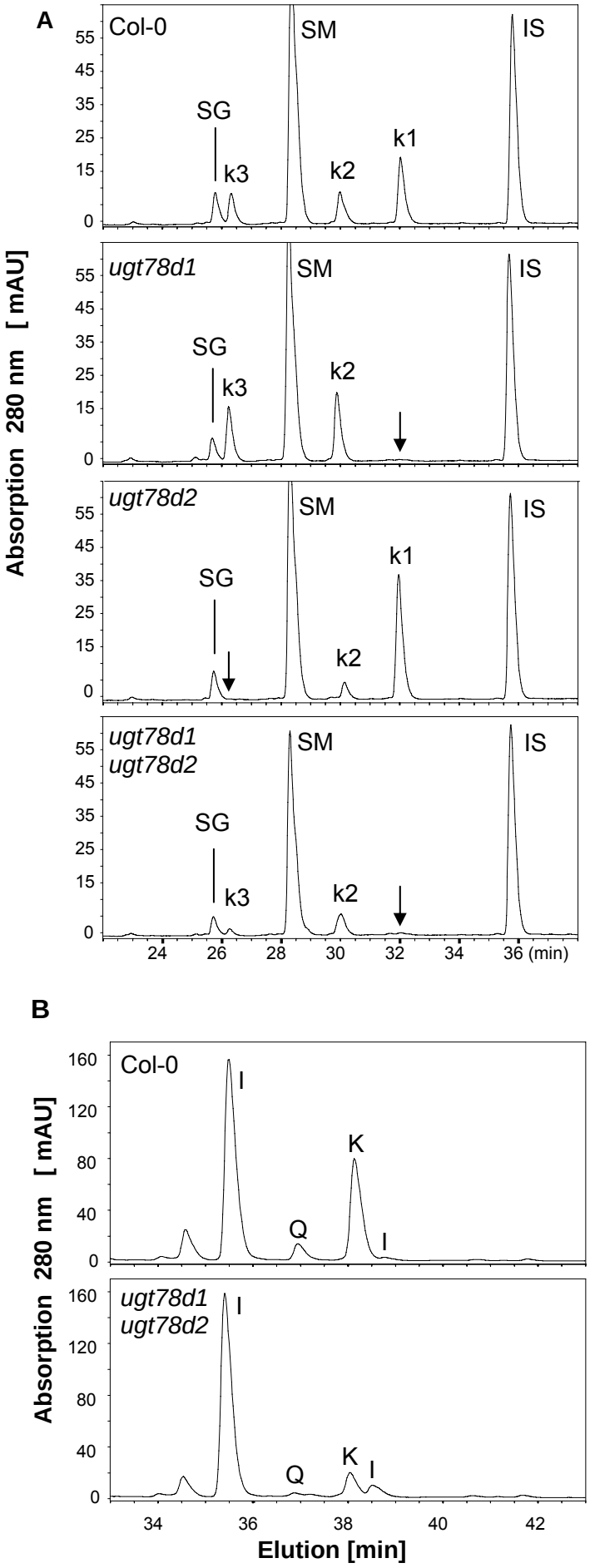
A
Col-0
SM
IS
SG
k3
k2
k1
ugt78d1
ugt78d2
ugt78d1
ugt78d2
Absorption 280 nm [mAU]
24
26
28
30
32
34
36 (min)
B
Col-0
I
K
Q
I
ugt78d1
ugt78d2
Absorption 280 nm [mAU]
34
36
38
40
42
Elution [min]

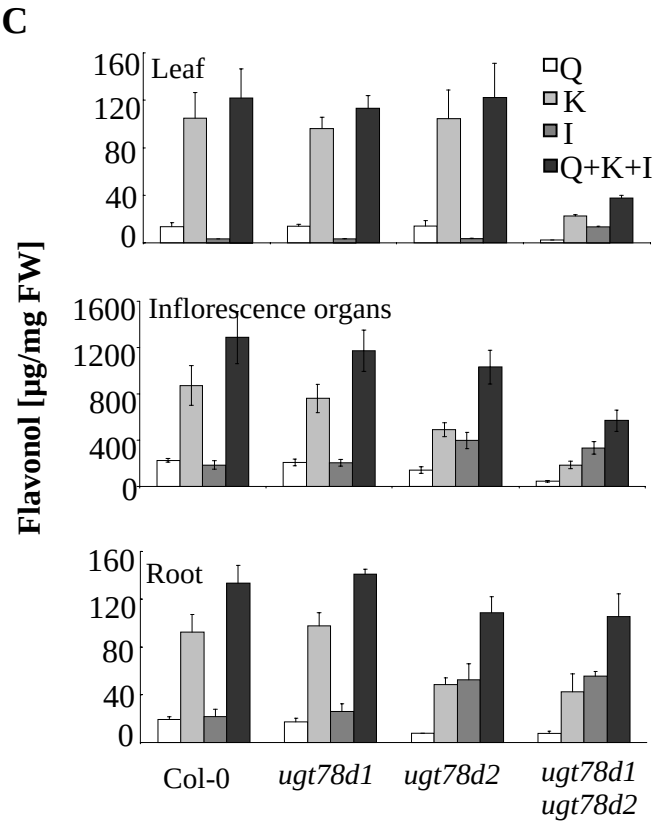

Figure 3. 1 Determination of flavonols from Col-0, *ugt78d1*, *ugt78d2* and *ugt78d1 ugt78d2* by HPLC analyses. *A*. Representative HPLC diagrams of the flavonol glycoside profiles from leaves of three-week-old plants. k1, kaempferol 3-*O*-rhamnoside-7-*O*-rhamnoside; k2, kaempferol 3-*O*-glucoside-7-*O*-rhamnoside; k3, kaempferol-3-*O*-[rhamnosyl (1->2glucoside)]-7-*O*-rhamnoside, IS, internal standard (naringenin), SM, sinapoyl malate, SG, sinapoyl glucose. Arrows indicate missing glycosides. *B*. Representative HPLC diagrams of flavonol aglycone profiles from leave extracts after acid hydrolysis. Q, quercetin; K, kaempferol; I, isorhamnetin, *C*. Total flavonol aglycone quantification after acid hydrolysis of the methanolic extracts from leaves and roots. Each bar represents the mean ± SD determined by three independent experiments. FW, fresh weight.

Table 3. 1 Detected metabolite levels in *ugt78d1 ugt78d2* and Col-0 leaves by LC-MS analysis.

Compounds	Col-0	*ugt78d1 ugt78d2*
Kaempferol 3-*O*-glucoside	29.92 ± 3.95	11.25 ± 3.05
Quercetin 3-*O*-glucoside	22.47 ± 2.55	3.19 ± 0.74
Isorhamnetin-glucoside-rhamnoside	9.71 ± 4.13	296.15 ± 35.85
Naringenin-glucoside	2.60 ± 0.64	2.02 ± 0.63
Sinapic acid	184.38 ± 37.02	125.93 ± 21.59
p-Coumaroyl-glucoside	1.14 ± 0.56	0.87 ± 0.50
p-Coumaroyl-glucose-ester	1.61 ± 0.44	2.03 ± 0.43
Caffeoyl-glucose-ester	6.90 ± 1.58	7.29 ± 1.35
p-Hydroxybenzoyl-glucose-ester	0.99 ± 0.42	1.04 ± 0.35

The flavonol glycosides shown in Figure 3. 1A are not shown here. In particular, no flavonol aglycones were detected in this analysis. Rosette leaves of three-week-old plants were used for the analysis. The values shown are the means of eight independent biological samples ± SD (µg/g dry weight equivalent 4-methyl-umbelliferyl-glucoside). Please note that the numbers do indicate relative quantities and cannot be compared to the values given in Figure 3. 1 and Figure 3. 5. These experiments were done in cooperation with Thomas Hoffmann and Wilfried Schwab, TU München.

3.3.2 Expression pattern of *UGT78D1* and *UGT78D2* matches organ-specific reduction in flavonols

The reduction of total flavonol content was organ-specific and different in inflorescences, stems and leaves from roots. Similar to leaves, the total flavonol content was strongly reduced in both inflorescences and stems of *ugt78d1 ugt78d2* plants as compared to the wild type counterpart (Figure 3. 1 C & Figure 4. 3). In roots, however, the total flavonol content of double mutants maintained at higher levels similar to *ugt78d2* single mutants (Figure 3. 1 C).

To study whether the organ-specific flavonol reduction in the *ugt78d1 ugt78d2* double mutant was correlated with the expression patterns of *UGT78D1* and *UGT78D2* in wild-type plants, the respective promoter reporter constructs were generated and introduced into wild-type *Arabidopsis* plants. In about two-week-old plants, both *UGT78D1* and *UGT78D2* were well expressed at the basal part of the young leaves (Figure 3. 2 A & B). The expression of

UGT78D2 was also observed along the central vein of the leaves as well as in the cotyledons (Figure 3. 2 B). In about three-week-old plants, the expression of both *UGT78D1* and *UGT78D2* was lower compared to that of two-week-old plants and predominantly at the basal part of leaf petioles (Figure 3. 2 C & D). Generally, the expression of both *UGT* genes was very low in roots relative to that in leaves. The expression of *UGT78D2* was not detectable in roots (Figure 3. 2 F). The expression of *UGT78D1* was observed along the root stele but was, however, absent in the region close to root tip (Figure 3. 2 E). Interestingly, strong expression of *UGT78D1* was observed in root tips (Figure 3. 2 E insert). Jones and colleagues (Jones *et al.,* 2003) also found that *UGT78D1* was well expressed at similar levels across leaves, flowers, siliques, and stems, whereas it was detectable only at very low levels in roots. These findings were further corroborated by examination of publicly available microarray data using the *Arabidopsis* eFP Browser (bar.utoronto.ca, developmental map) (Schmid *et al.,* 2005; Winter *et al.,* 2007), which showed that the expression of both *UGT78D1* and *UGT78D2* in roots was much lower than in leaves (Figure 3. 2 G). Taken together, both *UGT78D1* and *UGT78D2* exhibited a relatively much higher expression in plant aerial parts than in roots, which is positively correlated with the organ-dependent reduction of total flavonol content in the *ugt78d1 ugt78d2* double mutant.

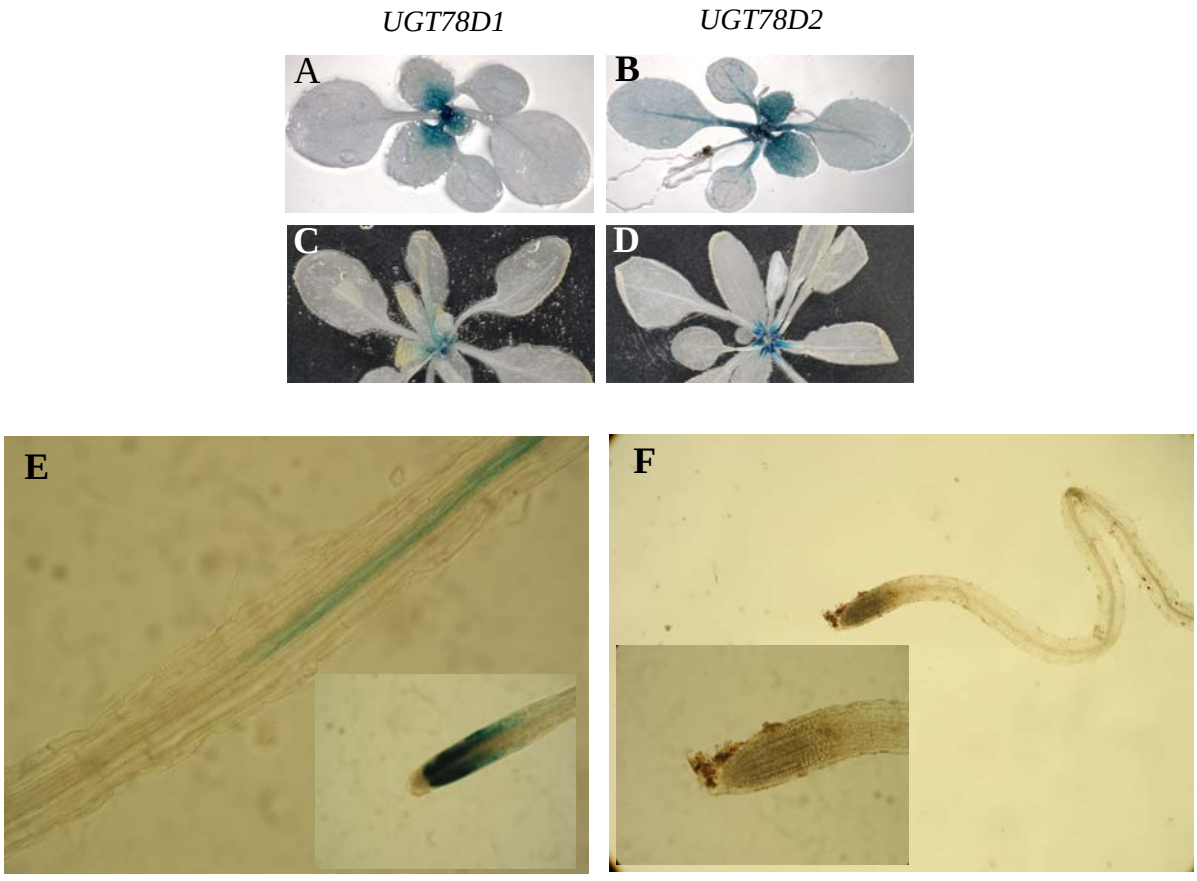

G

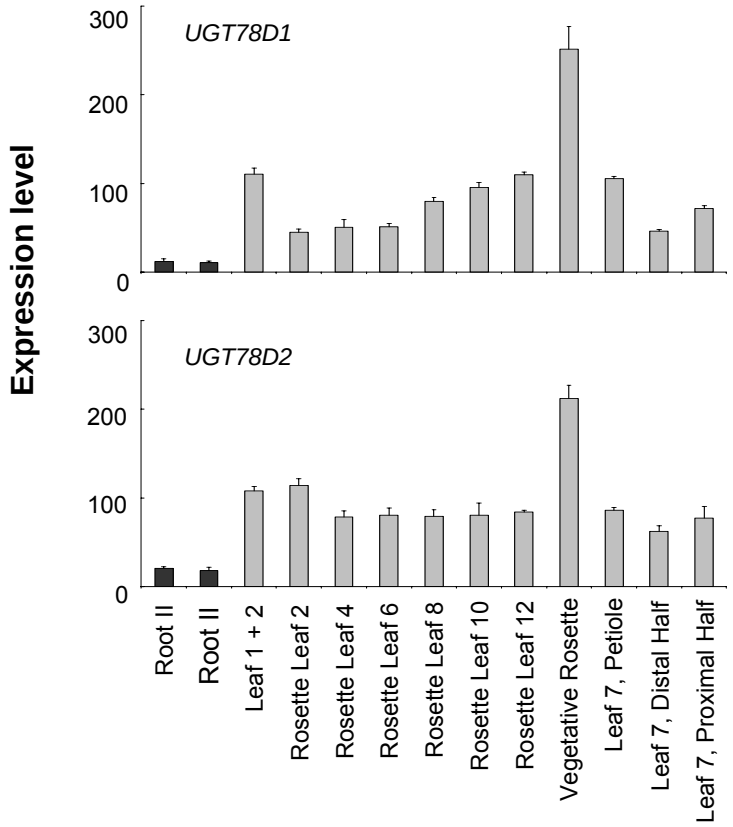

Figure 3. 2 Expression pattern of *UGT78D1* and *UGT78D2*. *A*, *B*, *C*, *D*, *E,* and *F,* transgenic promoter-GUS fusions were analyzed by histochemical staining with 5-bromo-4-chloro-3-indolyl-β-D-glucuronide. *A* and *B*, two-week-old plants. *C* and *D*, three-week-old plants. *G*, data from the public microarray database of both *UGT78D1* and *UGT78D2* genes obtained using the *Arabidopsis* eFP Browser (bar.utoronto.ca) (Schmid *et al.,* 2005, Winter *et al.,* 2007).

3.3.3 Flavonoid biosynthetic genes are transcriptionally down-regulated in *ugt78d1 ugt78d2* double mutant leaves

To examine whether the reduced flavonol content in leaves was accompanied by reduced transcript levels of the flavonoid biosynthetic genes, their mRNA abundance was assessed by quantitative RT-PCR in both *ugt78d1 ugt78d2* double mutant and wild-type plants. The primers used are listed in (Supplemental Table S1). In *ugt78d1 ugt78d2*, the transcripts of *CHS*, *F3'H*, *FLS1* and *DFR* were significantly lowered to about 50% in comparison to the wild-type counterpart (Figure 3. 3). However, the transcripts of *CHI* and *F3H* were of wild-type levels. Furthermore, genes in the general phenylpropanoid pathway upstream of the flavonoid branch including *PAL1*, *PAL2*, *PAL3*, *PAL4*, *4CL1*, *4CL2*, *4CL3* and *C4H* were also analyzed. *PAL1* and *4CL3* transcripts were almost reduced to half in the double mutant *vs*. wild type, whereas the reduction of *C4H* reduction was lower and *4CL1* mRNA levels were not altered. The lowly expressed *PAL2* showed only a tendency for repression (Figure 3. 3).

Eventually, the transcription of *PAL3*, *PAL4*, and *4CL2* in leaves was too low to allow and did not allow an unambiguous evaluation in both wild type and mutant (see Materials and methods). Thus, the committed steps of the phenylpropanoid pathway (*PAL1*) and of the flavonoid biosynthesis (*CHS*) along with several intermediate steps were suppressed at the transcriptional level in *ugt78d1 ugt78d2* to about one half of wild-type expression.

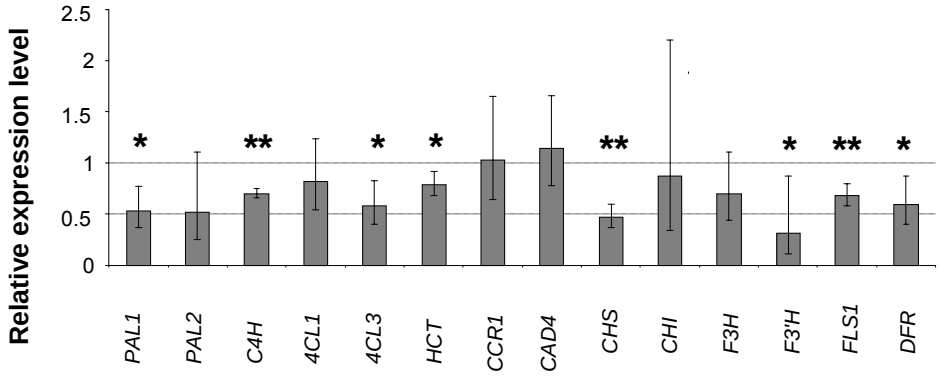

Figure 3. 3 Transcription of genes involved in phenylpropanoid and flavonoid biosynthetic pathways. Quantitative RT-PCR analyses were used to assess transcript levels of the indicated genes in the *ugt78d1 ugt78d2* double mutant relative to Col-0. Data were obtained from three independent experiments. Expression levels were normalized using *S16* and *TUB9* transcripts. The graphics shows the fold changes estimated for each comparison individually with 95%-confidence intervals. The R software was used for calculation. Stars indicate significance of the difference to Col-0 plants: *p-value < 0.05, **p-value < 0.01.

3.3.4 PAL Enzyme activity is reduced in the *ugt78d1 ugt78d2* double mutant

The decreased transcript levels of *PAL1* in the *ugt78d1 ugt78d2* double mutant prompted us to examine whether PAL activity was reduced as well. PAL activity was assayed in total protein extracts from *ugt78d1*, *ugt78d2*, *ugt78d1 ugt78d2* and wild-type leaves. Both *ugt78d1* and *ugt78d2* single mutants remained wild-type level of PAL activity, whereas the *ugt78d1 ugt78d2* double mutant showed a significant reduction to about 60% (Figure 3. 4).

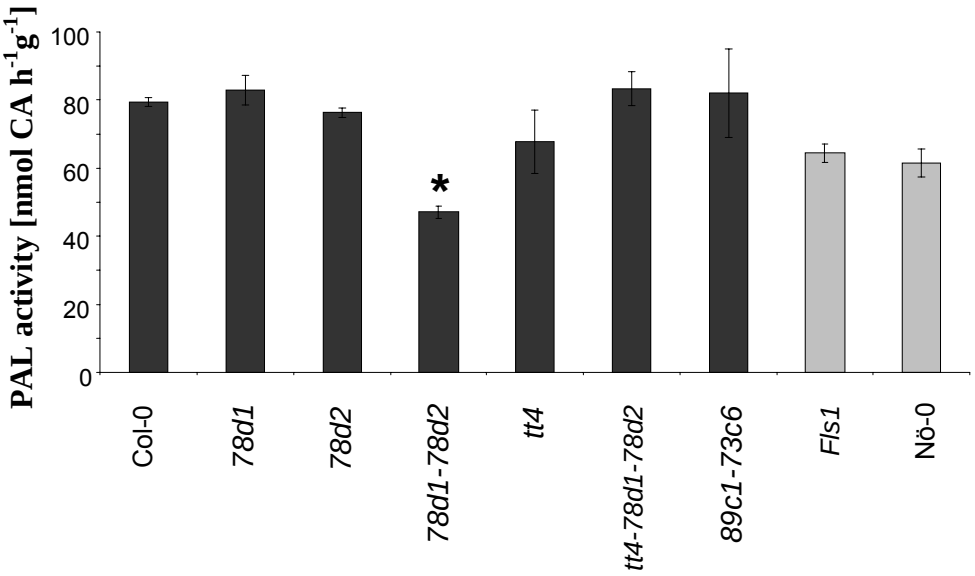

Figure 3. 4 Quantification of PAL activity of *ugt78d1*, *ugt78d2*, *ugt78d1 ugt78d2*, *tt4 ugt78d1 ugt78d2*, *ugt89c1 ugt73c6*, *fls1* and wild-type (Col-0, Nö-0) plants. Crude protein extract from leaves of three-week-old plants were assayed for PAL activity; CA, cinnamic acid. The mean values ± SE of three independent biological samples (pools of 4 to 6 plants per sample) are displayed. Multiple comparisons of different mutants with the corresponding wild-type background (Col-0) (dark bars) were performed using Dunnett's *t*-tests, which showed that Col-0 is significantly different only from *ugt78d1 ugt78d2* ($p < 0.05$), but not from the remaining genotypes. *fls1* was derived from Nö-0 background and compared to this wild type. No significant difference was found. The experiment was repeated three times with similar results.

3.3.5 The influence of reduced PAL activity on phenylpropanoid metabolism

In addition to the flavonol pathway the repression of PAL activity in *ugt78d1 ugt78d2* might also affect other phenylpropanoid-dependent branches, i.e. the biosynthesis of anthocyanins, sinapate esters, and lignin. *ugt78d1* accumulated essentially wild-type levels of total anthocyanins, while anthocyanin accumulation was already strongly suppressed in the *ugt78d2* single mutant without any inhibitory effect on PAL expression (Figure 3. 4 & Figure 3. 5A) (Tohge *et al*., 2003). Since *ugt78d1 ugt78d2* had comparably low amounts of anthocyanin like *ugt78d2* (Figure 3. 5*A*), the repression of PAL did not further impact this downstream branch. However, *DFR* transcription was slightly down-regulated in *ugt78d1 ugt78d2* in contrast to *ugt78d2* single mutant (Figure 3. 3 & Figure 3. 6).

Sinapate esters, particularly sinapoyl malate, are abundantly present in *Arabidopsis* leaves. The reduced PAL expression had a subtle inhibitory effect on sinapate ester accumulation.

The double mutant, in contrast to the single mutants, had a slightly, yet significantly reduced sinapoyl malate content compared to wild type (Figure 3. 5B).

To test whether lignin biosynthesis was affected, I first used quantitative RT-PCR analysis of key genes involved in lignin biosynthesis. The transcript abundance of *HCT* (encoding hydroxycinnamoyl-CoA shikimate/quinate hydroxycinnamoyl transferase) was marginally reduced. Transcription of *CCR1* (encoding cinnamoyl-CoA reductase Class I) and *CAD4* (encoding cinnamyl alcohol dehydrogenase Class II, isoform 4) was not affected in *ugt78d1 ugt78d2* leaves (Figure 3. 3). Thus, the biosynthesis of lignin precursors was essentially not affected at the transcriptional level. Secondly, total lignin was examined histochemically using phloroglucinol-HCl staining of leaves and stems. The flavonol glycoside content in inflorescence stems of *ugt78d1 ugt78d2* was also strongly reduced in leaves (Figure 4. 3). Lignin deposits in both leaves and stems of *ugt78d1 ugt78d2* appeared to be comparable to wild-type levels (Figure 3. 5C,D). Finally, LC-MS analysis was performed for the metabolites associated with the lignin biosynthesis pathway. No immediate monolignol precursor was detected in the leaf extracts. Nevertheless, LC-MS analysis showed that the *ugt78d1 ugt78d2* double mutant accumulated wild-type levels of the monolignol precursor-related derivatives *p*-coumaroyl-glucoside, *p*-coumaroyl-glucose-ester, and caffeoyl-glucose-ester (Table 3. 1). In summary, these results indicated that lignin biosynthesis was not significantly affected in *ugt78d1 ugt78d2*.

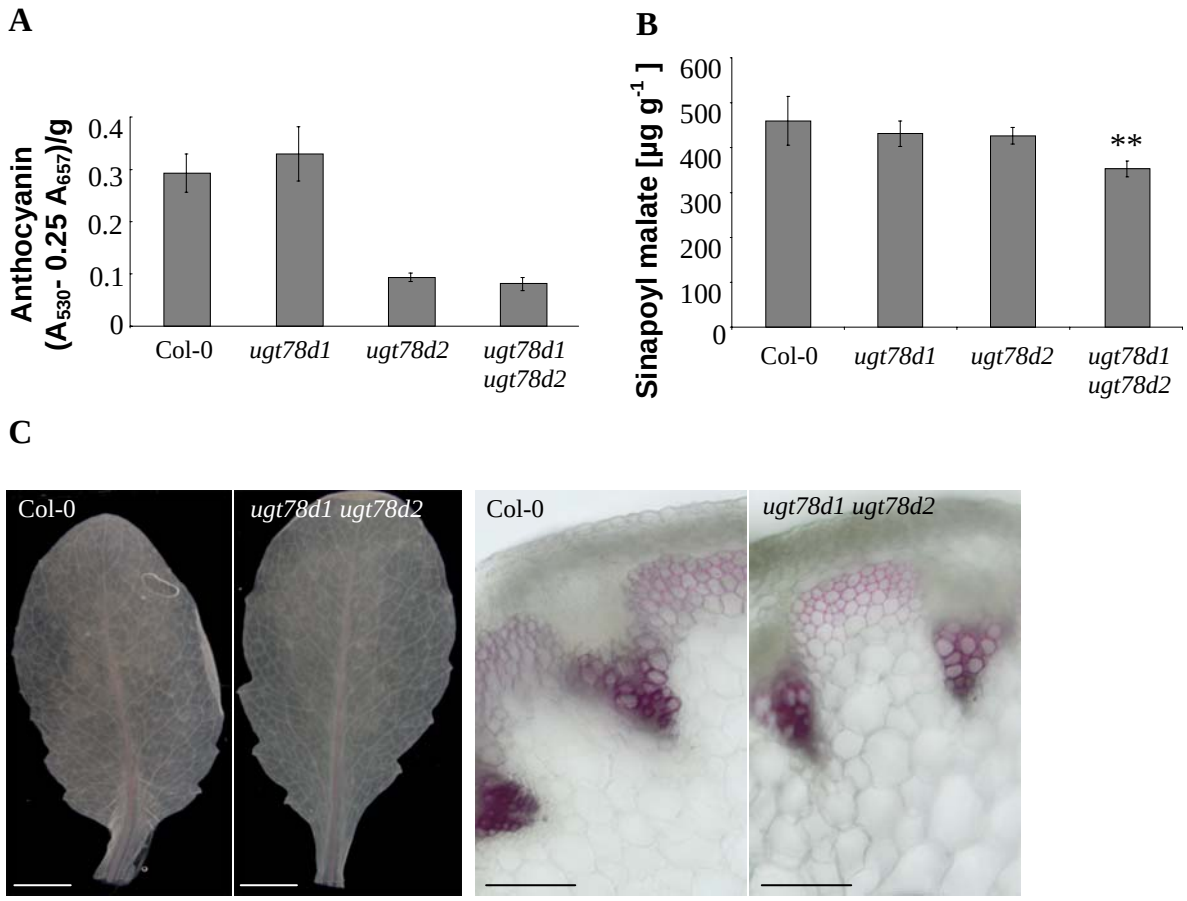

Figure 3. 5 Phenylpropanoid compounds of *ugt78d1 ugt78d2* and Col-0 plants. *A*, photometric determination of the anthocyanin content in acidic methanolic leaf extracts of *Arabidopsis* three-week-old plants: A_{530}, absorption at 530 nm; A_{657}, absorption at 657 nm. The mean values ± SD of three independent biological samples (pools of 4-6 plants per sample) are displayed. *B*, quantification of sinapoyl malate from *ugt78d1 ugt78d2* and Col-0 plants. The mean values ± SD of six independent biological samples (pools of 4-6 plants per sample) are displayed. $^{**}p < 0.01$; paired *t*-tests. This experiment was repeated three times with similar results. *C* and *D*, phloroglucinol-HCl-stained rosette leaves (*C*) from three-week-old plants and hand cross-sections of inflorescence stems (directly below the third internode) (*D*) from five-week-old plants. Bar = 3 mm in *C* and 100 µm in *D*.

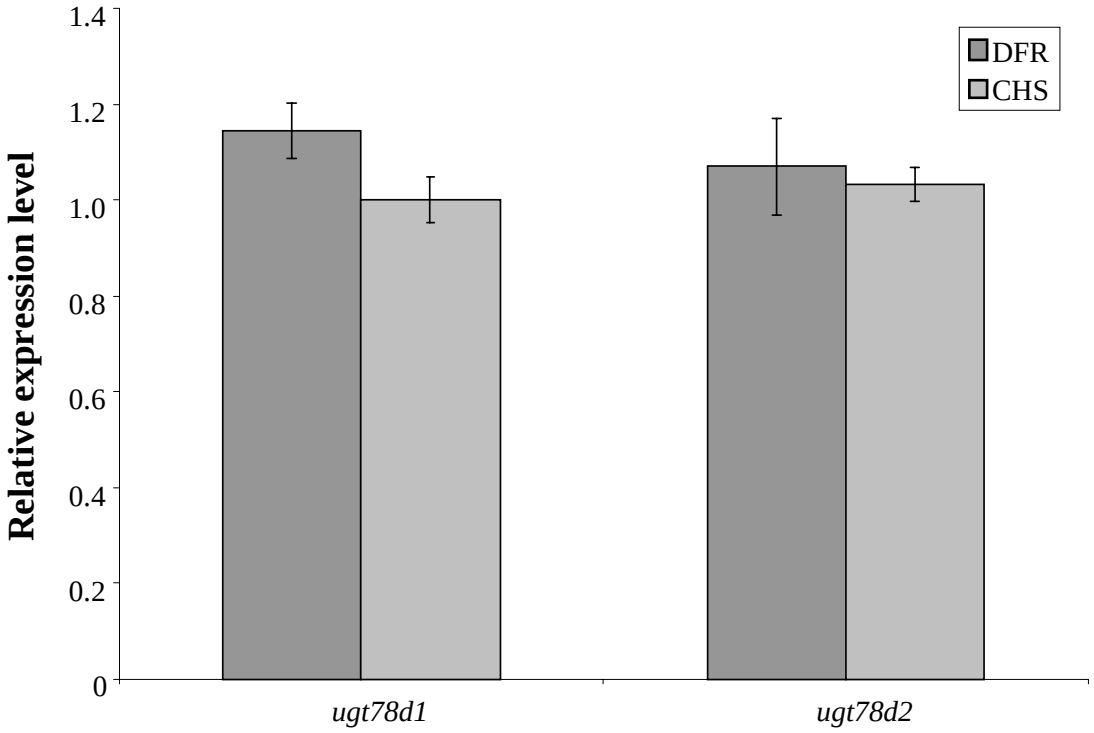

Figure 3. 6 Relative quantification of the expressions of *DFR* and *CHS* in *ugt78d1* and *ugt78d2* single mutants compared to wild-type (Col-0) by quantitative RT-PCR analysis. Leaves from about three-week-old plants were used for RNA isolation and cDNA synthesis. Each bar represents the mean ± SD by three independent experiments.

3.3.6 The reduction of PAL expression of *ugt78d1 ugt78d2* is dependent on flavonol aglycone formation

To examine whether flavonoids themselves could play a role in the flavonol-specific reduction in PAL expression, the *tt4 ugt78d1 ugt78d2* triple mutant was employed. The triple mutant *tt4 ugt78d1 ugt78d2* was blocked at the committed step into flavonoid biosynthesis in the glycosyltransferase double mutant background (Figure 1. 4). In contrast to the *ugt78d1 ugt78d2* line, *tt4 ugt78d1 ugt78d2* as well as the parent *tt4* had wild-type PAL activity (Figure 3. 4) and the transcripts of both *PAL1* and *PAL2* even showed a tendency of being up-regulated in the triple mutant (Figure 3. 7). Thus, the suppression of PAL expression in *ugt78d1 ugt78d2* was released either by the loss of flavonoids or by the loss of CHS activity. To distinguish these two possibilities, a chemical complementation approach was employed. The feeding of naringenin, an intermediate downstream of CHS/TT4, but upstream of FLS, to *tt4 ugt78d1 ugt78d2* could re-implement the inhibition of PAL expression. Naringenin feeding led to the repression of PAL activity and to the transcriptional down-regulation of *PAL1* similar to the extent observed for the glycosyltransferase double mutant (Figure 3. 8A). The

transcription of the much lower expressed *PAL2* was not significantly affected under this condition (Figure 3. 8B). Flavonols had been formed after administration of naringenin confirming the uptake and processing of the compound by *tt4 ugt78d1 ugt78d2* (Figure 3. 8C). Thus, the repression of PAL in the 3-*O*-glycosylation compromised *ugt78d1 ugt78d2* double mutant was flavonoid-dependent and related to naringenin or downstream naringenin-dependent steps. To further narrow down the key regulatory step, additional mutants defective in reactions either directly upstream or downstream of 3-*O*-glycosylation were examined for effects on PAL expression.

The *fls1* mutant severely blocked flavonol biosynthesis at its final step of the formation of the aglycone moiety (Figure 1. 4). However, PAL activity was not reduced, and transcription of *PAL1* and *PAL2* was even enhanced in the *fls1* background (Figure 3. 4 & Figure 3. 7), although this mutant showed a very strong reduction in flavonols (Stracke *et al*., 2009). Flavonol 3-*O*-glycosylation is followed by flavonol 7-*O*-glycosylation. To examine whether a compromised flavonol 7-*O*-glycosylation would also lead to a reduction in flavonol content and a concomitant repression of PAL activity, the *ugt89c1 ugt73c6* double mutant was generated (Figure 1. 4). The flavonol glycoside profile of *ugt89c1 ugt73c6* leaves indicated a strongly suppressed 7-*O*-conjugation. The contents of the three abundant, 7-*O*-conjugated wild-type flavonol glycosides (k1, k2 and k3) were strongly decreased, whereas two flavonol 3-*O*-monoglycosides, kaempferol 3-*O*-glucoside and kaempferol 3-*O*-rhamnoside accumulated (Figure 3. 9*A* & Figure 3. 10). Yet, *ugt89c1 ugt73c6* contained wild-type levels of total flavonols and had unchanged PAL enzyme activity (Figure 3. 4 & Figure 3. 9B).

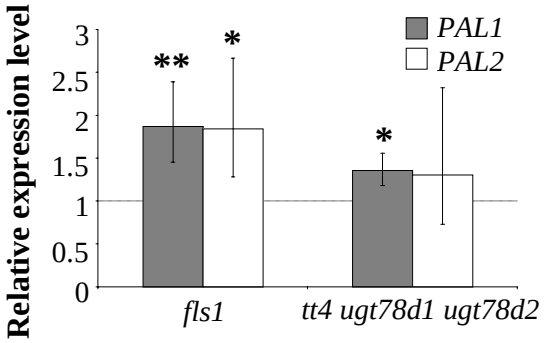

Figure 3. 7 Transcription of *PAL1* and *PAL2* genes in *fls1* and *tt4 ugt78d1 ugt78d2* mutants relative to the wild type. The *fls1* mutant was of Nö-0 background; *tt4 ugt78d1 ugt78d2* was of Col-0 background. The data were collected from three independent quantitative RT-PCR analyses. Expression levels were normalized using *S16* and *TUB9* transcripts. The graphics shows the fold changes estimated for each comparison individually with 95%-confidence

intervals. The R software was used for calculation. Stars indicate significance of the difference to corresponding wild-type plants: *p-value < 0.05, **p-value < 0.01.

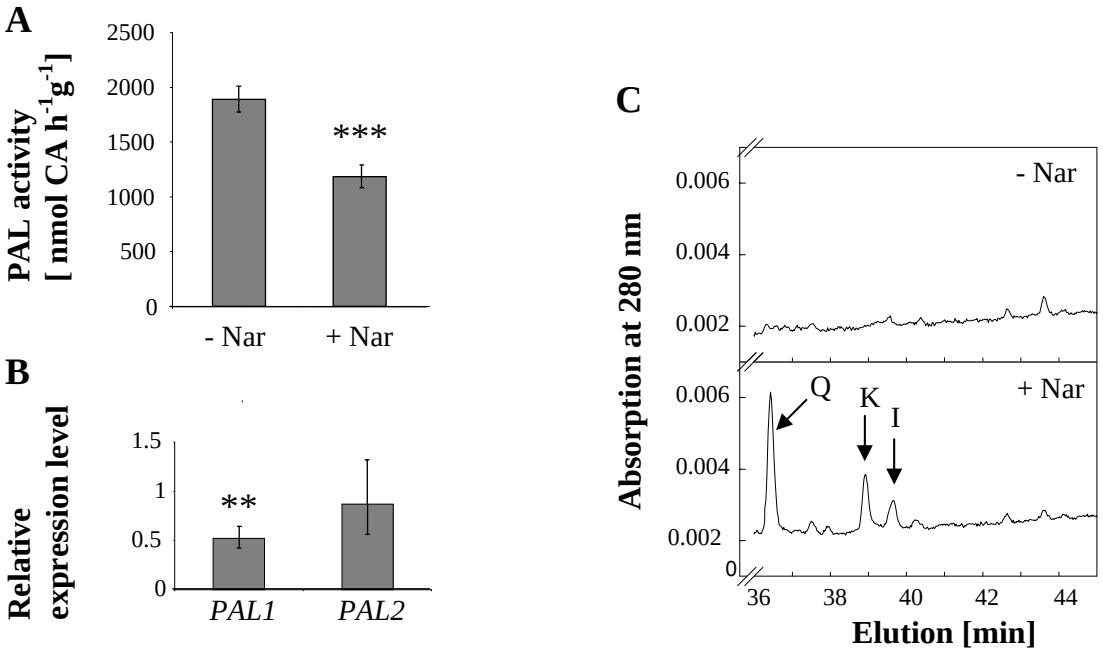

Figure 3. 8 Chemical complementation of *tt4 ugt78d1 ugt78d2* with naringenin. *A,* PAL activity of *tt4 ugt78d1 ugt78d2* with and without feeding of naringenin. The mean values ± SE of six independent biological samples (pools of 4-6 plants per sample) are displayed. CA is cinnamic acid. ****p* < 0.001; paired *t*-tests. The experiment was repeated twice with similar results. *B*, expression of *PAL1* and *PAL2* genes in the *tt4 ugt78d1 ugt78d2* triple mutant after naringenin feeding relative to non-fed triple mutant by quantitative RT-PCR analysis. Expression levels were normalized using *S16* and *TUB9* transcripts. The graphics shows the fold changes estimated for each comparison individually with 95%-confidence intervals. The R software was used for calculation. Stars indicate significance of the difference to non-fed mutant plants: **p-value < 0.01. Data obtained from six biological samples (pools of 4-5 seedlings per sample) were shown. The experiment was repeated twice with similar results. *C*, detected flavonols (after acid hydrolysis) from *tt4 ugt78d1 ugt78d2* fed with naringenin by HPLC analysis. Abbreviations: Q, quercetin; K, kaempferol; I, isorhamnetin.

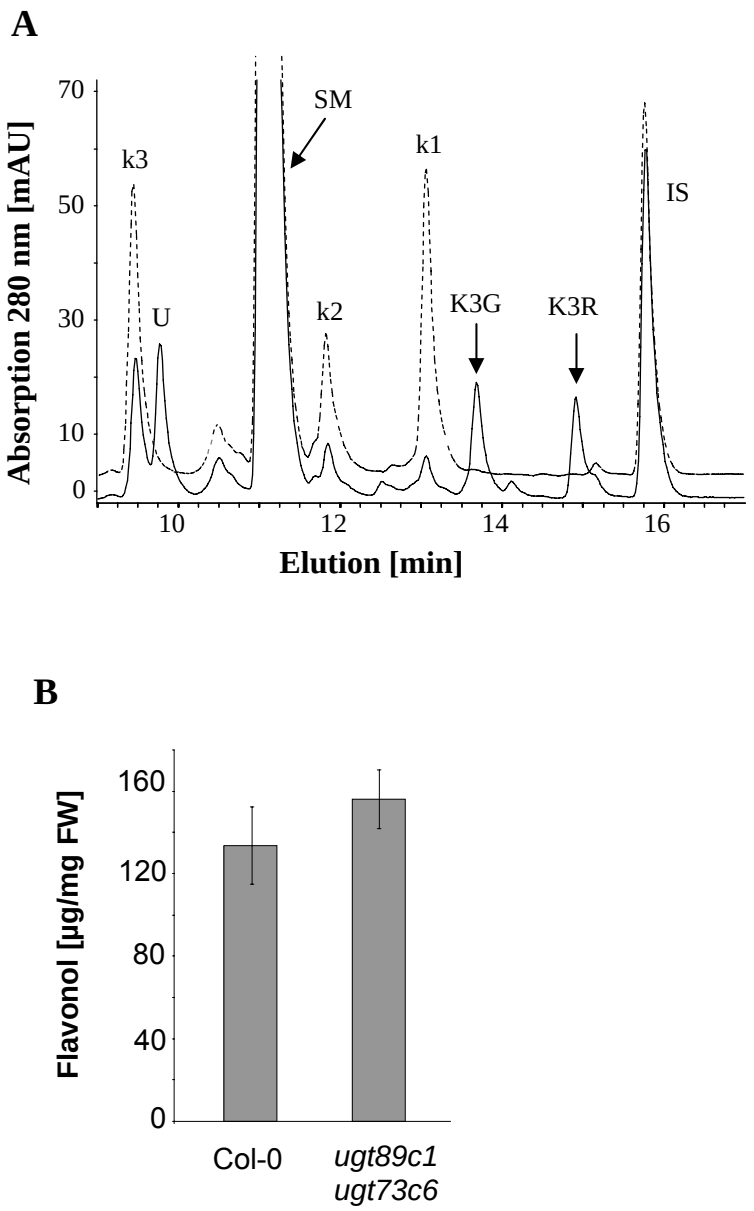

Figure 3. 9 Flavonol determination of *ugt89c1 ugt73c6* double mutant and Col-0 leaves. *A*. Representative HPLC diagrams of *ugt89c1 ugt73c6* and Col-0 (dashed line). Flavonols were extracted from the leaves of three-week-old plants. IS, internal standard (naringenin); SM, sinapoyl malate; U, unknown peak; K3G, kaempferol 3-*O*-monoglucoside; K3R, kaempferol 3-*O*-monorhamnoside. *B*. Total flavonol aglycone quantification after acid hydrolysis of the leaf extracts. Each bar represents the mean ± SD as determined by three independent experiments. FW, fresh weight.

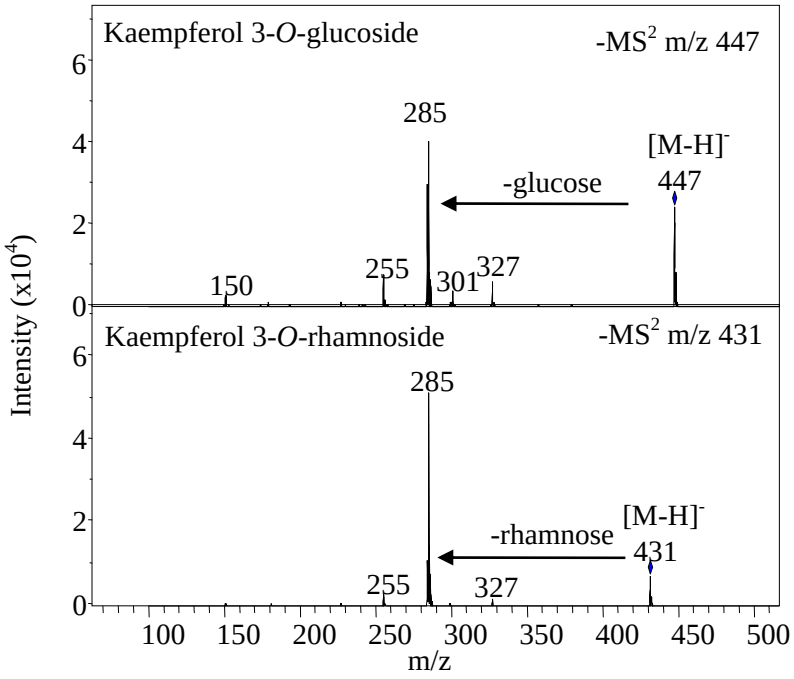

Figure 3. 10 The confirmation of kaempferol 3-*O*-monoglucoside and kaempferol 3-*O*-monorhamnoside by LC-MS analyses. The retention time and MS^2 spectra from *ugt89c1 ugt73c6* double mutant leaf extract and corresponding authentic standards (K3G and K3R) were identical.

3.4 DISCUSSION

A strongly compromised 3-*O*-glycosylation of flavonols led to a repression of the phenylpropanoid pathway and in particular the flavonol branch through transcriptional down-regulation of several biosynthetic key genes including *PAL1* and *CHS*. The wild-type PAL expression in *tt4 ugt78d1 ugt78d2* suggested that this feedback inhibition of PAL was not only linked to a suppression of flavonol biosynthesis due to a reduced initial 3-*O*-glycosylation, but at the same time dependent on an active flavonol aglycone formation. In contrast, no feedback inhibition of PAL expression occurred upon an almost complete loss of flavonol biosynthesis in *fls1*, instead an enhancement of *PAL* gene transcription was found (Figure 3. 4 & Figure 3. 7). Since the *ugt89c1 ugt73c6* double mutant, which is severely impaired in 7-*O*-glycosylation of flavonols, maintained wild-type PAL expression and total flavonol content, the feedback inhibition was specifically linked to the compromised 3-*O*-glycosylation step.

PAL1 and PAL2 control flavonol glycoside accumulation and lignin biosynthesis as demonstrated by analyzing the double mutant *pal1 pal2* (Rohde *et al*., 2004). I showed that a moderate reduction in PAL activity (about 40%) associated with a similar, about 50% reduction in *PAL1* transcription in *ugt78d1 ugt78d2* led to a strong decrease of the flavonol glycoside level (about 70%), whereas lignin biosynthesis appeared to be not affected. In contrast, the repression of lignin biosynthesis by silencing of hydroxycinnamoyl-CoA shikimate/quinate hydroxycinnamoyl transferase indicated a different link of the phenylpropanoid branches, since this blocking led to an increased production of flavonoids (Besseau *et al*., 2007). The apparently moderate repression of total PAL activity could still reflect a stronger suppression in relation to flavonol biosynthesis. First, even in the loss-of-function *pal1 pal2* line there was a 25% background level of residual PAL activity due to additional PAL isoforms (Rohde *et al*., 2004). In addition, flavonols are present mainly in epidermal cell layers, while lignin is more abundant in vascular tissues. Thus, it is conceivable that PAL expression in *ugt78d1 ugt78d2* was more severely repressed in flavonol synthesizing cells than in lignifying cells, which led to differential effects on the biosynthesis of flavonols and lignin. Two sinapate esters, sinapoyl malate and sinapoyl glucose, were not reduced in *pal1 pal2* leaves, but slightly decreased in *ugt78d1 ugt78d2* (Rohde *et al*., 2004) (Figure 3. 5B). This observation indicated that other genes were also affected in the production of sinapate esters in this glycosyltransferase double mutant.

The phenylpropanoid biosynthetic pathway is known to be metabolically regulated by phenylpropanoids. The transcription of *CHS* was shown to be inhibited by cinnamic acid, but stimulated by *p*-coumaric acid (Loake *et al.,* 1991; Loake *et al.,* 1992). PAL activity and transcription of *PAL* genes have been shown to be negatively regulated by its product cinnamic acid either via exogenous application of the compound or via blocking the downstream, cinnamic acid-metabolizing C4H activity (Bolwell 1986; Lamb 1979; Mavandad *et al.,* 1990; Blount *et al.,* 2000) (Figure 1. 4). In contrast to these known control mechanisms, a novel regulation was effective in *ugt78d1 ugt78d2* to repress PAL activity and flavonol biosynthesis. As deduced from the release of PAL repression upon completely blocking CHS in *tt4 ugt78d1 ugt78d2* and the restoration of inhibition by feeding of naringenin, the feedback regulation in *ugt78d1 ugt78d2* was rather dependent on flavonoids and a strongly compromised 3-*O*-glycosylation of flavonols. Moreover, this feedback inhibition did not only influence the committed steps of the phenylpropanoid and flavonoid pathways, but also several genes of the flavonoid branch and of flavonol-related steps of the general phenylpropanoid pathway. Within the general phenypropanoid pathway four active *4CL* genes have been identified in the genome of *A. thaliana*, for which different metabolic roles have been proposed. The isoforms 4CL1 and 4CL2 are considered to be important for

lignin biosynthesis, whereas 4CL3 is involved in flavonoid biosynthesis (Ehlting *et al.,* 1999; Costa *et al*., 2005). Consistent with the specific repression of flavonoids, only the transcription of 4CL3 was down-regulated in *ugt78d1 ugt78d2* (Figure 3. 3).

The transcriptional regulation of the phenylpropanoid pathway has been intensely studied. Several families of transcription factors, including R2R3-MYB, WD40, BZIP, WRKY, MADS-box and BHLH proteins, are involved in the control of general phenylpropanoid and flavonoid-biosynthetic genes (Stracke *et al*., 2007; Quattrocchio *et al*., 2006). The general phenypropanoid pathway and flavonoid biosyntheses are widely controlled by the PRODUCTION OF ANTHOCYANIN PIGMENT1 (PAP1/MYB75) transcription factor as well as related proteins. PAP1-overexpressing plants showed a coordinated up-regulation of *PAL1*, *4CL-like5*, *CHS*, *CHI*, *F3H*, *F3´H*, *DFR*, and *ANTHOCYANIN SYNTHASE* (Tohge *et al*., 2005; Borevitz *et al*., 2000). There is an additional level of control through flavonol-specific transcription factors, *i.e.* MYB11, MYB12 and MYB111, which activate transcription of *4CL3*, *CHS*, *CHI*, *F3H*, *F3'H* and *FLS1*(Stracke *et al*., 2007). The transcription factor MYBL2 on the other hand was found to suppress *e.g*. *CHS*, *F3H*, *F3'H*, and *DFR*, but not *CHI* (Dubos *et al*., 2008). Such a pattern was widely overlapping with the situation found in *ugt78d1 ugt78d2*, which repressed transcription of *CHS*, *F3'H* and *DFR*, but did not affect *CHI* (Figure 3. 3). These MYB transcription factors are also known to interact and depend on the other partners like BHLH proteins to generate the eventual readouts via such transcriptional networks (Ramsay *et al*., 2005; Nesi *et al*., 2001; Zimmermann *et al*., 2004). Thus, it is suggestive to hypothesize that the transcriptional repression of the genes observed in *ugt78d1 ugt78d2* is involving and is finally mediated by MYB factors and/or their combinatorial action with other proteins.

Although transcriptional regulation of *PAL* genes and *CHS* plays an import role, an additional, direct regulation at the protein level in *ugt78d1 ugt78d2* cannot be excluded. Although previous *in vitro* studies showing direct flavonol-protein interaction may not be completely transferable to an *in vivo* situation and may lack in part specificity, these reports point to the potential of the hydrophobic flavonols to interfere with enzymatic activities (Cos *et al*., 2001; Attridge *et al*., 1971; Sato and Sankawa 1983; Shimmyo *et al*., 2008). Since phenylpropanoid and flavonoid-biosynthetic enzymes have been proposed to be organized as multienzyme complexes (Winkel-Shirley 2004), any flavonol aglycone formed upon the strongly compromised 3-*O*-glycosylation in *ugt78d1 ugt78d2* could interact *in situ* with and inhibit PAL or other flavonoid-biosynthetic enzymes. Such low levels of flavonol aglycones could escape detection in leaf extracts (Table 3. 1). Alternatively, low and undetectable levels of flavonol aglycones *per se* or in combination with biosynthetic enzymes could also provide

a link to the specific transcriptional feedback regulation observed in *ugt78d1 ugt78d2*. Flavonols are known to bind to proteins including histones, mammalian DNA polymerases and nucleic acids and thus have the potential to interfere with gene transcription (Solimani 1997; Ramadass *et al*., 2003; Mizushina *et al.*, 2003). In plants, flavonols have been shown to directly or indirectly control the transcription of genes encoding auxin transporters (Peer *et al.,* 2004). Furthermore, flavonol metabolites as well as the cytosolic CHS and CHI proteins have been detected in nuclei of *Arabidopsis* cells (Saslowsky and Winkel-Shirley 2001; Saslowsky *et al.,* 2005). Thus, one could speculate that they were also involved in regulatory processes. Nevertheless, CHS being a major player with such a dual function is less likely based on the re-establishment of PAL repression in the CHS-lacking *tt4 ugt78d1 ugt78d2* line after feeding of naringenin. Although the molecular mechanism of flavonol-dependent feedback inhibition therefore remains obscure, this regulation may serve as a mean to avoid the accumulation of hydrophobic and potentially toxic flavonol aglycones.

4 Chapter 4: THE OVER-ACCUMULATION OF KAEMPFEROL 3-*O*-RHAMNOSIDE-7-*O*-RHAMNOSIDE IN THE UGT78D2 MUTANT RESULTS IN DECREASED BASIPETAL AUXIN TRANSPORT AND PLANT GROWTH DEFECTS

4.1 ABSTRACT

Flavonoids and in particular flavonols have been postulated to modulate auxin transport. However, the active flavonoids involved in this process have not yet been identified in plants. The *ugt78d2* mutant, which is defective in flavonoid 3-*O*-glucosylation and possesses an altered flavonol glycoside pattern, showed severe shoot growth defects including dwarfism and loss of apical dominancy. The *ugt78d2* growth defects were eliminated by blocking flavonoid biosynthesis, suggesting that they were flavonoid-dependent. The modular combination of mutants in flavonoid biosynthesis or glycosylation and their flavonol glycoside profiles identified kaempferol 3-*O*-rhamnoside-7-*O*-rhamnoside (k1) as the *ugt78d2* phenotype-inducing metabolite. Furthermore, basipetal auxin transport was reduced in the k1-overaccumulating *ugt78d2* mutant. Preliminary data showed that auxin transport was almost revered to wild-type level in an *ugt78d2* mutant complemented line. The expression of *UGT78D1*, which is required for the synthesis of k1, was detected in all the tissues examined, but particularly high in the tissues where the modulation of auxin transport by flavonoids occurs. These results suggest that k1 is an endogenous auxin transport inhibitor.

4.2 INTRODUCTION

The phytohormone auxin, or indole-3-acetic acid (IAA), plays an important role in plant growth and development. Auxin needs to be transported from the sites of synthesis mainly in the apices to distal parts of the plants to exert its function (Berleth *et al.* 2007). So far, a number of auxin transporters including ABC transporters (ABCB1/PGP1, ABCB4/MDR4, ABCB19/PGP19), AUX1/LAX family members (LAX1, LAX2, and LAX3), and PIN proteins (PIN1-PIN8) have been well characterized (reviewed in Friml 2003 and Zažímalová *et al.,* 2010). However, to understand how auxin is transported into different parts of the plant, we need to extend our understanding of the regulation of this process.

Flavonoids, in particular flavonols, have been suggested to modulate auxin transport, because flavonol aglycones were shown to be able to displace binding of synthetic auxin transport inhibitors *in vitro* and the supply of flavonol aglycones to detached zucchini hypocotyls or clover roots resulted in decreased polar auxin transport (Jacobs and Rubery, 1988; Mathesius *et al*., 1998; Morris 2000). Further *in vivo* evidence for the modulation of auxin transport by flavonoids was obtained mainly by analyzing auxin transport in three *Arabidopsis transparent testa* (*tt*) mutants, i.e. *tt3*, *tt4* and *tt7*, which are defective in various steps of flavonoid biosynthesis. No flavonoids are synthesized in *tt4*, as it is lacking chalcone synthase catalyzing the committed step of flavonoid biosynthesis. Enhanced level of kaempferols, but no quercetins are formed in *tt7* devoid of flavonol 3´-hydroxylase. Flavonols, but no anthocyanins accumulate in *tt3*, where dihydroflavonol reductase is missing (Figure 4. 1) (Shirley *et al.*, 1995). Auxin transport in the *tt4* mutant was elevated compared to wild type, while the flavonol-overproducing mutant *tt3* exhibited reduced auxin transport (Brown *et al.*, 2001; Peer *et al.*, 2004; Buer *et al.,* 2004). Interestingly *tt7*, which accumulates exclusively kaempferol conjugates, exhibited reduced auxin transport, suggesting the involvement of kaempferol derivatives in the inhibition of auxin transport (Peer *et al.*, 2004). Despite these substantial pieces of evidence supporting a role of flavonols in the modulation of auxin transport, specific flavonol aglycones or derivatives being active in this process have not been pinpointed in plants so far.

The biosynthesis of flavonoids is tissue specific, developmentally regulated and dependent on environmental factors, e.g. light and temperature (Taylor and Grotewold 2005; Shirley 2006). *Arabidopsis* plants accumulate different subclasses of flavonoids, i.e. flavonols, anthocyanins and proanthocyanins, in a spatiotemporal manner. Virtually all the organs contain flavonols. Anthocyanins accumulate in organs such as hypocotyls of emerging seedlings, leaves, stems, siliques and seed coats. The accumulation of proanthocyanins is confined to the endothelial cell layer of the seed coat.

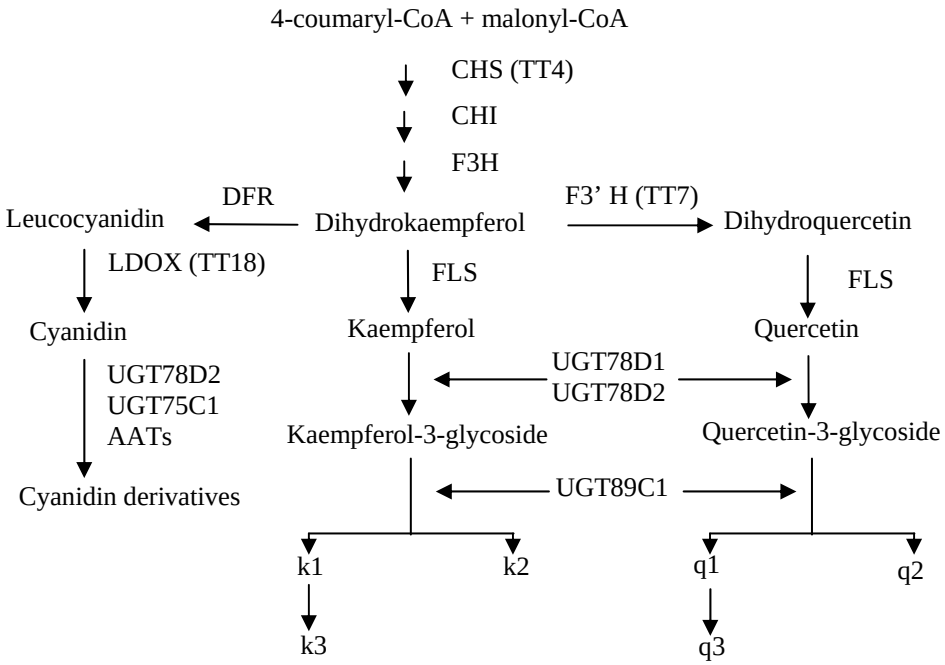

Figure 4. 1 The *Arabidopsis* flavonoid biosynthesis pathway.
LDOX, leucoanthocyanidin dioxygenase; TT18, transparent testa 18; UGT75C1, anthocyanin 5-*O*-glucosyltransferase; AATs, anthocyanin acyltransferase. Major flavonol glycosides: k1, kaempferol 3-*O*-rhamnoside-7-*O*-rhamnoside; k2, kaempferol 3-*O*-glucoside-7-*O*-rhamnoside; k3, kaempferol 3-*O*-rhamnosyl (1->2) glucoside-7-*O*-rhamnoside; q1, quercetin 3-*O*-rhamnoside-7-*O*-rhamnoside; q2, quercetin 3-*O*-glucoside-7-*O*-rhamnoside; q3, quercetin 3-*O*-rhamnosyl (1->2) glucoside-7-*O*-rhamnoside.

In *Arabidopsis* cells, flavonols usually are glycosylated. Five UDP-dependent glycosyltransferases (UGTs) including UGT78D1, UGT78D2, UGT78D3, UGT73C6 and UGT89C1 have been demonstrated to be involved in flavonol glycosylation (Figure 4. 1) (Jones *et al*., 2003; Tohge *et al*., 2005; Yonekura-Sakakibara *et al.,* 2007; Yonekura-Sakakibara *et al.,* 2008). The high degree of specificity of these five UGTs and the uniqueness of UGT78D1 and UGT89C1 for 3-*O*-rhamnosylation and 7-*O*-rhamnosylation, respectively, greatly facilitate to genetically manipulate *Arabidopsis* plants to synthesize or deplete specific flavonol glycosides. Recently, a comprehensive flavonol glycoside analysis revealed that flavonol glycosides are distributed in an organ-dependent manner (Yonekura-Sakakibara *et al.,* 2008). In contrast to flowers, the flavonol pattern in leaves and particularly in inflorescence stems was rather simple. Only three kaempferol glycosides and three structurally equivalent quercetin glycosides were detected in stems (Yonekura-Sakakibara *et al.*, 2008).

In this work, I showed that the loss of the flavonoid-3-*O*-glucosyltransferase UGT78D2 led to a reduced plant height and increased branching. Blocking flavonoid biosynthesis and/ or conjugation at specific positions clearly related the excess accumulation of kaempferol 3-*O*-rhamnoside-7-O-rhamnoside (k1) to the growth defects of *ugt78d2*. Since basipetal auxin transport in k1 over-accumulating influorescence stems was repressed, the genetic study also proposed that k1 acts as an endogenous auxin transport inhibitor.

4.3 RESULTS

4.3.1 Height and stature of *ugt78d2* plants are altered

Bolting of the *ugt78d2* mutant inflorescence stem was delayed about 2-3 days on average relative to wild type. The mutant eventually reached only about 50% of wild-type height (Figure 4. 2 A, B, D & E). To elucidate the underlying mechanism of this dwarfism, cellular architecture of both the mutant and wild-type inflorescence stem was compared. In *ugt78d2*, cell length was significantly reduced compared to the wild type (Table 4. 1). Its vascular system showed no obvious anatomical aberrations, but contained an increased number of vascular bundles (Kerstin Schuster, unpublished data) At a later growth stage, *ugt78d2* developed more lateral and axillary branches, indicating that apical dominance was reduced (Figure 4. 2D,E & Table 4. 1). The reduction in length of the *ugt78d2* lateral branches was not as pronounced as that of the primary stem. The silique length of *ugt78d2* was similar to wild type (Table 4. 1). Complementation of *ugt78d2* with a genomic fragment covering the complete *UGT78D2* gene led to a reversion of the observed *ugt78d2* growth phenotype to wild-type appearance and reverted the altered flavonol glycosides to a wildtype-like pattern (Figure 4. 2 C, F & Figure 4. 3a). Thus, the lesion in *UGT78D2* was responsible for the observed growth defects of *ugt78d2*.

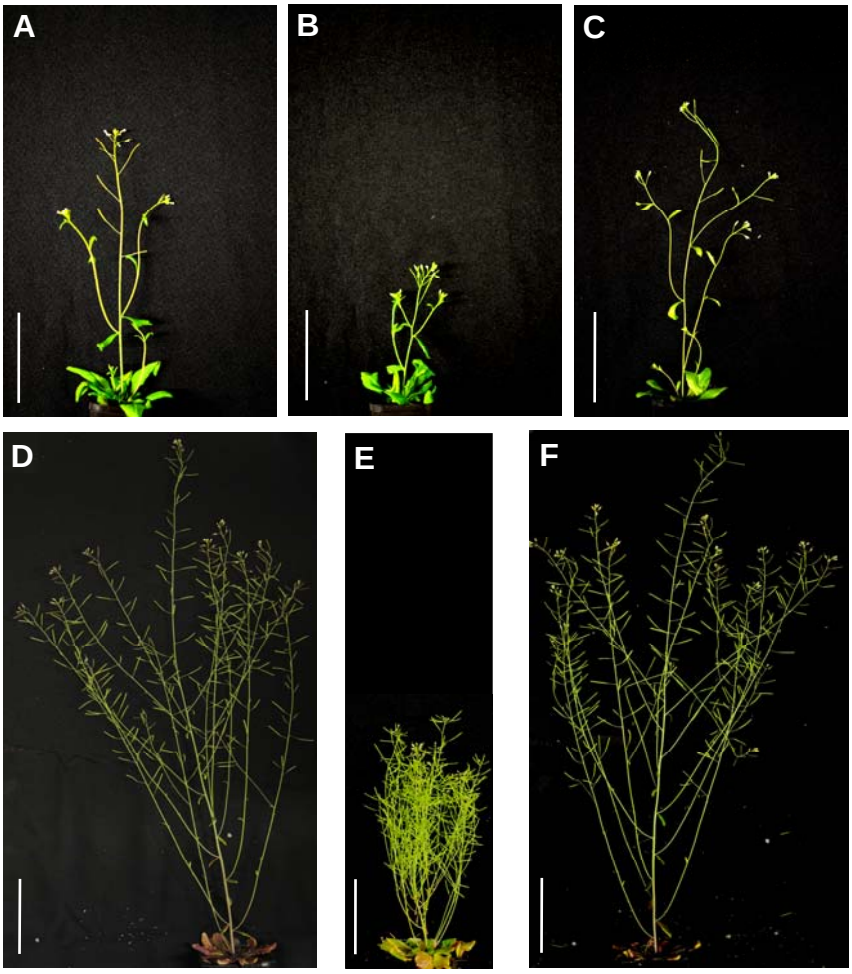

Figure 4. 2 The growth defects of the *ugt78d2* mutant.

(A-C) The *ugt78d2* mutant (B) has partially lost apical dominance and is dwarfed compared to wild-type plants (A). The *ugt78d2* mutant can be complemented by a genomic fragment containing the *UGT78D2* gene (C). Pictures were taken after 28 days of growth. Scale bar, 5 cm.

(D-F) The *ugt78d2* mutant (E) growth defects are more pronounced compared with wild-type plants (D) at a later growth stage. (F) depicted here is a genetically complemented plant. Pictures were taken after 50 days of growth. Scale bar, 5 cm.

Table 4. 1 Phenotypic analysis of Col-0 and *ugt78d2* plants.

	Col-0	*ugt78d2*
Length of Primary inflorescence (cm)	35.3 ± 0.9	17.7 ± 0.8 **
Length of lateral branches (cm)	22.3 ± 2.4	16.2 ± 0.8 **
Number of lateral branches	5.3 ± 0.4	9.0 ± 0.5 **
Number of axillary branches	0.1 ± 0.1	3.2 ± 0.6 **
Length of siliques (mm)	12.2 ± 0.3	12.3 ± 0.3
Length of parenchyma cells (μm)	186.1 ± 3.7	158.9 ± 3.3**

For the first five traits ten individual 50-day-old plants were analyzed. For parenchyma cell length measurement, basal stems from five individual 33-day-old plants of each genotype were analyzed by microscopy. About 30 cells of each stem segment were measured. The mean values ± SE are displayed. Statistical analyses were performed by a paired t-test for uneven variance for each trait between these two genotypes (**$p < 0.01$). The experiment of cell length measurement was repeated three times with similar results. The parenchyma cell length measurements were performed by Kerstin Schuster.

4.3.2 The *ugt78d2* growth defects are flavonoid-dependent

As UGT78D2 had been characterized as a flavonoid 3-*O*-glucosyltransferase (Tohge *et al.,* 2005; Lee *et al.,* 2005), it was possible that the altered flavonoid glycoside pattern in *ugt78d2* plants caused the *ugt78d2* phenotype. To test this possibility, a flavonoid-deficient *tt4 ugt78d2* double mutant was generated (Figure 4. 3A). The growth defects in *ugt78d2* were eliminated in *tt4 ugt78d2*, indicating that they were flavonoid-dependent (Figure 4. 4).

4.3.3 Kaempferol 3-*O*-rhamnoside-7-*O*-rhamnoside is the *ugt78d2* phenotype-inducing flavonol

To identify the *ugt78d2* phenotype-inducing flavonoid, a genetic approach using various mutants defective in flavonol biosynthetic and/or conjugating steps was employed in order to link specific flavonol glycoside patterns in stems to growth phenotypes. Similar to the recently published data obtained by LC-MS analyses, only six flavonol glycosides were detected in wild-type stem extracts (Figure 4. 3A) (Yonekura-Sakakibara *et al.,* 2008). Three kaempferol glycosides (k1-k3) were the most abundant flavonols, while three quercetin glycosides (q1-q3) were present at much lower levels. No flavonol aglycones were detected. The flavonol glycoside pattern of *ugt78d2* was altered. In accordance with the loss of the 3-*O*-glucosyltransferase activity the 3-*O*-glucoside derivatives (k2, k3, q2 and q3) were strongly repressed, whereas the 3-*O*-rhamnoside derivatives k1 and q1 were elevated compared to the wild-type counterpart (Figure 4. 3A). A similar alteration of the flavonol glycoside pattern in *ugt78d2* was also observed in leaves (Tohge *et al.,* 2005). k1 and q1 were positively correlated with the *ugt78d2* growth defects, and hence, were good candidates for inducing the *ugt78d2* phenotype.

Both k1 and q1 contain a 3-*O*-rhamnosyl and a 7-*O*-rhamnosyl residue. These features offered the opportunity to examine by depletion of either of these two conjugating residues whether k1 and q1 were the true *ugt78d2* phenotype-inducing flavonol glycosides. The attachment of the 3-*O*- and 7-*O*-rhamnosyl residues to both k1 and q1 is catalyzed by

UGT78D1 and UGT89C1, respectively (Jones *et al.,* 2003; Yonekura-Sakakibara *et al.* 2008). Thus, either knock-out of *UGT78D1* or *UGT89C1* would compromise the biosynthesis of k1 and q1 and would allow testing the role of k1 and q1 in the development of the *ugt78d2* growth defects. The effect of the *ugt89c1* mutation on the accumulation of k1 and q1 was confirmed in the *ugt78d2 ugt89c1* double mutant. None of the six flavonol glycosides (k1-k3, q1-q3) were detected, yet new ones accumulated in the *ugt78d2 ugt89c1* double mutant (Figure 4. 3A). It did not develop any *ugt78d2*-like phenotype (Figure 4. 4).

Likewise, *ugt78d1 ugt78d2* double mutant plants did not develop any *ugt78d2*-like phenotype (Figure 4. 4). Among the six common flavonol derivatives only the formation of the 3-*O*-rhamnosylated k1 and q1 is dependent on UGT78D1. Accordingly, the *ugt78d1 ugt78d2* double mutant turned out to be devoid of k1 and q1 (Figure 4. 3A). Thus, eliminating either 3-*O*- or 7-*O*-rhamnosylation and thereby depleting both k1 and q1 supported the notion that k1 and/or q1 were inducing the *ugt78d2* growth phenotype.

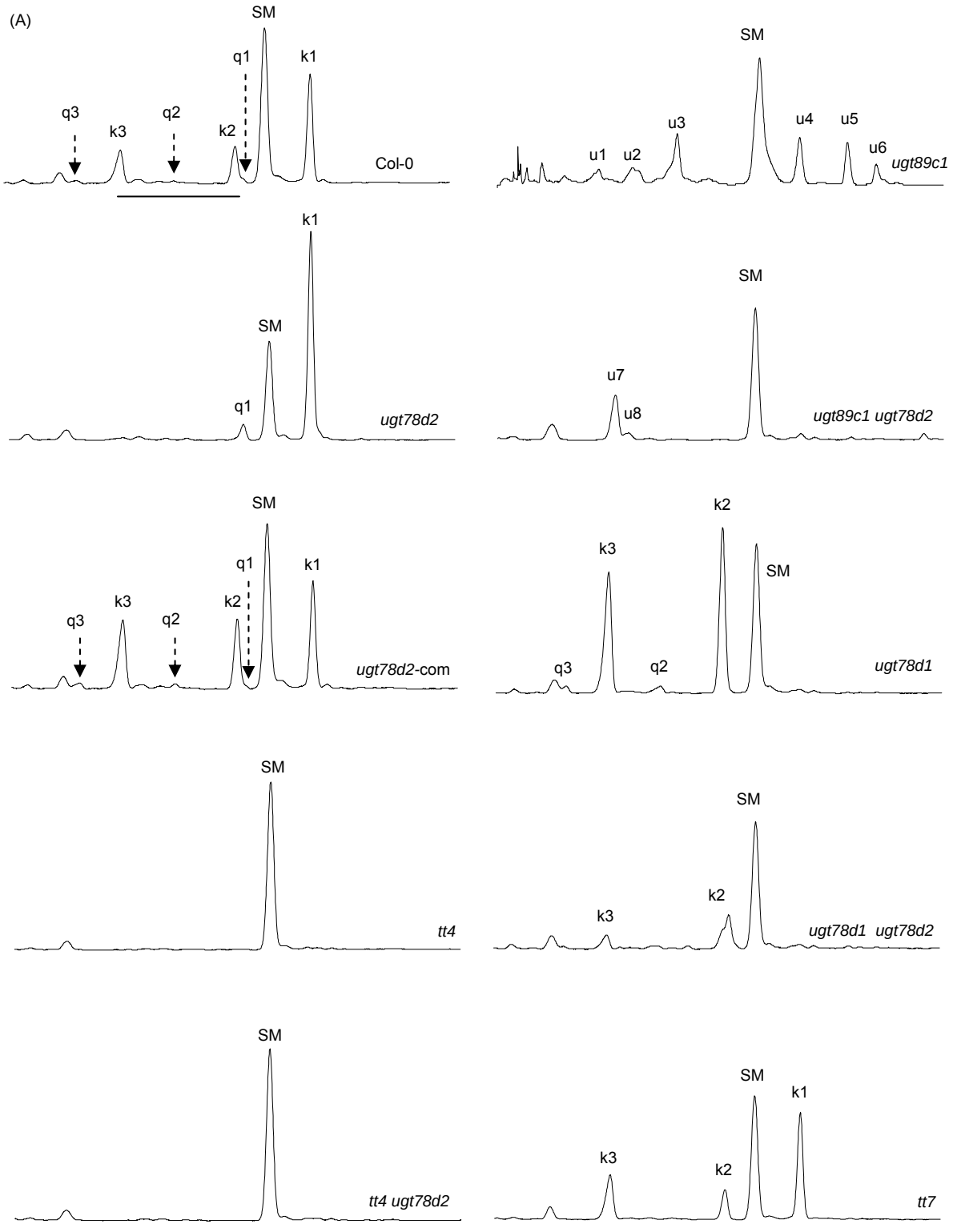

continued on next page

Figure 4. 3 continued

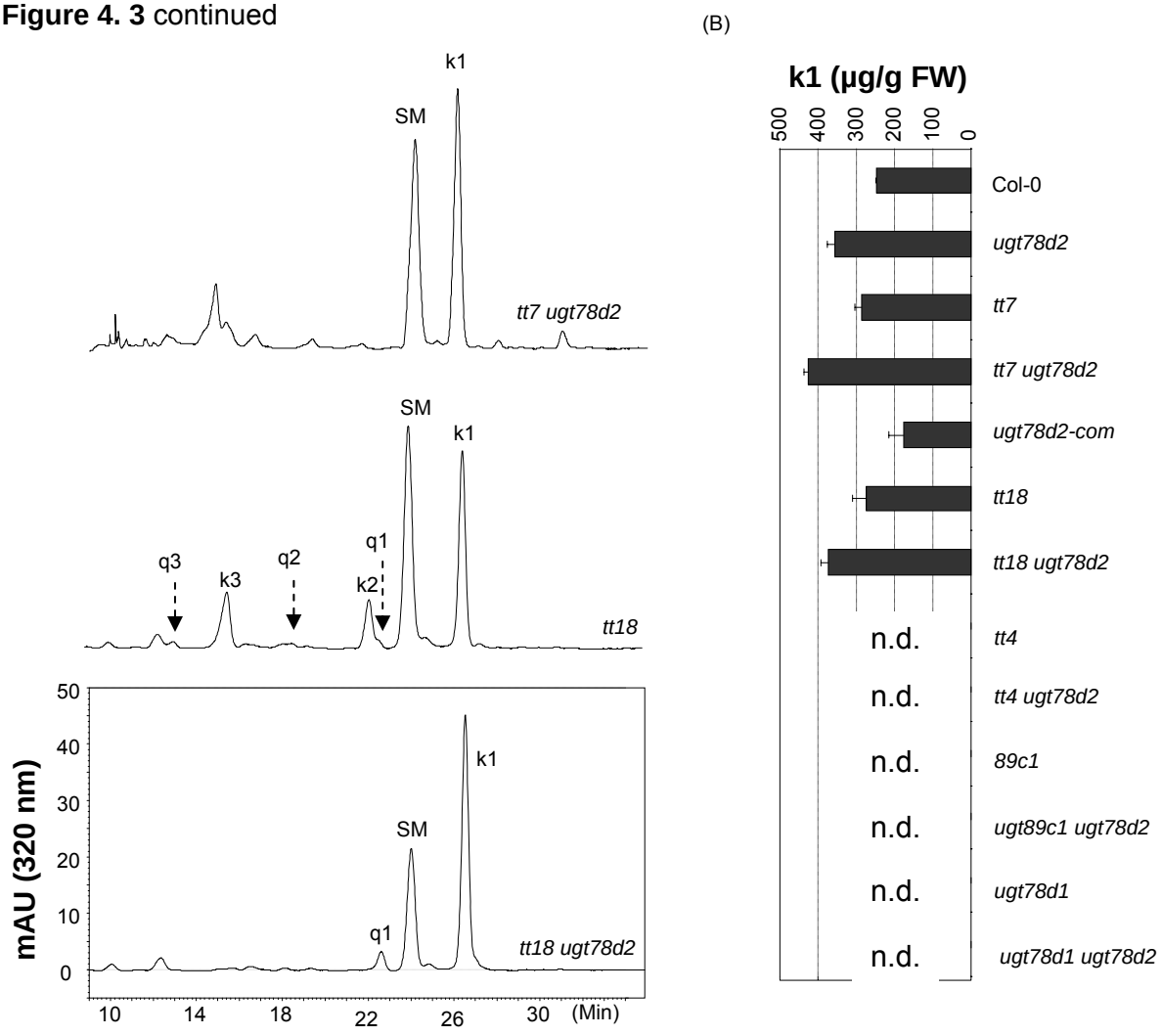

Figure 4. 3 Flavonol analyses in various mutants by HPLC.

(A) Representative chromatograms of flavonols from Col-0 and various mutants. The scale of all chromatograms is the same as in the last one. *ugt78d2*-com represents an *ugt78d2* mutant genetically complemented line. Kaempferol (k) and quercetin (q) glycosides were identified by their retention times as well as UV-spectra. The published flavonol glycoside patterns of various mutants are also referred to for flavonol identification (Jones *et al.,* 2003; Tohge *et al.,* 2005; Yonekura-Sakakibra *et al.,* 2008). u1-u8 represent unknown flavonoids according to their UV spectra. SM represents sinapoyl malate. k2 and q1 were eluted close to each other. q1 appears as a shoulder of the k2 peak.

(B) Quantification of k1. The mean of k1 ± standard deviation from 4 biological samples (a pool of 3-5 individual stem segments for one sample) are shown. Basal stems of 28-day-old plants were used for flavonol analyses. n.d., not detectable.

To further distinguish whether k1 and/or q1 were the causal metabolites leading to the *ugt78d2* growth phenotype, a *tt7 ugt78d2* double mutant was generated. The conversion of kaempferol into quercetin was blocked in *tt7*, thus kaempferols including k1 were increased,

whereas quercetins including q1 were absent (Figure 4. 3A) (Schoenbohm *et al.,* 2000; Abrahams *et al.,* 2002). This effect of the *tt7* mutation on the accumulation of k1 and q1 was maintained in the *tt7 ugt78d2* double mutant, which accumulated an even higher amount of k1 than the *ugt78d2* mutant and was devoid of q1 (Figure 4. 3A,B). *tt7 ugt78d2* was more severely dwarfed than *ugt78d2*, indicating that a further enhanced k1 level led to a more severe *ugt78d2*-like phenotype. Interestingly, the lateral branches of *tt7 ugt78d2* were strikingly shorter than those of *ugt78d2*. These observations indicated that the development of the *ugt78d2* growth defects was independent of quercetin derivatives. Together, these results demonstrated that k1 was sufficient to induce the *ugt78d2* phenotype.

4.3.4 Anthocyanins are not responsible for the *ugt78d2* growth defects

Besides flavonol aglycones, UGT78D2 also recognizes anthocyanidins as substrate (Tohge *et al.*, 2005; Lee *et al.,* 2005). Therefore, it was possible that anthocyanins were also involved in the development of *ugt78d2* growth defects. To test this possibility, an anthocyanin-deficient *tt18 ugt78d2* double mutant was generated. The anthocyanin-deficient *tt18* single mutant, devoid of anthocyanidin synthase, did not develop any *ugt78d2*-like growth defects, whereas the growth defects of *ugt78d2* were retained in the *tt18 ugt78d2* double mutant (Figure 4. 4). The flavonol glycoside pattern of *tt18 ugt78d2* was similar to that of *ugt78d2* (Figure 4. 3A). These observations indicated that anthocyanins were not responsible for the *ugt78d2* growth defects.

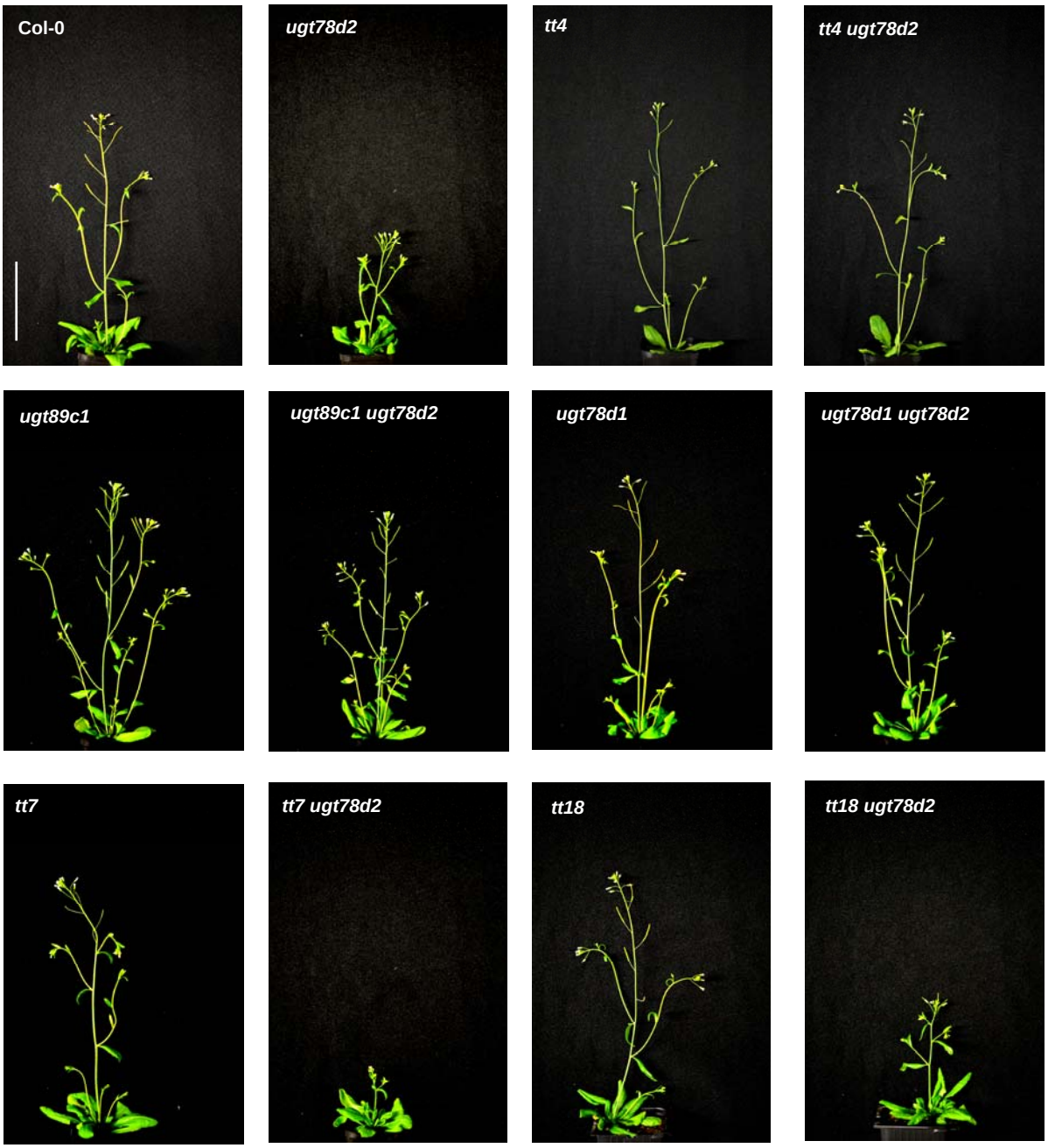

Figure 4. 4 Depicting *ugt78d2*-like growth defects of various mutants.

Wild type (Col-0) and various mutant plants were grown under long-day conditions at ~ 230 µmol m^{-2} sec^{-1}, and were photographed for shoot morphological phenotype after 28 days of growth. Scale bar, 5 cm.

4.3.5 Basipetal auxin transport is reduced in inflorescence stem of *ugt78d2*

The *ugt78d2* growth phenotype resembled to a variable extent *pgp1 pgp19* and *twd1*, which are greatly impaired in auxin transport (Noh *et al.,* 2001; Geisler *et al.,* 2003). As flavonols have been postulated to be endogenous auxin transport inhibitors, I reasoned that the altered flavonol glycoside pattern in *ugt78d2* influenced auxin transport in inflorescence stems, which led to the growth defects. Therefore, polar transport of [^{3}H]-IAA was compared in *ugt78d2* and wild-type plants. Basal stem segments were chosen for the experiment, because the emergence of side-branches as well as pedicels from stem segments close to the inflorescence apex might interfere with the auxin transport assay. The flavonol glycoside pattern was examined in adjacent segments along the primary stem. Importantly, the pattern was similar for all the segments, but the upper segment accumulated a higher level of flavonol glycosides than the lower ones (Figure 4. 5).

Basipetal auxin transport was significantly reduced to about 45% of the wild-type level in *ugt78d2* (Figure 4. 6). The low levels of acropetal auxin transport did not differ in wild type and mutant (Figure 4. 7). The auxin transport inhibitor 1-naphthylphthalamic acid (NPA) almost completely blocked basipetal auxin transport in both *ugt78d2* and wild-type stems. Thus, *ugt78d2* exhibited a strongly reduced NPA-sensitive basipetal auxin transport in its inflorescence stems.

Preliminary data were also obtained for *tt7 ugt78d2* and *ugt78d2* genetically complemented line. The *tt7 ugt78d2* double mutant, which had a further enhanced k1 level, showed a more pronounced reduction in basipetal auxin transport activity (Figure 4. 6). Thus, basipetal auxin transport activity appeared to be inversely correlated with k1 content. However, whether auxin transport could be reverted to wild-type level in the *ugt78d2* mutant genetically complemented plants need further assays, as preliminary data showed a discrepancy among the independed complementation lines. One line can complement, whereas another obviously not. This discrepancy might due to the over-complementaion, which can lead to the production of excess k2 and k3 (Figure 4. 3). These k2, k3 might inhibit auxin transport.

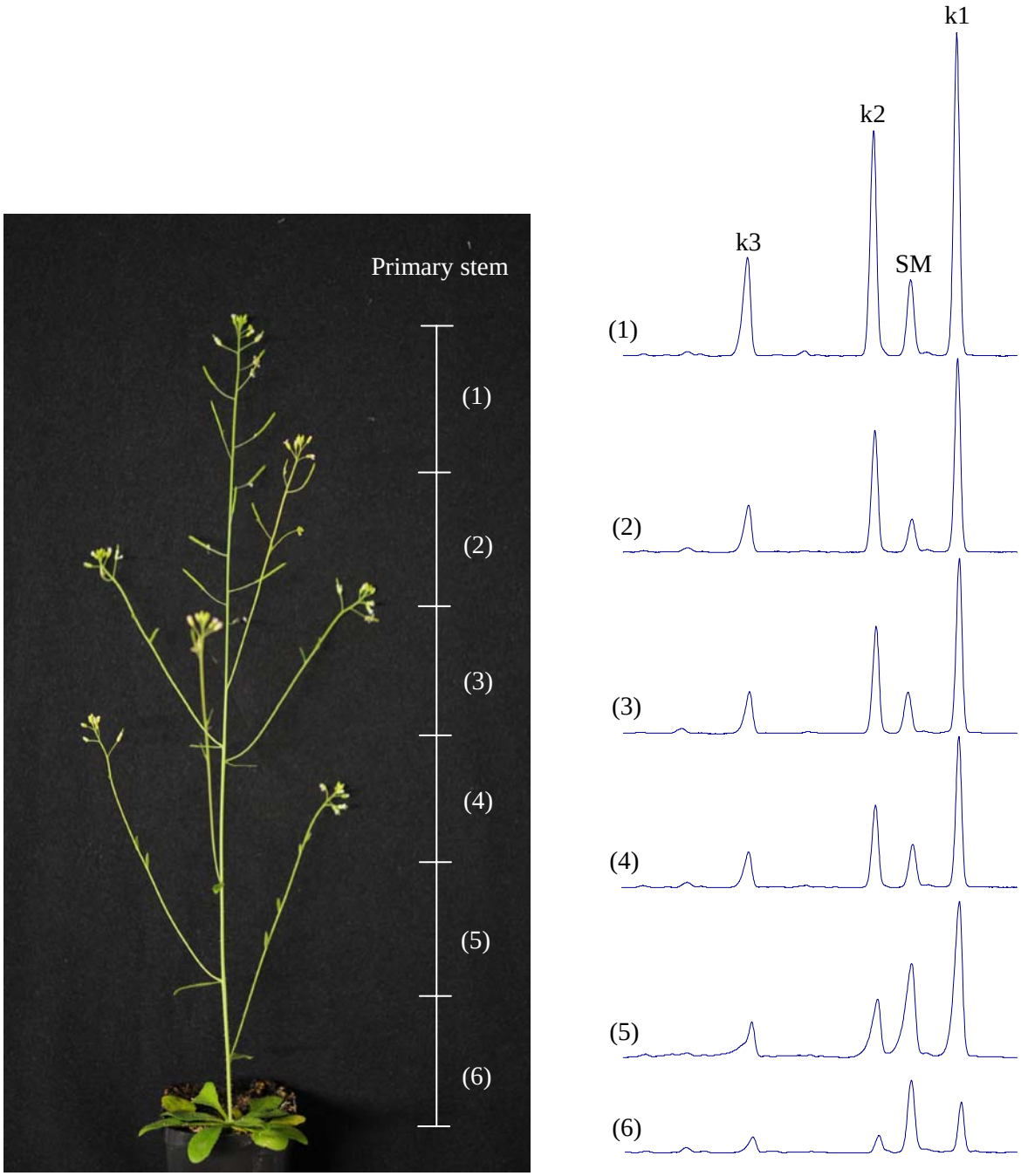

Figure 4. 5 Flavonol glycoside pattern in consecutive primary stem segments of Col-0 plants. Primary stems were cut in six segments with each segment approximately 2.5 cm long. Flavonol glycosides were analyzed by HPLC. All the chromatograms were adjusted to the same scale. k1-k3 represent the three major kaempferol glycosides. q1-q3 are not indicated due to low abundance. SM represents sinapoyl malate.

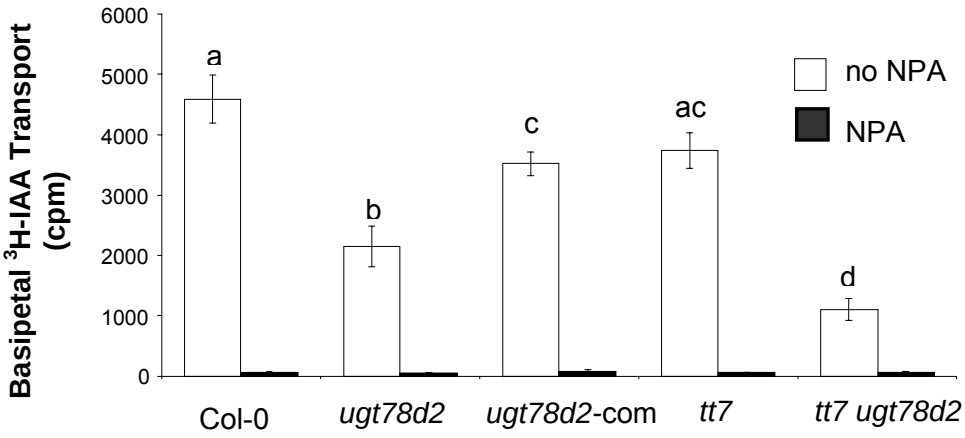

Figure 4. 6 Basipetal auxin transport activity in inflorescence stems.
ugt78d2-com represents a genetically complemented line. Data are presented as mean ± SE obtained from ten individual plants without NPA treatment. For NPA treatment, data were obtained from two individual plants. All genotypes not treated with NPA were compared against each other by a paired t-test. The same letters above the error bars indicate that there is no significant difference between genotypes ($p>0.05$), whereas different letters represent a significant difference between genotypes ($p<0.05$). (These experiments were performed together, but mainly by Kerstin Schuster).

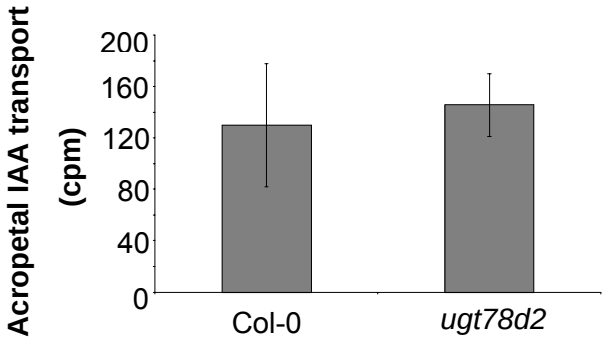

Figure 4. 7 Acropetal auxin transport activity in inflorescence stems of Col-0 and *ugt78d2*. Mean values are shown by the columns, and the standard deviations are indicated by the error bars. Data collected from ten individual plants are shown here. These experiments were repeated twice with similar results.

4.3.6 Free IAA quantification in WT and *ugt78d2* plants

To examine whether the reduced auxin transport influenced IAA homeostasis in *ugt78d2* stems, the endogenous levels of free IAA in three consecutive stem segments of *ugt78d2* and wild type were compared. The endogenous levels of free IAA in the inflorescence apex segments were not different from wild type levels ($p > 0.05$), whereas the middle and basal stems of *ugt78d2* contained lower steady-state IAA levels than the wild-type counterparts ($p < 0.05$; Table 4. 2), suggesting that the decreased IAA in the lower parts of the inflorescence stem of *ugt78d2* was due to reduced basipetal auxin transport.

Table 4. 2 Free IAA quantification in *Arabidopsis* inflorescence stem segments

	Apical segment	Middle segment	Basal segment
WT	207 ± 50	253 ± 23	247 ± 27
ugt78d2	194 ± 17	118 ± 14 **	142 ± 18 *

Stem segments of 2.5 cm length from different locations of the inflorescence stems were collected for free IAA quantification (pmol/g FW). The mean values ± SE of three independent biological samples (one sample is a pool of 4-6 individual stem segments) are displayed. Statistical analyses were performed by a paired t-test for uneven variance for each part of the stem between these two genotypes (*$p < 0.05$).

4.3.7 Expression profile of *UGT78D1* points to k1 as an endogenous auxin transport inhibitor

In *Arabidopsis* seedlings, flavonoids were shown to directly modulate auxin transport at the sites of auxin synthesis (shoot apex) and redirection (root tip) (Peer *et al*., 2004). If k1 was an endogenous auxin transport inhibitor, then k1 should be localized in those regions. Since the expression of *UGT78D1* is essential for the formation of k1 (Jones *et al.,* 2003), it was interesting to examine its expression pattern in more detail. A survey of publicly available microarray data using the *Arabidopsis* eFP Browser (bar.utoronto.ca) revealed that the expression of *UGT78D1* was high in the shoot apex during vegetative growth and particularly high in the inflorescence shoot apex (Figure 4. 8) (Schmid *et al*., 2005; Winter *et al*., 2007). This shoot apex specific expression of *UGT78D1* was confirmed by analyzing promoter::*GUS* fusions of young seedlings (Figure 4. 9a). Moreover, the expression of *UGT78D1* was also observed at root tips (Figure 4. 9b). Thus the expression of *UGT78D1* would be in agreement with k1 acting as an endogenous auxin transport modulator.

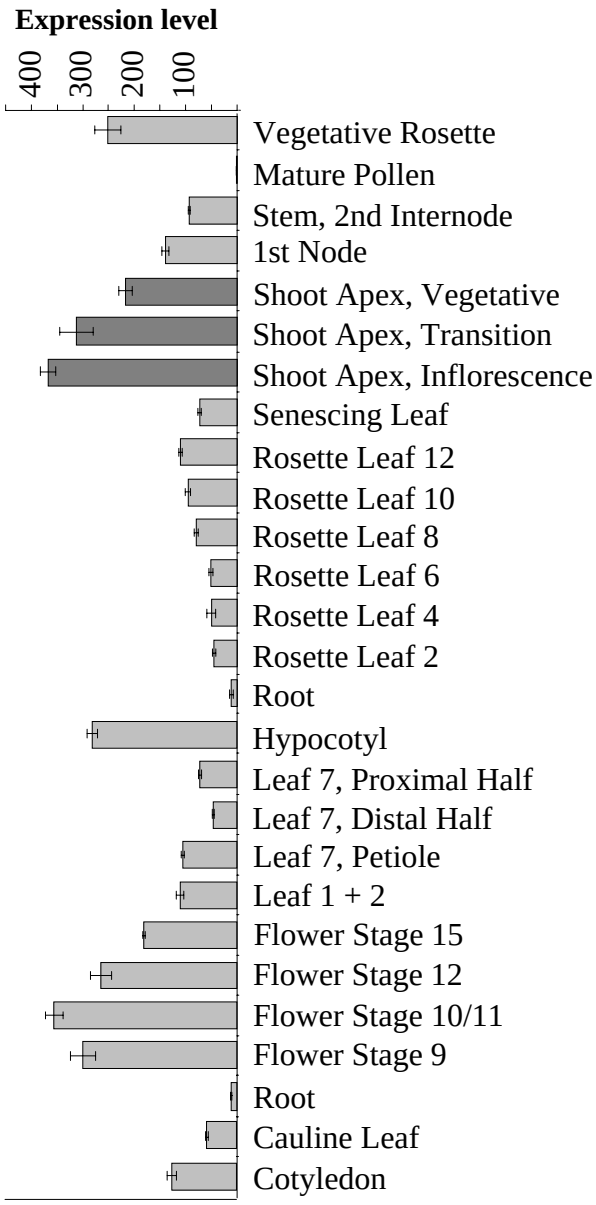

Figure 4. 8 Data from the public microarray database for *UGT78D1* gene obtained using the *Arabidopsis* eFP Browser (Schmid *et al*., 2005; Winter *et al*., 2007). Particularly high expression was observed in shoot apices (black columns).

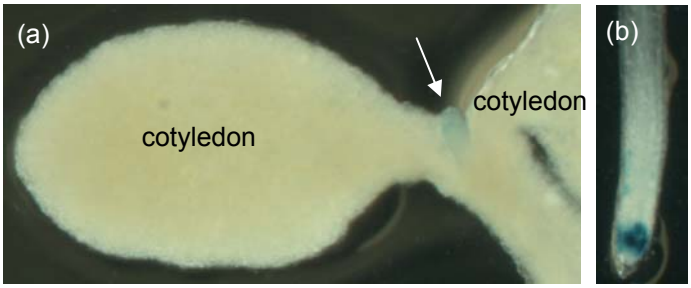

Figure 4. 9 Tissue specific expression of *UGT78D1*.
Three-day-old transgenic plants harbouring *promoter*$_{UGT78D1}$*:GUS-GFP* construct analyzed by histochemical staining with 5-bromo-4-chloro-3-indolyl-β-D-glucuronide. The expression of *UGT78D1* was mainly detected in the shoot apex (a) and root tips (b). Arrow indicates expression at the shoot apex.

4.4 DISCUSSION

4.4.1 The role of k1 in repressing plant growth

In this work, the growth defects of *ugt78d2* could be related to the accumulation of k1, kaempferol-3-*O*-rhamnoside-7-*O*-rhammoside, by several pieces of evidence. First, the accumulation of k1 was positively correlated with the *ugt78d2* growth defects. Second, the requirement of k1 for the development of *ugt78d2*-like growth defects was tested by depleting either its 3-*O*-rhamnosyl or 7-*O*-rhamnosyl residue in *ugt78d1 ugt78d2* and *ugt78d2 ugt89c1,* respectively. Last, a further increase of k1 quantity led to more severe *ugt78d2*-like growth defects in the *tt7 ugt78d2* double mutant.

The identification of k1 through a genetic approach was greatly facilitated by two features of *Arabidopsis*. The enzymes in the central flavonoid pathway, including CHS, CHI, F3H, F3'H, DFR and LDOX, are encoded by single genes with only one exception (FLS), which enables to genetically block specific branches of the flavonoid pathway (Lillo *et al*., 2008; Owens *et al.,* 2008). Furthermore, many flavonoid glycosyltransferases have already been identified. Since they exhibit strict specificity for the respective sugar donors it is possible to genetically manipulate the formation or depletion of specific flavonol glycosides. This genetic approach was superior to feeding experiments, where an administered chemical would be metabolized by endogenous enzymatic activities.

k1 and q1 are very similar in chemical structure with q1 carrying one additional hydroxyl group in its B-ring in comparison to k1. However, by examining *tt7 ugt78d2*, q1 was shown to be dispensable for developing *ugt78d2*-like growth defects.

In wild-type plants (Columbia accession) k1 is the most abundant flavonol glycoside in inflorescence stems (Figure 4. 3). A slight increase of k1 in *tt7* did not obviously influence plant growth (Figure 4. 3 and Figure 4. 4). However, a stronger increase of k1 as observed in *ugt78d2* led to obvious growth defects, which were even more severe along with a further enhancement of k1 levels in *tt7 ugt78d2*. Interestingly, the absence of k1 in other mutants, e.g. *tt4, ugt78d1,* or *ugt89c1,* did not obviously influence plant growth under our growth

conditions; in particular it did not have an enhancing effect. These observations suggested that wild-type levels of k1 were tolerated without any impact, yet starting from a threshold above this level, k1 was related to the repression of plant growth. Flavonol biosynthesis is regulated by environmental conditions. In particular, UV-B radiation enhances flavonol glycoside accumulation, with a strong increase of quercetin glycosides and a moderate increase of kaempferol glycosides including k1 (Götz *et al.,* 2010). Accordingly, a reduced plant growth phenotype could be postulated, which is actually a well-known feature of UV-B-dependent effects (Caldwell, 1971; Tevini *et al.,* 1981).

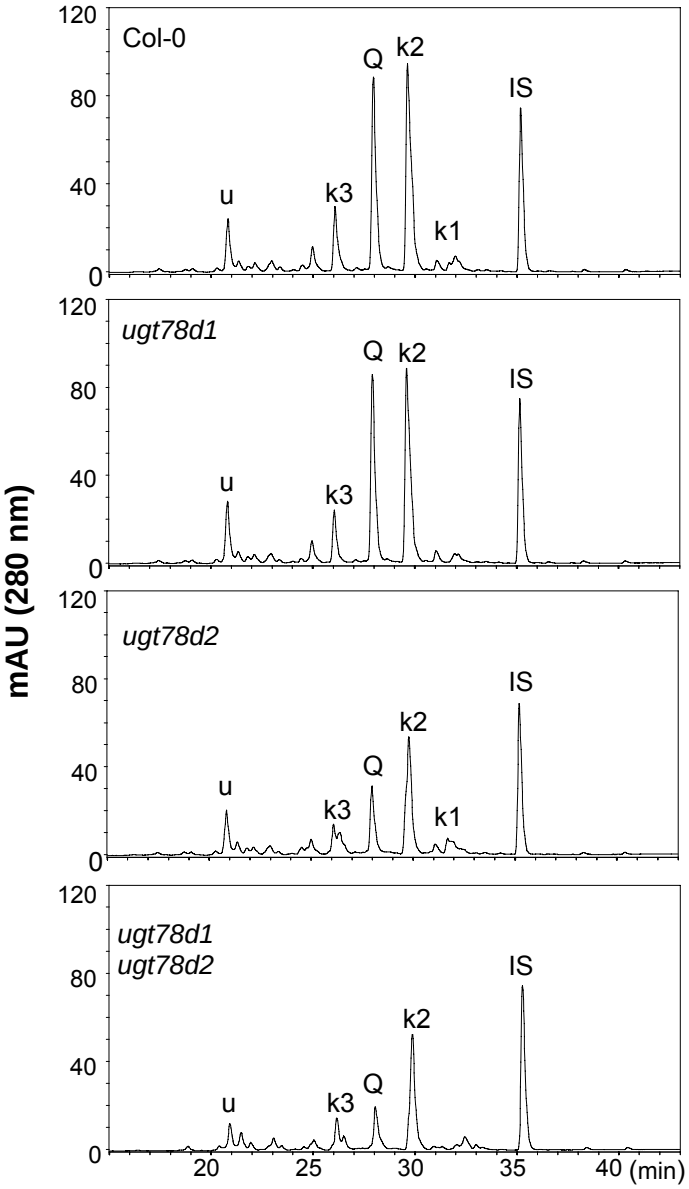

Figure 4. 10 Representative HPLC chromatograms of the root flavonol glycoside patterns. Plants were cultured vertically on ½ MS solid medium containing 1.5% sucrose for about 14 days. The flavonol glycosides were extracted and analyzed

according to the Experimental Procedures. IS, internal standard (naringenin). Q, quercetin 3-*O*-glucoside-7-*O*-rhamnoside. U, an unknown peak.

The expression of *UGT78D1* and *UGT78D2* was low in roots (Figure 3. 2). Accordingly, flavonol glycoside pattern in roots was not very much altered in the two single mutants or the *ugt78d1 ugt78d2* double mutant (Figure 4. 10). Therefore, it is less likely that auxin transport was significantly altered in roots of these mutants.

Both *UGT78D1* and *UGT78D2* were expressed in basal part of young leaves and young leaf petioles (Figure 3. 2), where auxin biosynthesis and transport are highly active. This observation may suggest that flavonoid modulation of auxin transport also occurs at these regions. In fact, during vegetative growth it was frequently observed that *ugt78d2* leaf petioles were shorter than wild type ones (Figure 4. 11), which could be a consequence of altered auxin transport in this tissue.

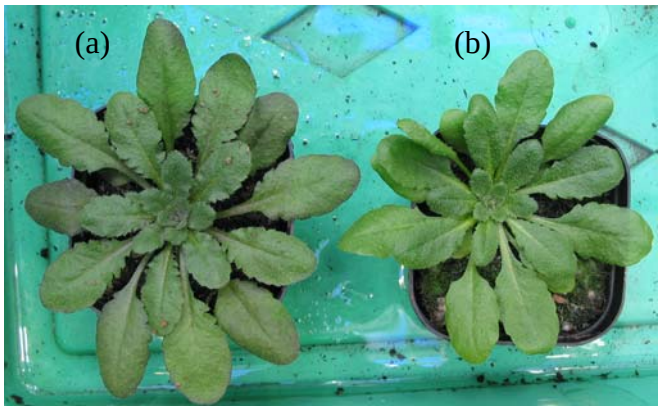

Figure 4. 11 The morphology of Col-0 and *ugt78d2* plants at the rosette stage.
Leaf petioles in *ugt78d2* mutant (b) appear to be shorter than that in Col-0 (a). Pictures were taken after 20 days of growth in a growth chamber providing well controlled condition with a 16/8 hr photoperiod at 200–230 µmol m^{-2} s^{-1} and at 22°C.

4.4.2 Kaempferol 3-*O*-rhamnoside-7-*O*-rhamnoside is an endogenous auxin transport inhibitor

In an effort to examine the mechanism of the over-accumulation of k1 leading to the *ugt78d2* growth defects, I found that basipetal auxin transport was strongly reduced in *ugt78d2* inflorescence stems. It has been shown that the modulation of auxin transport by flavonoids takes place at shoot apex and root tips. According to the expression of *UGT78D1*, k1 should be localized in shoot apex and root tips. These results strongly suggest that k1 is an endogenous auxin transport inhibitor. Although q1 has been shown to be dispensable for

developing *ugt78d2*-like growth defects, a possible contribution of q1 to the reduction in auxin transport can not be ruled out in *ugt78d2*. Preliminary data already showed that auxin transport was almost reverted to wild-type level in one *ugt78d2* mutant complemented line. At the mean time, together with Kerstin, I am performing more auxin transport experiments using *ugt78d2* mutant complemented line.

4.4.3 Are Flavonol aglycones involved in the inhibition of auxin transport in *ugt78d2*?

Feeding of flavonol aglycones to detached zucchini hypocotyls or clover roots led to a reduced polar auxin transport (Jacobs and Rubery, 1988; Mathesius *et al.,* 1998). Based on these observations, flavonol aglycones were postulated to be endogenous auxin transport inhibitors. However, several independent observations could argue against a direct involvement of flavonol aglycones. First, flavonol aglycones applied to plants might be rapidly conjugated or metabolized. Thus, such flavonol derivatives could not be excluded as the active auxin transport inhibitors. Second, flavonol aglycones were not detected with the up-to-date liquid chromatography or mass spectrometric approaches in extracts from *Arabidopsis* plants (Böttcher *et al.,* 2008, Yonekura-Sakakibara *et al.,* 2008; Kitamura *et al.,* 2010) except for one report (Peer *et al.,* 2001). Likewise, flavonol aglycones could not be detected in this work as well as by additional approaches employing LC-MS and FT-ICR-MS analyses of *Arabidopsis* extracts (Figure 3. 1 & Table 3. 1). In contrast, flavonol aglycones exerted their functions at micromolar concentrations in the cited *in vitro* experiments (Jacobs and Rubery, 1988; Mathesius *et al.,* 1998). Flavonol aglycones would not escape detection, if such high concentrations were only roughly reached in plants. Nevertheless, it is still possible that the level of flavonol aglycones is below the detection limits of the approaches, but high enough to modulate auxin transport in cells.

In wild-type *Arabidopsis* plants, UGT78D1 and UGT78D2 compete for flavonol aglycones as substrates to form flavonol 3-*O*-monorhamnosides and flavonol-3-*O*-monoglucosides, respectively. The loss of flavonol 3-*O*-glucosyltransferase in the *ugt78d2* mutant leads to an increase of flavonol 3-*O*-rhamnosylation, as evidenced by the increase of flavonol 3-*O*-rhamnoside derivatives, i.e. k1 and q1. Therefore, it can be stated that no flavonol aglycones could be accumulated in the *ugt78d2* mutant, as they are alternatively conjugated.

4.4.4 Possible mechanisms how flavonols modulate auxin transport

Although several possibilities were proposed (Buer and Muday 2004), the mechanisms by which flavonols modulate auxin transport remain to be elucidated. The site of regulation might be at the level of PGP transporters by inhibiting their activity. In fact, PGP proteins were shown to be able to bind to kaempferol and quercetin aglycones (Murphy *et al.,* 2002).

One striking feature of these PGP proteins is that they can bind structurally unrelated substrates. This might facilitate the direct regulation of PGP activity by binding of diverse flavonol glycosides. Under our growth conditions, neither *pgp1* nor *pgp19* single mutant exhibited an *ugt78d2*-like phenotype (data not shown). It is possible that multiple PGP proteins involved in auxin transport are affected in *ugt78d2*, which leads to growth defects. In fact, the *pgp1 pgp19* double mutant was shown to be dwarf and delayed in bolting time in previous studies (Noh *et al.,* 2001; Geisler *et al.,* 2003).

The immunophilin-like FKBP42 TWISTED DWARF1 (TWD1) acts *in planta* as a positive regulator of PGP1- and PGP-19 mediated auxin efflux through protein-protein interaction (Geisler *et al.,* 2003; Bouchard *et al.,* 2006; Bailly *et al.,* 2008). TWD1 was shown to mediate the modulation of PGP1-mediated auxin transport by flavonols. Importantly, flavonol glycosides were shown to be as effective as their aglycones in disrupting PGP1-TWD1 interaction (Bailly *et al.,* 2008). Even though k1 was not tested in that study, it is tempting to speculate that it inhibits auxin transport in the same way, as the reduction in plant height of *ugt78d2* resembles *twd1*.

Polar localization of PIN proteins determines the direction of local intercellular auxin transport (Wisniewska *et al.,* 2006). The PINOID kinase and PP2A phosphatase act antagonistically on the phosphorylation of the central hydrophilic loop of PINs, thereby mediating polar targeting of PIN proteins (Michniewicz *et al.,* 2007). Recently, It was found that PINOID-dependent PIN phosphorylation at one single site is sufficient to change PIN polarity (Zhang *et al.,* 2009). Flavonols have long been known as protein kinase inhibitors (Graziani *et al.,* 1983). Thus, flavonols might regulate the level of phosphorylation of auxin transport proteins through their kinase inhibiting function (Garbers *et al.,* 1996; DeLong *et al.,* 2002). PIN1 localization is responsive to flavonols; it is delocalized from the plasma membrane in the flavonoid-deficient *tt4* mutant and its localization was extended in *tt3*, which produces excess flavonols (Peer *et al*, 2004). It would be interesting to examine whether PIN1 localization is altered in the *ugt78d2* mutant.

In conclusion, the work presented here demonstrates that kaempferol 3-*O*-rhamnoside-7-*O*-rhamnoside (k1) is responsible for the repression of growth in the *ugt78d2* mutant. Furthermore, k1 has been identified as an endogenous auxin transport inhibitor.

5 Chapter 5: *ARABIDOPSIS* UGT74F1 AND UGT74F2 ARE NOT RESPONSIBLE FOR STRESS-RELATED SALICYLIC ACID GLUCOSYLATION

5.1 INTRODUCTION

Previously, recombinant UGT74F1 and UGT74F2 were shown to glucosylate salicylic acid (SA) *in vitro* (Lim *et al.,* 2002). In our laboratory, previous work by Meßner *et al*. (unpublished data) showed that ectopic overexpression of both enzymes in transgenic *Arabidopsis thaliana* resulted in increased SA glucosides with UGT74F1 being more efficient. However, single knock-out mutants of either gene did not lead to a reduction in SA glucosides under both non-stressed and SA-inducing conditions, i.e. spraying with benzothiadiazol (BTH). Since UGT74F1 and UGT74F2 are two close homologues and share a high degree of sequence similarity (82% amino acid identity), it is possible that these two glycosyltransferases have over-lapping functions in conjugating SA *in vivo*. The *ugt74f1 ugt74f2* double mutant might have less SA glucosides. However, genetic crossing of two single mutants to generate a double mutant is not feasible, because these two genes are located on the same chromosome in close proximity, about 5 Kb in distance. Therefore, I generated a *ugt74f2* knock-down line with an artificial miRNA approach in the *ugt74f1* knock-out background to yield a plant material, which was almost void of the gene products of both *UGT74F1* and *UGT74F2*. For simplicity, this mutant will be referred as the *ugt74f1 ugt74f2* double mutant. I quantified free SA and SA glucosides, including SA glucoside and SA ester. However, both, under non-stressed and SA-inducing conditions the *ugt74f1 ugt74f2* double mutant accumulated wild-type levels of free SA as well as SA glucosides. This work revealed that UGT74F1 and UGT74F2 are not responsible for stress-related salicylic acid glucosylation *in Arabidopsis*.

5.2 RESULTS

5.2.1 *UGT74F2* is efficiently silenced by the amiRNA

Seeds from transgenic plants were selected according to the seed coat specifically expressed GFP signal using fluorescence microscopy (Figure 5. 1). Quantitative real time PCR analysis showed that the transcript of *UGT74F2* was drastically reduced in the rosette leaves of the T1 primary transformants (Figure 5. 2). Two of the most strongly silenced independent lines, i.e. line 4 and 5, were chosen for further analysis. The two plants were

self-pollinated and homozygous lines selected among individuals. Homozygous transgenic T2 plants were used for salicylic acid quantification. The *UGT74F2* transcript level in the T2 plants used for SA quantification was also determined (Figure 5. 3), which showed that the silencing efficiency was stably inherited to the T2 generation.

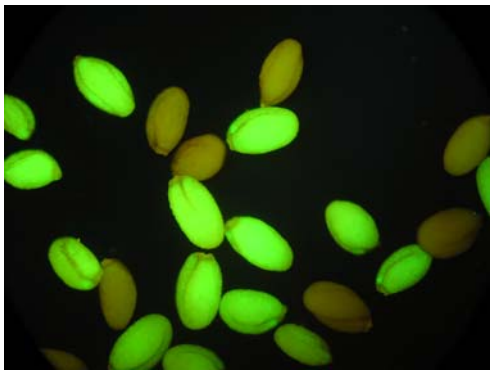

Figure 5. 1 Selection of transgenic seeds with the aid of the seed coat specific expression of GFP by fluorescence microscopy. The light green seeds are transgenic, whereas the brown ones are not (Bensmihen *et al*., 2004).

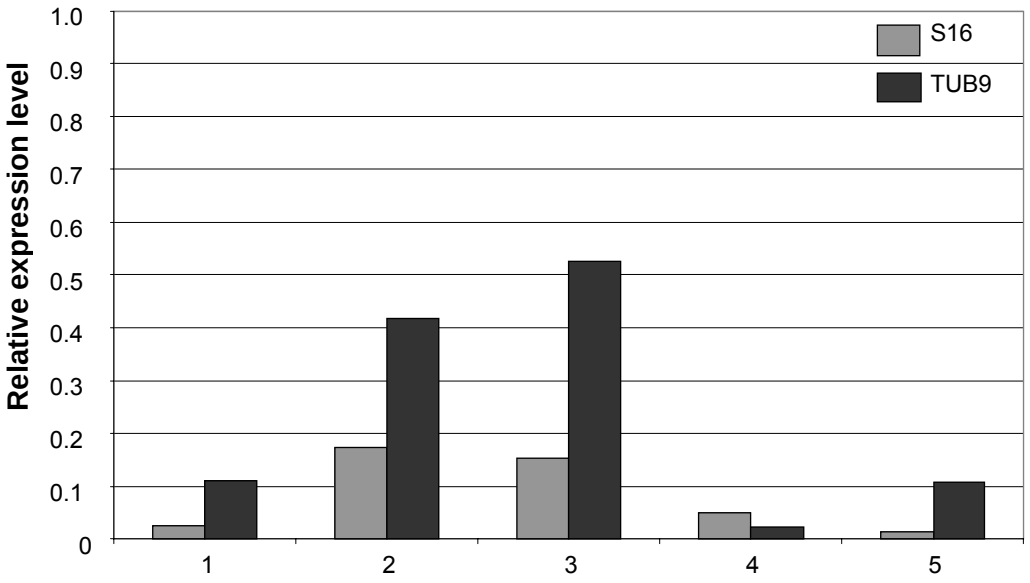

Figure 5. 2 Transcript level of *UGT74F2* in amiRNA-UGT74F2 containing transgenic plants of the T1 generation. Total RNA was extracted from the rosette leaves (a pool of leaves from 4-6 plants) of 4-week-old plants and transcript level was determined by quantitative RT-PCR analysis. Five independent transgenic lines (1-5) were analyzed.

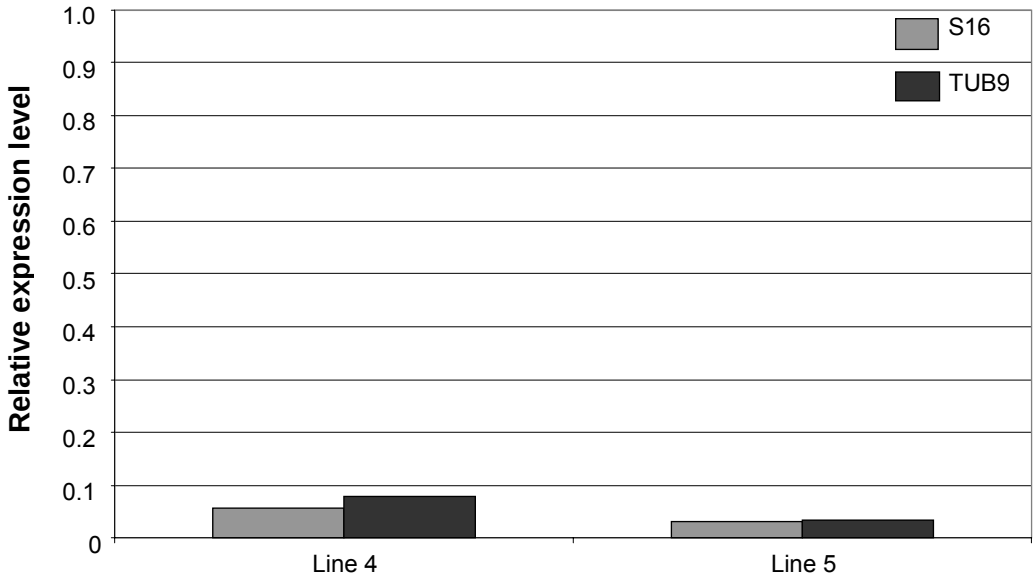

Figure 5. 3 Transcript levels of *UGT74F2* in two independent lines of amiRNA-UGT74F2 containing homozygous transgenic plants of the T2 generation. Total RNA was extracted from the rosette leaves (a pool of leaves from 4-6 plants) of 4-week-old plants and transcripts levels were determined by the quantitative RT-PCR analysis. Homozygous mutants from line 4 and line 5 were analyzed.

5.2.2 The *ugt74f1 ugt74f2* double mutant has wild-type SA levels

Free salicylic acid and salicylic acid glucosides analyses were performed with two independent *ugt74f1 ugt74f2* double mutant lines as well as wild-type plants. The *ugt74f1 ugt74f2* double mutant and wild-type plants contained comparable levels of free SA as well as SA glucosides in response to both BTH-sprayed and non-stressed conditions (Figure 5. 4 & Figure 5. 5), suggesting that UGT74F1 and UGT74F2 are not the true SA glucosyltransferases in plants.

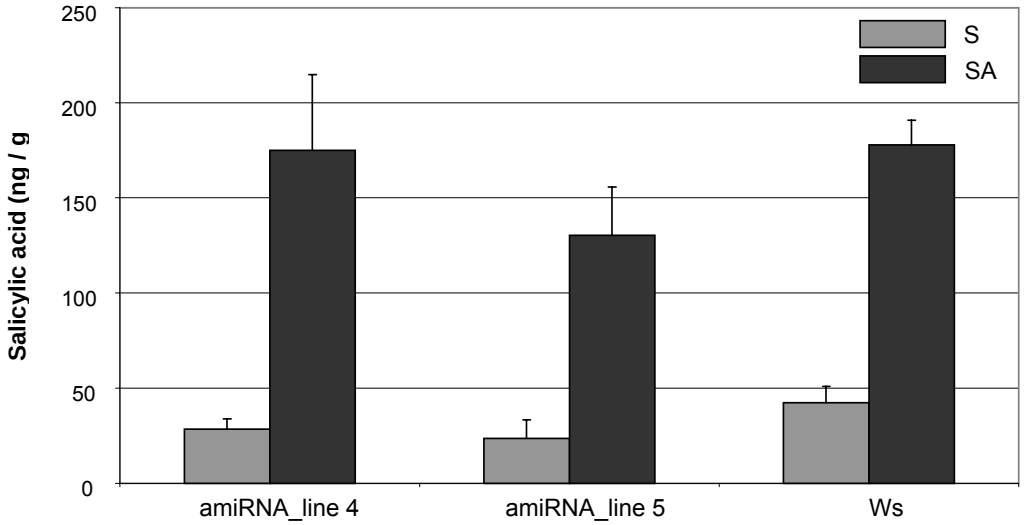

Figure 5. 4 Contents of free salicylic acid (SA) and salicylic acid glucosides (SAG) in unstressed amiRNA-UGT74F2 mediated double mutant lines and wild-type background (Wassilewskija, Ws). The mean values ± SD of four independent biological samples in two independent experiments are displayed.

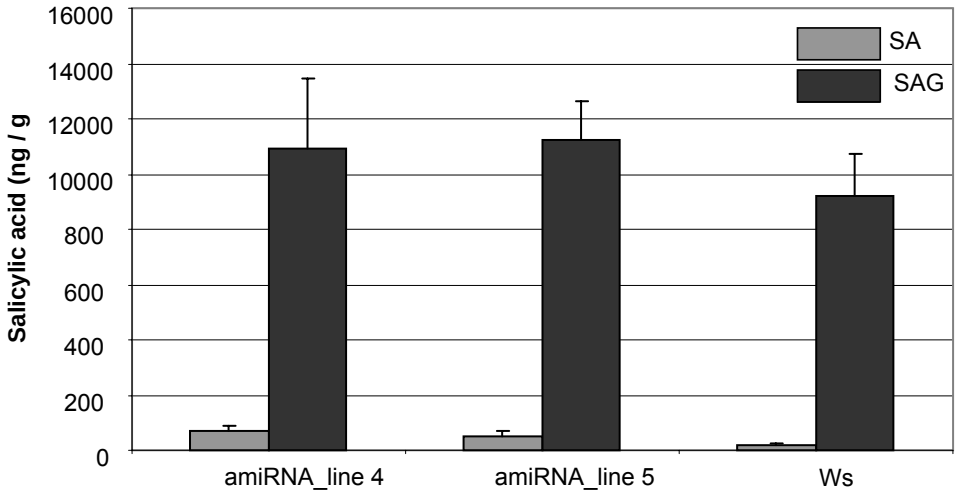

Figure 5. 5 Contents of free salicylic acid (SA) and salicylic acid glucosides (SAG) in BTH-sprayed amiRNA-UGT74F2 mediated double mutant lines. The mean values ± SD of four independent biological samples in two independent experiments are displayed.

5.3 DISCUSSION

In vitro study showed that of ninety tested UGT enzymes only two, i.e. UGT74F1 and UGT74F2, were active toward salicylic acid, suggesting that they were the *Arabidopsis* salicylic acid glucosyltransferase (Lim *et al.,* 2002). However, the wild-type levels of salicylic acid and its glucoside in the *ugt74f1 ugt74f2* double mutant demonstrated that both UGT74F1 and UGT74F2 could not be the salicylic acid glucosyltransferases under non-stressed and salicylic acid-inducing condition (using BTH) in plants. Although unlikely, I still cannot completely rule out the possibility that the remaining activity of UGT74F2 in the amiRNA-containing transgenic plants was enough to glucosylate SA to wild-type level.

The key question is to which extent any of these *in vitro* biochemical studies can suggest UGT activity and physiological function in plants (Bowles *et al*., 2006). Some important factors, such as cofactors and metabolite channelling, cannot be addressed *in vitro*. Another important factor is the substrate availability. If the native enzyme has the capability to recognize multiple substrates in plants, their availability to act as acceptors will be critical. In accordance with the *in vitro* studies by Lim and colleagues (2002), the increase of salicylic acid and salicylic acid glucosides in the ectopic overexpression lines (Meßner *et al.*, unpublished data) of both *UGT74F1* and *UGT74F2* confirmed the ability of these two enzymes to glucosylate salicylic acid. The wild-type levels of salicylic acid and salicylic acid glucosides in both single and double mutants may imply that localizations of these two proteins do not coincide with those of salicylic acid in plants.

6 REFERENCES

Abrahams, S., Tanner, G. J., Larkin P. J., Ashton, A. R. (2002) Identification and biochemical characterization of mutants in the proanthocyanidin pathway in Arabidopsis. *Plant Physiol.* **130:** 561-576

Attridge, T. H., Stewart, G. R., Smith, H. (1971) End-product inhibition of Pisum phenylalanine ammonia-lyase by the Pisum flavonoids. *FEBS Lett.* 17**:** 84-86

Bailly, A., Sovero, V., Vincenzetti, V., Santelia, D., Bartnik, D., Koenig, B.W., Mancuso, S., Martinoia, E. and Geisler, M. (2008) Modulation of P-glycoproteins by auxin transport inhibitors is mediated by interaction with immunophilins. *J. Biol. Chem.* **283**, 21817-21826.

Bate, N.J., Orr, J., Ni, W., Meromi, A., Nadler-Hassar, T., Doerner, P.W., Dixon, R.A., Lamb, C.J. and Elkind, Y. (1994) Quantitative relationship between phenylalanine ammonia-lyase levels and phenylpropanoid accumulation in transgenic tobacco identifies a rate-determining step in natural product synthesis. *Proc. Natl. Acad. Sci. USA*, **91**, 7608-7612.

Bensmihen, S., To, A., Lambert, G., Kroj, T., Giraudat, J. and Parcy, F. (2004) Analysis of an activated ABI5 allele using a new selection method for transgenic *Arabidopsis* seeds. *FEBS Lett*. **561**, 127-131.

Berleth, T., Scarpella, E. and Prusinkiewicz, P. (2007) Towards the systems biology of auxin-transport-mediated patterning. *Trends Plant Sci*. **12**, 151-159.

Besseau, S., Hoffmann, L., Geoffroy, P., Lapierre, C., Pollet, B. and Legrand, M. (2007) Flavonoid accumulation in Arabidopsis repressed in lignin synthesis affects auxin transport and plant growth. *Plant Cell*, **19**, 148-162.

Bloor, S.J. and Abrahams, S. (2002) The structure of the major anthocyanin in *Arabidopsis thaliana*. *Phytochemistry*, **59**, 343-346.

Blount, J.W., Korth, K.L., Masoud, S.A., Rasmussen, S., Lamb, C. and Dixon, R.A. (2000) Altering expression of cinnamic acid 4-hydroxylase in transgenic plants

provides evidence for a feedback loop at the entry point into the phenylpropanoid pathway. *Plant Physiol*. **122**, 107-116.

Böttcher, C., von Roepenack-Lahaye, E., Schmidt, J., Schmotz, C., Neumann, S., Scheel, D. and Clemens, S. (2008) Metabolome analysis of biosynthetic mutants reveals a diversity of metabolic changes and allows identification of a large number of new compounds in Arabidopsis. *Plant Physiol*. **147**, 2107-2120.

Borevitz, J.O., Xia, Y., Blount, J., Dixon, R.A. and Lamb, C. (2000) Activation tagging identifies a conserved MYB regulator of phenylpropanoid biosynthesis. *Plant Cell*, **12**, 2383-2394.

Bouchard, R., Bailly, A., Blakeslee, J.J., Oehring, S.C., Vincenzetti, V., Lee, O.R., Paponov, I., Palme, K., Mancuso, S., Murphy, A.S., Schulz, B. and Geisler, M. (2006) Immunophilin-like TWISTED DWARF1 modulates auxin efflux activities of Arabidopsis P-glycoproteins. *J. Biol. Chem.* **281**, 30603-30612.

Bowles, D., Lim, E.K., Poppenberger, B. and Vaistij, F.E. (2006) Glycosyltransferases of lipophilic small molecules. *Annu. Rev. Plant Biol.* **57**, 567-597.

Brown, D.E., Rashotte, A.M., Murphy, A.S., Normanly, J., Tague, B.W., Peer, W.A., Taiz, L. and Muday, G.K. (2001) Flavonoids act as negative regulators of auxin transport in vivo in arabidopsis. *Plant Physiol*. **126**, 524-535.

Buer, C.S., Imin, N. and Djordjevic, M.A. (2010) Flavonoids: new roles for old molecules. *J. Integr. Plant Biol*. **52**, 98-111.

Buer, C.S. and Muday, G.K. (2004) The transparent testa4 mutation prevents flavonoid synthesis and alters auxin transport and the response of Arabidopsis roots to gravity and light. *Plant Cell*, **16**, 1191-1205.

Burbulis, I.E., Iacobucci, M. and Shirley, B.W. (1996) A null mutation in the first enzyme of flavonoid biosynthesis does not affect male fertility in Arabidopsis. *Plant Cell*, **8**, 1013-1025.

Buttery, B.R. and Buzzell, R.I. (1987) Leaf Traits Associated with Flavonol Glycoside Genes in Soybean. *Plant Physiol*. **85**, 20-21.

Cos, P., Calomme, M., Sindambiwe, J.B., De Bruyne, T., Cimanga, K., Pieters, L., Vlietinck, A.J. and Vanden Berghe, D. (2001) Cytotoxicity and lipid peroxidation-inhibiting activity of flavonoids. *Planta Med*. **67**, 515-519.

Costa, M.A., Bedgar, D.L., Moinuddin, S.G., Kim, K.W., Cardenas, C.L., Cochrane, F.C., Shockey, J.M., Helms, G.L., Amakura, Y., Takahashi, H., Milhollan, J.K., Davin, L.B., Browse, J. and Lewis, N.G. (2005) Characterization in vitro and in vivo of the putative multigene 4-coumarate:CoA ligase network in Arabidopsis: syringyl lignin and sinapate/sinapyl alcohol derivative formation. *Phytochemistry*, **66**, 2072-2091.

Debeaujon, I., Leon-Kloosterziel, K.M. and Koornneef, M. (2000) Influence of the testa on seed dormancy, germination, and longevity in Arabidopsis. *Plant Physiol.* **122**, 403-414.

Debeaujon, I., Nesi, N., Perez, P., Devic, M., Grandjean, O., Caboche, M. and Lepiniec, L. (2003) Proanthocyanidin-accumulating cells in Arabidopsis testa: regulation of differentiation and role in seed development. *Plant Cell*, **15**, 2514-2531.

DeLong, A., Mockaitis, K., Christensen, S. (2002) Protein phosphorylation in the delivery of and response to auxin signals. *Plant Mol. Biol*. **49:** 285-303

Deruere, J., Jackson, K., Garbers, C., Soll, D., Delong, A. (1999) The RCN1-encoded A subunit of protein phosphatase 2A increases phosphatase activity in vivo. *Plant J.* **20:** 389-399

Dixon, R.A. and Steele, C.L. (1999) Flavonoids and isoflavonoids - a gold mine for metabolic engineering. *Trends Plant Sci.* **4**, 394-400.

Dobrev, P.I., Kaminek, M. (2002) Fast and efficient separation of cytokinins from auxin and abscisic acid and their purification using mixed-mode solid-phase extraction. *J. Chromatogr. A* **950:** 21-29

Dubos, C., Le Gourrierec, J., Baudry, A., Huep, G., Lanet, E., Debeaujon, I., Routaboul, J.M., Alboresi, A., Weisshaar, B. and Lepiniec, L. (2008) MYBL2 is a new regulator of flavonoid biosynthesis in *Arabidopsis thaliana*. *Plant J*. **55**, 940-953.

Ehlting, J., Buttner, D., Wang, Q., Douglas, C.J., Somssich, I.E. and Kombrink, E. (1999) Three 4-coumarate:coenzyme A ligases in *Arabidopsis thaliana* represent two evolutionarily divergent classes in angiosperms. *Plant J*. **19**, 9-20.

Franken, P., Niesbach-Klosgen, U., Weydemann, U., Marechal-Drouard, L., Saedler, H. and Wienand, U. (1991) The duplicated chalcone synthase genes C2 and Whp (white pollen) of Zea mays are independently regulated; evidence for translational control of Whp expression by the anthocyanin intensifying gene in. *EMBO J*. **10**, 2605-2612.

Garbers, C., DeLong, A., Deruere, J., Bernasconi, P. and Soll, D. (1996) A mutation in protein phosphatase 2A regulatory subunit A affects auxin transport in Arabidopsis. *EMBO J*. **15**, 2115-2124.

Geisler, M., Kolukisaoglu, H.U., Bouchard, R., Billion, K., Berger, J., Saal, B., Frangne, N., Koncz-Kalman, Z., Koncz, C., Dudler, R., Blakeslee, J.J., Murphy, A.S., Martinoia, E. and Schulz, B. (2003) TWISTED DWARF1, a unique plasma membrane-anchored immunophilin-like protein, interacts with Arabidopsis multidrug resistance-like transporters AtPGP1 and AtPGP19. *Mol. Biol. Cell*, **14**, 4238-4249.

Götz, M., Albert, A., Stich, S., Heller, W., Scherb, H., Krins, A., Langebartels, C., Seidlitz, H.K. and Ernst, D. (2010) PAR modulation of the UV-dependent levels of flavonoid metabolites in *Arabidopsis thaliana* (L.) Heynh. leaf rosettes: cumulative effects after a whole vegetative growth period. *Protoplasma*, **243**, 95-103.

Graziani, Y., Erikson, E. and Erikson, R.L. (1983) The effect of quercetin on the phosphorylation activity of the Rous sarcoma virus transforming gene product in vitro and in vivo. *Eur. J. Biochem*. **135**, 583-589.

Harborne, J.B. and Williams, C.A. (2000) Advances in flavonoid research since 1992. *Phytochemistry* **55:** 481-504

Harborne, J.B. and Williams, C.A. (2001) Anthocyanins and other flavonoids. *Nat. Prod. Rep.* **18:** 310-333

Harrison, M.J. (2005) Signaling in the arbuscular mycorrhizal symbiosis. *Annu. Rev. Microbiol.* **59:** 19-42

Hennig, L., Gruissem, W., Grossniklaus, U. and Kohler, C. (2004) Transcriptional programs of early reproductive stages in Arabidopsis. *Plant Physiol*. **135**, 1765-1775.

Hrazdina, G. and Wagner, G.J. (1985) Metabolic pathways as enzyme complexes: evidence for the synthesis of phenylpropanoids and flavonoids on membrane associated enzyme complexes. *Arch. Biochem. Biophys*. **237**, 88-100.

Hrazdina, G., Zobel, A.M. and Hoch, H.C. (1987) Biochemical, immunological, and immunocytochemical evidence for the association of chalcone synthase with endoplasmic reticulum membranes. *Proc. Natl. Acad. Sci. USA*, **84**, 8966-8970.

Jacobs, M. and Rubery, P.H. (1988) Naturally Occurring Auxin Transport Regulators. *Science* **241:** 346-349

Jones, P., Meßner, B., Nakajima, J., Schäffner, A. R. and Saito, K. (2003) UGT73C6 and UGT78D1, glycosyltransferases involved in flavonol glycoside biosynthesis in *Arabidopsis thaliana*. *J. Biol. Chem.* **278**, 43910-43918.

Kaffarnik, F., Seidlitz, H.K., Obermaier, J., Sandermann, H., Jr. and Heller, W. (2006) Environmental and developmental effects on the biosynthesis of UV-B screening pigments in Scots pine (Pinus sylvestris L.) needles. *Plant Cell Environ*. **29**, 1484-1491.

Karimi, M., Inze, D. and Depicker, A. (2002) GATEWAY vectors for Agrobacterium-mediated plant transformation. *Trends Plant Sci*. **7**, 193-195.

Kubasek, W.L., Shirley, B.W., McKillop, A., Goodman, H.M., Briggs, W. and Ausubel, F.M. (1992) Regulation of Flavonoid Biosynthetic Genes in Germinating Arabidopsis Seedlings. *Plant Cell*, **4**, 1229-1236.

Li, J., Ou-Lee, T.M., Raba, R., Amundson, R.G. and Last, R.L. (1993) Arabidopsis Flavonoid Mutants Are Hypersensitive to UV-B Irradiation. *Plant Cell*, **5**, 171-179.

Li, Y., Baldauf, S., Lim, E.K. and Bowles, D.J. (2001) Phylogenetic analysis of the UDP-glycosyltransferase multigene family of *Arabidopsis thaliana*. *J. Biol. Chem*. **276**, 4338-4343.

Lin, J.K. and Weng, M.S. (2006) Flavonoids as nutraceuticals. In *The Science of Flavonoids* (Grotewold, E. ed. New York: Springer Science+Business Media, Inc., pp. 213-238.

Lillo, C., Lea, U.S. and Ruoff, P. (2008) Nutrient depletion as a key factor for manipulating gene expression and product formation in different branches of the flavonoid pathway. *Plant Cell Environ*. **31**, 587-601.

Lim, E.K., Doucet, C.J., Li, Y., Elias, L., Worrall, D., Spencer, S.P., Ross, J. and Bowles, D.J. (2002) The activity of Arabidopsis glycosyltransferases toward salicylic acid, 4-hydroxybenzoic acid, and other benzoates. *J. Biol. Chem*. **277**, 586-592.

Loake, G.J., Choudhary, A.D., Harrison, M.J., Mavandad, M., Lamb, C.J. and Dixon, R.A. (1991) Phenylpropanoid pathway intermediates regulate transient expression of a chalcone synthase gene promoter. *Plant Cell*, **3**, 829-840.

Loake, G.J., Faktor, O., Lamb, C.J. and Dixon, R.A. (1992) Combination of H-box [CCTACC(N)7CT] and G-box (CACGTG) cis elements is necessary for feed-forward stimulation of a chalcone synthase promoter by the phenylpropanoid-pathway intermediate p-coumaric acid. *Proc. Natl. Acad. Sci. USA*, **89**, 9230-9234.

Mathesius, U., Schlaman, H.R., Spaink, H.P., Of Sautter, C., Rolfe, B.G. and Djordjevic, M.A. (1998) Auxin transport inhibition precedes root nodule formation in white clover roots and is regulated by flavonoids and derivatives of chitin oligosaccharides. *Plant J*. **14**, 23-34.

Mehrtens, F., Kranz, H., Bednarek, P. and Weisshaar, B. (2005) The Arabidopsis transcription factor MYB12 is a flavonol-specific regulator of phenylpropanoid biosynthesis. *Plant Physiol*. **138**, 1083-1096.

Meßner, B., Thulke, O. and Schäffner, A.R. (2003) Arabidopsis glucosyltransferases with activities toward both endogenous and xenobiotic substrates. *Planta*, **217**, 138-146.

Meyerowitz, E.M., Bowman, J.L., Chang, C. and Kempin, S. (1990) RFLP map of *Arabidopsis thaliana*. In *Genetic Maps* (O'Brien, S.J. ed. New York: Cold Spring Harbor Laboratory Press, pp. 98-99.

Michniewicz, M., Zago, M.K., Abas, L., Weijers, D., Schweighofer, A., Meskiene, I., Heisler, M.G., Ohno, C., Zhang, J., Huang, F., Schwab, R., Weigel, D., Meyerowitz, E.M., Luschnig, C., Offringa, R. and Friml, J. (2007) Antagonistic regulation of PIN phosphorylation by PP2A and PINOID directs auxin flux. *Cell*, **130**, 1044-1056.

Mizushina, Y., Ishidoh, T., Kamisuki, S., Nakazawa, S., Takemura, M., Sugawara, F., Yoshida, H. and Sakaguchi, K. (2003) Flavonoid glycoside: a new inhibitor of eukaryotic DNA polymerase alpha and a new carrier for inhibitor-affinity chromatography. *Biochem. Biophys. Res. Commun*. **301**, 480-487.

Mo, Y., Nagel, C. and Taylor, L.P. (1992) Biochemical complementation of chalcone synthase mutants defines a role for flavonols in functional pollen. *Proc. Natl. Acad. Sci. USA*, **89**, 7213-7217.

Moreira, M.R., Kanashiro, A., Kabeya, L.M., Polizello, A.C., Azzolini, A.E., Curti, C., Oliveira, C.A., A, T.d.A. and Lucisano-Valim, Y.M. (2007) Neutrophil effector functions triggered by Fc-gamma and/or complement receptors are dependent on B-ring hydroxylation pattern and physicochemical properties of flavonols. *Life Sci*. **81**, 317-326.

Morris, D.A. (2000) Transmembrane auxin carrier systems--dynamic regulators of polar auxin transport. *Plant Growth Regul*. 32, 161-172.

Murphy, A., Peer, W.A. and Taiz, L. (2000) Regulation of auxin transport by aminopeptidases and endogenous flavonoids. *Planta* **211:** 315-324

Murphy, A.S., Hoogner, K.R., Peer, W.A. and Taiz, L. (2002) Identification, purification, and molecular cloning of N-1-naphthylphthalmic acid-binding plasma membrane-associated aminopeptidases from Arabidopsis. *Plant Physiol.* 128, 935-950.

Nesi, N., Jond, C., Debeaujon, I., Caboche, M. and Lepiniec, L. (2001) The Arabidopsis TT2 gene encodes an R2R3 MYB domain protein that acts as a key determinant for proanthocyanidin accumulation in developing seed. *Plant Cell*, 13, 2099-2114.

Noh, B., Murphy, A.S. and Spalding, E.P. (2001) Multidrug resistance-like genes of Arabidopsis required for auxin transport and auxin-mediated development. *Plant Cell*, **13**, 2441-2454.

Okada, K., Ueda, J., Komaki, M.K., Bell, C.J. and Shimura, Y. (1991) Requirement of the Auxin Polar Transport System in Early Stages of Arabidopsis Floral Bud Formation. *Plant Cell*, **3**, 677-684.

Olsen, K.M., Lea, U.S., Slimestad, R., Verheul, M. and Lillo, C. (2008) Differential expression of four Arabidopsis PAL genes; PAL1 and PAL2 have functional specialization in abiotic environmental-triggered flavonoid synthesis. *J. Plant Physiol*. **165**, 1491-1499.

Ossowski, S., Schwab, R. and Weigel, D. (2008) Gene silencing in plants using artificial microRNAs and other small RNAs. *Plant J*. **53**, 674-690.

Owens, D.K., Alerding, A.B., Crosby, K.C., Bandara, A.B., Westwood, J.H. and Winkel, B.S. (2008) Functional analysis of a predicted flavonol synthase gene family in Arabidopsis. *Plant Physiol*. **147**, 1046-1061.

Pairoba, C.F. and Walbot, V. (2003) Post-transcriptional regulation of expression of the Bronze2 gene of Zea mays L. *Plant Mol. Biol*. **53**, 75-86.

Peer, W.A., Bandyopadhyay, A., Blakeslee, J.J., Makam, S.N., Chen, R.J., Masson, P.H. and Murphy, A.S. (2004) Variation in expression and protein localization of the PIN family of auxin efflux facilitator proteins in flavonoid mutants with altered auxin transport in *Arabidopsis thaliana*. *Plant Cell*, **16**, 1898-1911.

Peer, W.A., Brown, D.E., Tague, B.W., Muday, G.K., Taiz, L. and Murphy, A.S. (2001) Flavonoid accumulation patterns of transparent testa mutants of arabidopsis. *Plant Physiol*. **126**, 536-548.

Peer, W.A. and Murphy, A.S. (2007) Flavonoids and auxin transport: modulators or regulators? *Trends Plant Sci*. **12**, 556-563.

Prescott, A.G., Stamford, N.P., Wheeler, G. and Firmin, J.L. (2002) In vitro properties of a recombinant flavonol synthase from *Arabidopsis thaliana*. *Phytochemistry*, **60**, 589-593.

Preston, J., Wheeler, J., Heazlewood, J., Li, S.F. and Parish, R.W. (2004) AtMYB32 is required for normal pollen development in *Arabidopsis thaliana*. *Plant J*. **40**, 979-995.

Preuß, A., Stracke, R., Weisshaar, B., Hillebrecht, A., Matern, U. and Martens, S. (2009) *Arabidopsis thaliana* expresses a second functional flavonol synthase. *FEBS Lett*. **583**, 1981-1986.

Przemeck, G.K., Mattsson, J., Hardtke, C.S., Sung, Z.R. and Berleth, T. (1996) Studies on the role of the Arabidopsis gene MONOPTEROS in vascular development and plant cell axialization. *Planta*, **200**, 229-237.

Quattrocchio, F., Baudry, A., Lepiniec, L. and Grotewold, E. (2006) The Regulation of Flavonoid Biosynthesis. In *The Science of Flavonoids* (Grotewold, E. ed. New York: Springer Science & Business Media, pp. 97-122.

Raes, J., Rohde, A., Christensen, J.H., Van de Peer, Y. and Boerjan, W. (2003) Genome-wide characterization of the lignification toolbox in Arabidopsis. *Plant Physiol*. **133**, 1051-1071.

Ramadass, P., Meerarani, P., Toborek, M., Robertson, L.W. and Hennig, B. (2003) Dietary flavonoids modulate PCB-induced oxidative stress, CYP1A1 induction, and AhR-DNA binding activity in vascular endothelial cells. *Toxicol. Sci*. **76**, 212-219.

Ramsay, N.A. and Glover, B.J. (2005) MYB-bHLH-WD40 protein complex and the evolution of cellular diversity. *Trends Plant Sci.* **10**, 63-70.

Rayle, D.L., Ouitrakul, R., and Hertel, R. (1969) Effect of auxins on the auxin transport system in coleoptiles. *Planta* **87:** 49-53

R-Development-Core-Team (2009), R: A Language and Environment for Statisticalal computing. R. Foundation for Statisticalal Computing, Vienna, Austria. http://www.R-project.org.

Ringli, C., Bigler, L., Kuhn, B.M., Leiber, R.M., Diet, A., Santelia, D., Frey, B., Pollmann, S. and Klein, M. (2008) The modified flavonol glycosylation profile in the Arabidopsis rol1 mutants results in alterations in plant growth and cell shape formation. *Plant Cell*, **20**, 1470-1481.

Rodney, G., LSW, L. M., Wheeler, G. N. Smith and C.S. Worrel (1950) The effect of a series of flavonoids on hyaluronidase and some other related enzymes. *J. Biol. Chem.* **183:** 739-747

Rohde, A., Morreel, K., Ralph, J., Goeminne, G., Hostyn, V., De Rycke, R., Kushnir, S., Van Doorsselaere, J., Joseleau, J.P., Vuylsteke, M., Van Driessche, G., Van Beeumen, J., Messens, E. and Boerjan, W. (2004) Molecular phenotyping of the

pal1 and pal2 mutants of *Arabidopsis thaliana* reveals far-reaching consequences on phenylpropanoid, amino acid, and carbohydrate metabolism. *Plant Cell*, **16**, 2749-

Ross, J., Li, Y., Lim, E. and Bowles, D.J. (2001) Higher plant glycosyltransferases. *Genome Biol*. **2**, REVIEWS3004.

Rubio, V., Shen, Y., Saijo, Y., Liu, Y., Gusmaroli, G., Dinesh-Kumar, S.P. and Deng, X.W. (2005) An alternative tandem affinity purification strategy applied to Arabidopsis protein complex isolation. *Plant J*. **41**, 767-778.

Santelia, D., Henrichs, S., Vincenzetti, V., Sauer, M., Bigler, L., Klein, M., Bailly, A., Lee, Y., Friml, J., Geisler, M., Martinoia, E. (2008) Flavonoids redirect PIN-mediated polar auxin fluxes during root gravitropic responses. *J. Biol. Chem.* **283:** 31218-31226

Saslowsky, D. and Winkel-Shirley, B. (2001) Localization of flavonoid enzymes in Arabidopsis roots. *Plant J*. **27**, 37-48.

Saslowsky, D. E., Warek, U. and Winkel, B. S. (2005) Nuclear localization of flavonoid enzymes in Arabidopsis. *J. Biol. Chem*. **280**, 23735-23740.

Sato, T. and Sankawa, U. (1983) Inhibition of Phenylalanine Ammonia - lyase by Flavonoids. *Chem. Pharm. Bull.* **31:** 149-155

Schmid, M., Davison, T.S., Henz, S.R., Pape, U.J., Demar, M., Vingron, M., Scholkopf, B., Weigel, D. and Lohmann, J.U. (2005) A gene expression map of *Arabidopsis thaliana* development. *Nat Genet*. **37**, 501-506.

Schoenbohm, C., Martens, S., Eder, C., Forkmann, G. and Weisshaar, B. (2000) Identification of the *Arabidopsis thaliana* flavonoid 3'-hydroxylase gene and functional expression of the encoded P450 enzyme. *Biol. Chem*. **381**, 749-753.

Sewalt, V., Ni, W., Blount, J.W., Jung, H.G., Masoud, S.A., Howles, P.A., Lamb, C. and Dixon, R.A. (1997) Reduced Lignin Content and Altered Lignin Composition in Transgenic Tobacco Down-Regulated in Expression of L-Phenylalanine Ammonia-Lyase or Cinnamate 4-Hydroxylase. *Plant Physiol*. **115**, 41-50.

Shimmyo, Y., Kihara, T., Akaike, A., Niidome, T. and Sugimoto, H. (2008) Flavonols and flavones as BACE-1 inhibitors: structure-activity relationship in cell-free, cell-based

and in silico studies reveal novel pharmacophore features. *Biochim. Biophys. Acta*. **1780**, 819-825.

Solimani, R. (1997) The flavonols quercetin, rutin and morin in DNA solution: UV-vis dichroic (and mid-infrared) analysis explain the possible association between the biopolymer and a nucleophilic vegetable-dye. *Biochim. Biophys. Acta.* **1336**, 281-294.

Stafford, H. (1974) Possible multi-enzyme complexs regulating the formation of C_6-C_3 phenolic compounds and lignins in higher plants. *Rec. Adv. Phytochem.* **8:** 53-79

Stracke, R., De Vos, R.C., Bartelniewoehner, L., Ishihara, H., Sagasser, M., Martens, S. and Weisshaar, B. (2009) Metabolomic and genetic analyses of flavonol synthesis in *Arabidopsis thaliana* support the in vivo involvement of leucoanthocyanidin dioxygenase. *Planta*, **229**, 427-445.

Stracke, R., Ishihara, H., Huep, G., Barsch, A., Mehrtens, F., Niehaus, K. and Weisshaar, B. (2007) Differential regulation of closely related R2R3-MYB transcription factors controls flavonol accumulation in different parts of the *Arabidopsis thaliana* seedling. *Plant J*. **50**, 660-677.

Taylor, L.P. and Grotewold, E. (2005) Flavonoids as developmental regulators. *Curr Opin Plant Biol*. **8**, 317-323.

Tohge, T., Nishiyama, Y., Hirai, M. Y., Yano, M., Nakajima, J., Awazuhara, M., Inoue, E., Takahashi, H., Goodenowe, D. B., Kitayama, M., Noji, M., Yamazaki, M. and Saito, K. (2005) Functional genomics by integrated analysis of metabolome and transcriptome of Arabidopsis plants over-expressing an MYB transcription factor. *Plant J*. **42**, 218-235.

Turnbull, J.J., Nakajima, J., Welford, R.W., Yamazaki, M., Saito, K. and Schofield, C.J. (2004) Mechanistic studies on three 2-oxoglutarate-dependent oxygenases of flavonoid biosynthesis: anthocyanidin synthase, flavonol synthase, and flavanone 3beta-hydroxylase. *J. Biol. Chem*. **279**, 1206-1216.

Vandesompele, J., De Preter, K., Pattyn, F., Poppe, B., Van Roy, N., De Paepe, A. and Speleman, F. (2002) Accurate normalization of real-time quantitative RT-PCR data by geometric averaging of multiple internal control genes. *Genome Biol*, **3**, RESEARCH0034.

Veit, M. and Pauli, G.F. (1999) Major flavonoids from *Arabidopsis thaliana* leaves. *J. Nat. Prod*. **62**, 1301-1303.

von Roepenack-Lahaye, E., Degenkolb, T., Zerjeski, M., Franz, M., Roth, U., Wessjohann, L., Schmidt, J., Scheel, D. and Clemens, S. (2004) Profiling of Arabidopsis secondary metabolites by capillary liquid chromatography coupled to electrospray ionization quadrupole time-of-flight mass spectrometry. *Plant Physiol*. **134**, 548-559.

Wasson, A.P., Pellerone, F.I., Mathesius, U. (2006) Silencing the flavonoid pathway in Medicago truncatula inhibits root nodule formation and prevents auxin transport regulation by rhizobia. *Plant Cell,* **18:** 1617-1629

Winkel-Shirley, B. (1999) Evidence for enzyme complexes in the phenylpropanoid and flavonoid pathways. *Physiol. Plant.* **107:** 142-149

Winkel-Shirley, B. (2001) Flavonoid biosynthesis. A colorful model for genetics, biochemistry, cell biology, and biotechnology. *Plant Physiol.* **126:** 485-493

Winkel-Shirley, B. (2004) Metabolic channeling in plants. *Annu. Rev. Plant Biol*. **55**, 85-107.

Winkel-Shirley, B. (2006) The Biosynthesis of Flavonoids. *In* E Grotewold, ed, The Science of Flavonoids. Springer Science&Business Media, New York, pp 71-95

Winkel-Shirley, B., Kubasek, W.L., Storz, G., Bruggemann, E., Koornneef, M., Ausubel, F.M., Goodman, H.M. (1995) Analysis of Arabidopsis mutants deficient in flavonoid biosynthesis. *Plant J.* **8:** 659-671

Winter, D., Vinegar, B., Nahal, H., Ammar, R., Wilson, G.V. and Provart, N.J. (2007) An "electronic fluorescent pictograph" browser for exploring and analyzing large-scale biological data sets. *PLoS One*, **2**, e718.

Wisniewska, J., Xu, J., Seifertova, D., Brewer, P.B., Ruzicka, K., Blilou, I., Rouquie, D., Benkova, E., Scheres, B. and Friml, J. (2006) Polar PIN localization directs auxin flow in plants. *Science*, **312**, 883.

Xiao, J. Cao, H., Wang, Y., Zhao, J. and Wei, X. (2009) Glycosylation of dietary flavonoids decreases the affinities for plasma protein. *J. Agric. Food Chem*. **57**, 6642-6648.

Yonekura-Sakakibara, K., Tohge, T., Matsuda, F., Nakabayashi, R., Takayama, H., Niida, R., Watanabe-Takahashi, A., Inoue, E. and Saito, K. (2008) Comprehensive flavonol profiling and transcriptome coexpression analysis leading to decoding gene-metabolite correlations in Arabidopsis. *Plant Cell*, **20**, 2160-2176.

Yonekura-Sakakibara, K., Tohge, T., Niida, R. and Saito, K. (2007) Identification of a flavonol 7-O-rhamnosyltransferase gene determining flavonoid pattern in *Arabidopsis* by transcriptome coexpression analysis and reverse genetics. *J. Biol. Chem*. **282**, 14932-14941.

Zažímalová, E., Murphy, A.S., Yang, H., Hoyerova, K. and Hosek, P. Auxin transporters--why so many? *Cold Spring Harb Perspect Biol*, **2**, a001552.

Zhang, J., Nodzynski, T., Pencik, A., Rolcik, J. and Friml, J. (2009) PIN phosphorylation is sufficient to mediate PIN polarity and direct auxin transport. *Proc. Natl. Acad. Sci. USA*, **107**, 918-922.

Zimmermann, I. M., Heim, M. A., Weisshaar, B. and Uhrig, J. F. (2004) Comprehensive identification of *Arabidopsis thaliana* MYB transcription factors interacting with R/B-like BHLH proteins. *Plant J.* **40**, 22-34.

7 SUPPPLEMENTAL DATA

Supplemental Table 1 Primers used in this thesis. The AGI code of each gene is given in the middle of the primer name.

Primer name (including AGI code)	Sequence (5'->3')
PAL1-At2g37040-f	TGCAGTGACTTCAATCTTCCA
PAL1-At2g37040-r	TTCGGGATAGCCGATGTT
PAL2-At3g53260-f	GGTTCCACGGAGAGGTAGTG
PAL2-At3g53260-f	CATGCTCGTCAGAGTCAACAC
PAL3-At5g04230-f	TGGAACGAGTCAGGACAGAGT
PAL3-At5g04230-f	TTAGCAACCTCGTCTCGAGTT
PAL4-At3g10340-f	TCCCTGCAGCCTCACTTAC
PAL4-At3g10340-r	GCTCCGATTTTGTGGAAAAC
4CL1-At1g51680-f	GTAGATATGAAACATGGGCAAAAC
4CL1-At1g51680-r	GATGCTGACTCACAAGGGACTA
4CL2-At3g21240-f	AGCTGGAGCCACTTGAAATC
4CL2-At3g21240-r	GATAAAGATGGTTGGCTTCACA
4CL3-At1g65060-f	AGGAGATTTAGGAATGGAAGCA
4CL3-At1g65060-r	GTGCGATCAAATGGAAATGA
C4H-At2g30490-f	AGGATGTGCAAGCTGAATTG
C4H-At2g30490-r	TTGGCATTGCCTATTTTGG
CHS-At5g13930-f	GTCACGTGTTGAGCGAGTATG
CHS-At5g13930-r	CCCCACTCCAACCCTTCT
CHI-At3g55120-f	AGCGAAGAGGATCGATGAAC
CHI-At3g55120-r	CGGAGAATTGTGTGGCTATATG
F3H-At3g51240-f	CACTGACCCTGGAACCATTAC
F3H-At3g51240-r	TTGACGACAAACGCTCCTT
F3'H-At5g07990-f	TCGCTCAGCTTCCTTACCTT
F3'H-At5g07990-r	GGGATATGGTAGCCGTTGAT
FLS1-At5g08640-f	TCCTCGGCCGGATTTAG
FLS1-At5g08640-r	GCATCGAACCAGTGATCATC
DFR-At5g42800-f	GCATTTGGACGACTTATGCA
DFR-At5g42800-r	GGCCTGAGAAATTTGGAGATAG

ABBREVIATIONS

aa	amino acid
bp	base pairs
cDNA	complementary DNA
CPM	count per minute
DNA	deoxyribonucleic acid
dNTP	deoxyribonucleotide triphosphate
EDTA	ethylene diamine tetraacetic acid
FW	fresh weight
g	gram
GUS	β-glucuronidase
HPLC	high performance liquid chromatography
IAA	indole-3-acetic acid
Kb	kilo base
LC-MS	liquid chromatography mass spectrometry
min	minute
OD	optical density
PAT	polar auxin transport
PCR	polymerase chain reaction
RNA	ribonucleic acid
RNase	ribonuclease
RT	room temperature
RT-PCR	reverse transcriptase-PCR
SDS	sodium dodecyl sulphate
TEMED	N,N,N,N-tetramethyl ethylene diamine
Tris	2-amino-2-hydroxymethyl-1,3-propanediol
UDP	uridine 5’-diphosphate
UGT	UDP dependent glycosyltransferase
UV	ultra violet
v/v	volume per volume
X-glc	5-bromo-4-chloro-3-indolyl- β-D-glucuronide

ACKNOWLEDGEMENTS

I am heartily thankful to my supervisor, PD Dr. Schäffner, whose education, supervision and support from the preliminary to the concluding level enabled me to develop an understanding of the projects. Moreover, his enthusiasm and stringency to science have influenced me and will continue to benefit me beyond these projects.

My special thanks go to Dr. Heller. His expertise and enthusiasm in flavonoid research have always supported me throughout my thesis. PD Dr. Glawischnig (TUM, Weihenstephan) has brought me into scientific field. It has been wonderful to work together with him before I started my research in Helmholtz Zentrum München. This thesis would not have been possible without the initial work from Dr. Meßner. His excellent previous work laid a solid foundation for this thesis. I am grateful to Kerstin Schuster. Her passion and contribution to the auxin transport related project supported me to complete this project. Stephan Dräxl provided kind help with auxin transport at the end of my PhD work. I also thank Veronica von Saint Paul for her kind help me with the initial statistical analysis and FT-ICR-MS measurement. I also would like thank Dr. Albert and other colleagues from EUS group for their help in the access to sun simulators. Without their contributions, the auxin transport related project would not have progressed that smoothly. I would like to thank Birgit Geist, Susanne Stich, Lucia Gößl and Susanna Holzinger for excellent technical assistance.

I also want to thank Dr. Hoffmann and Prof. Dr. Schwab (TUM, Weihenstephan) for metabolite analysis using LC-MS, Dr. Dobrev and Dr. Zažímalová (Prague, Czech Rep) for phytohormone measurement. Dr. Stracke (Universität Bielefeld) has generously provided many valuable mutants deficient in flavonoid pathway. His support definitely speeded up my doctoral thesis. I would like to than Dr. Hutzler for instructions of confocal laser scanning microscopy. I would like to thank Dr. Scherb (Helmholtz Zentrum München) and Theresa Faus-Kessler for assistants in statistical analyses.

I would like to express my sincere gratitude to Prof. Dr. Beckmann (Gene Center; Department of Chemistry and Biochemistry, University of Munich) for acting as the second referee of my thesis.

My deep thanks go to Wei Zhang, Antonie Sophie Bernhard, Jin Zhao, Kerstin Schuster and Dr. Das for enjoying lunch together and beyond. Special thanks come to Dr. Bahnweg for his kind help of English proofreading and scientific comments. I would also like to thank Dr.

Frank Gaupels, my officemate, for interesting discussions. It is a pleasure to thank all the people who made this thesis possible with contributions from different aspects.

My deep thank comes to Prof. Dr. Durner for his support in various aspects of my project. In the institute (BIOP), I enjoyed to work together with Christian Holzmeister, Birgit Geist, Dr. Sell, Dr. Lindermayr, Stephan Dräxl, Veronica von Saint Paul, Gitto Kuruthukulangarakoola and Dr. Uta v. Rad. I would like to thank Frau Bieber for help with fixing computer problems. My special thank goes to Frau Stoll for her kind help with signing contract, filling difficult official forms and discussion about Chinese language.

I owe my deepest gratitude to my dear wife Dr. Lin. Her encouragement, understanding, experience and direct help have always been the most important support for my research.

Ruohe Yin